DUBLIN CITY UNIVERSITY

School of Electronic Engineering

Control Technology Research Unit

Self Tuning Control of Fermentation Processes

by

Philip Comerford, B Eng

A thesis submitted for the degree of Master of Engineering

Supervisor: Dr John Ringwood

September, 1990

ABSTRACT

SELF TUNING CONTROL OF FERMENTATION PROCESSES

Control of fermentation processes is a complex problem due to the inherent non-linearities and time varying characterstics of the process The application of conventional single loop analogue controllers provides poor control due to problems in tuning individual loops and the lack of ability to implement complex controllers The application of standard optimal techniques is compounded both by the complexity of the process and the lack of adequate models as a result of poorly understood dynamics The lack of important transducers for product measurement coupled with the time varying parameters in a fermentation process provides a natural test for adaptive control techniques

This thesis includes details of modelling and simulation studies carried out on a Bakers Yeast fermentation process A mathematical model of the growth of *Saccharomyces Cerevisiae* which describes oxidative and aerobic fermentative growth on glucose is presented The parameters which influence the growth phases of the yeast organism are identified by Recursive Least Squares as part of an overall adaptive control technique

An integrated approach is presented for the on-line estimation of the state of a biochemical reactor from presently attainable real time measurments State estimation by the presented method of Kalman filtering and the above parameter estimation technique is used for the development of an adaptive control scheme

Details of the pilot-plant, instrumentation and computer systems are described highlighting the practical problems in these areas and the means by which these problems have been overcome

Results are presented to show the sucessful performance of the adaptive technique and this work indicates that the application of an adaptive technique could provide great opportunities for the enhancement of conventional control of fermentation processes

ACKNOWLEDGEMENTS

The continued help and encouragment from my project supervisor, Dr John Ringwood is greatly appreciated Special thanks also to Jim Dowling for his assistance during the course of the project To the staff at the School of Electronic Engineering at Dublin City University especially fellow postgrads Fred Jones and Paddy Gibbs and the electronics technicians who supplied technical and social expertise when necessary throughout this project.

This was a bioengineering project and the help of the staff in the School of Biological Science at Dublin City University is acknowledged Special thanks to Brian Corcoran and Peter Canavan for their help in the pilot plant and to Monica Byrne, Roseanne Comerford and the other biology technicians for their help in the biology laboratory

DECLARATION

I herby declare that this thesis is entirely of my own work and has not been submitted as an exercise to any other university

Philip Comerford

Philip Comerford

DEDICATION

Dedicated to my parents as they enter their golden years

NOMENCLATURE

C^* saturated concentration of CO_2 in the broth (g/l)

C the broth concentration of dissolved $C0_2$ (g/l)

D the dilution rate (hr^{-1})

d_b the air bubble diameter in the broth (cm)

d_i the impeller diameter (cm)

D_{02} the diffusion coefficient for oxygen (cm^2/s)

E the ethanol concentration in the broth (g/l)

F the input flow rate of air to the vessel(l/min)

H Henry's constant for gases

K absolute temperature in Kelvin (Degrees Kelvin)

K_d the factor by which the volumetric absorption coefficient for $C0_2$ is greater than that of oxygen

k_{02} the saturation constant for dissolved oxygen tension.

k_La the mass transfer or absorption coefficient for oxygen (hr^{-1})

k_S Blackman's constant

L the air bubble membrane thickness (cm)

N_g the mole concentration of a gas (mole)

N_S the stirrer rotation speed (rpm)

O^* the saturation concentration of dissolved oxygen in the liquid (g/l)

O the dissolved oxygen concentration in the liquid (g/l)

P pressure in the vessel (bar)

p_O the partial pressure of oxygen in the gas phase (atm)

R gas constant

Re Reynolds number for a fluid

S substrate concentration (g/l)

Sh Sherwood number for the broth.

S_i the feed concentration of glucose (g/l)

V volume of liquid in the vessel(l)

v_b the ascending bubble velocity (cm/sec)

V_g volume of the gas phase (l)

X cell concentration (g/l)

$Y_{x\,s}$ the yield coefficient of biomass on substrate (g/g)

$Y_{x\,o}$ the yield coefficient of biomass on oxygen (g/g)

$Y_{x\,c}$ the yield coefficient of CO_2 on biomass (g/g)

GREEK

μ specific biomass growth rate (hr^{-1})

μ_c broth viscosity (g/cm sec)

τ specific ethanol growth rate (hr^{-1})

δ surface density of the broth (g/cm^3)

ϵ_f liquid holdup fraction in the reactor

ϵ_g liquid holdup fraction in the gas

ρ_c continous phase density (g/cm^3)

ρ_ℓ density of the broth (g/cm^3)

λ forgetting factor

CONTENTS

CHAPTER 1	**INTRODUCTION**	
1 1	Evolution of Fermentation Control	1
1 2	Control of Fermentation Processes	2
1 3	Motivation for Research	4
1 4	Thesis Structure	4
CHAPTER 2	**MODELLING AND SIMULATION OF FERMENTATION PROCESSES**	
2 1	Biochemical Fundamentals	6
2 1 1	Bioreactor Techniques	7
2 1 2	Metabolism of Bakers Yeast	8
2 2	Modelling of Kinetics	10
2 2 1	Cell growth	10
2 2 2	Substrate Utilisation	11
2 2 3	Dissolved Oxygen Utilisation	11
2 2 4	Ethanol Production and Consumption	12
2 2 5	Carbon Dioxide Production	13
2 2 6	Models of the Specific Growth Rate μ	14
2 3	Modelling of Transport	16
2 3 1	Oxygen Transfer	17
2 3 2	Carbon Dioxide Transfer	18
2 3 3	Absorption Coefficient	18
2 3 4	Gas Phase Concentrations	20
2 4	Fed Batch Fermenter Simulation	22
2 4 1	Numerical Integration Methods	23

2 4 2	Simulation Program Structure	24
2 5	Summary	25

CHAPTER 3 **PARAMETERIZATION AND IDENTIFICATION OF THE FERMENTATION PROCESS**

3 1	Introduction	26
3 2	Least Squares Identification	27
3 2 1	Recursive Least Squares	27
3 3 2	Recursive Least Squares for Time Varying Systems	28
3 3	Identification Models	30
3 3 1	Unstructured Model	30
3 3 2	Monod Model	32
3 3 2	Ollson Model	33
3 3 4	Comprehensive Model	34
3 4	Simulation Results	35
3 5	Discussion	37
3 6	Summary	38

CHAPTER 4 **STATE ESTIMATION TECHNIQUES FOR BIOREACTORS**

4 1	Introduction	39
4 2	Observability of Non-Linear Systems	41
4 3	State Estimation	43
4 3 1	Non-Linear Observer	44
4 3 2	Non-Adaptive Observer	46
4 3 3	Extended Kalman Filter	47

4 4	Combined State and Parameter Estimation	52
4 4 1	Partially Adaptive Observer	52
4 4 2	Fully Adaptive Observer	53
4 5	Simulation Results	55
4 6	Discussion	56
4 7	Summary	57

CHAPTER 5 SELF TUNING CONTROL OF FERMENTATION PROCESSES

5 1	Introduction	58
5 2	Process Model	60
5 3	Process Model Lineasization	61
5 3 1	Linearised State Space Model - Single-Input Single-Output	62
5 3 2	Linearised State Space Model - Multi-Input Multi-Output	63
5 3 3	Controllability	64
5 4	Regulation Based on Pole Placement by State Feedback	67
5 5	Simulation Results	68
5 5 1	Non-Linear and Linearised Plant Comparsion	69
5 5 2	Fixed Parameter Controller	69
5 5 3	Self Tuning Controller	71
5 6	Conclusions	73

CHAPTER 6 EXPERIMENTAL RESULTS AND MODEL VALIDATION

6 1	Process Instrumentation	74
6 2	Materials and Methods	76
6 2 1	Innoculum Preparation	76
6 2 2	Medium Preparation	76
6 3	Production of Laboratory Results	77
6 3 1	Wet cell Weight/Dry Yeast Weight	77
6 3 2	Sugar Level Determination	78
6 4	Model Validation	79
6 4 1	Validation of Substrate and Biomass Measurements	79
6 4 2	Validation of Dissolved Oxygen Measurement	77
6 4 3	Validation of Gas Analysis	80
6 5	Identification using Experimental Results	80
6 5 1	Unstructured Growth Rate Model	81
6 5 2	Monod and Ollson Growth Rate Models	82
6 6	Discussion	83
6 6 1	Model Validation	83
6 6 2	Experimental Identification of Parameters	85
6 7	Summary	87

CHAPTER 7 CONCLUSIONS 88

REFERENCES 92

FIGURES 97

APPENDIX A 136

CHAPTER 1

INTRODUCTION

1 1 EVOLUTION OF FERMENTATION CONTROL

Ancient man was well aware of fermentations even though he had little knowledge of what caused them He was aware of such fundamentals as making intoxicating drinks from grains and fruit The aging of meat and the manufacture of alcoholic beverages were man's first uses of fermentation. The discovery of fruit fermentation was made so long ago that the ancient Greeks believed that wine had been invented by the god Dionysus The manufacture of beer is only slightly less ancient than that of wine An Assyrian tablet of 2000 B C even lists beer among the commodities that Noah took aboard his Ark In those early days man considered fermentation as some sort of mystical process, he did not know that he was profiting from the activity of invisible microorganisms

During the Middle Ages, experimenters learned how to improve the taste of wine, beer and cheese Yet, after thousands of years of experience, man still did not realise that in fermentations he was dealing with a form of life However, in 1857, Pasteur proved that alcoholic fermentation was brought about by yeast and that yeasts were living cells This discovery was a major turning point and considered the birth of microbiology With the discovery of additional products and chemicals produced by fermentations the inheritors of Pasteur's knowledge pushed fermentation processes towards commercial practice

The technical innovation that the microprocessor brought to engineering systems did not rapidly become apparent in its application to control of biological systems In fact, in 1973 when the first conference on Computer Process Control in Fermentation was held in Dijon[1], reports on the application of computer

control had only been published for two production plants and one pilot plant in the fermentation industry Not only were the applications few but it was also indicated that not all applications were sucessful Special purpose software in machine language code made modifications and correction of errors difficult. Combined with limited reliability of computer hardware, sensors and transmitters, this resulted in overall unsatisfactory performance

Fermentors, before microprocessors, were controlled by analog systems Control action was generated by pneumatic or electrical elements with physically defined characterstics so as to generate proportional, integral and derivative response to error signals When microprocessors became readily available the most natural evolution was to append the microprocessor to the existing analog system so as to obtain digital logs and supervisory control of the process set points [2] Such control techniques were at the time practicable but certainly not optimal

Overall at present the fermentation industry has widely accepted computer based systems Alford [3] describes the evolution of a computer system at Eli Lilly & Co at their plant in Indinia, U S A from the early 1970's to early 1980's Microcomputer development allied with real time operating systems, standard modular control languages, realistic process models and on-line programming facilities has completely changed the approach to fermentation system design.

1.2 CONTROL OF FERMENTATION PROCESSES

The feasibility of applying control techniques to fermentation processes is today expanding in application Increasing production costs have led to a greater interest in data acquisition for performance analysis and on-line control of the process The ability to control fermentation accurately and automatically would enable a reduction in production costs and an increase in yield whilst maintaining

the quality, uniformity and reproductibility of the product

Analysis of fermentation processes reveal that many problems face any prospective control system designer Until recently the fermentation industry had lagged behind in the application of control techniques and especially computer control Progress in the application of computer control techniques has been hampered by many of the following practical problems

Firstly, the development of suitable instruments for the measurment of biological variables has lagged behind the development of computer control schemes In particular instruments for the measurement of biomass (e g bakers yeast) and substrate concentrations have not gained wide acceptance as they do not withstand the rigorous sterility requirements and those that pass the above test prove to be less than durable [4]

Secondly, the fermentation process is more complex than many chemical and other types of processes It contains non–linearities and parameters which change with time and from batch to batch Hence conventional two and three term controllers are difficault to tune and cannot provide optimal performance over the whole range of the process

Thirdly, the development of mathematical models to describe the fermentation process has been restricted by their complexity Models have been proposed using differental equations describing the microbial kinetics [5,6] These require assumptions that the parameters of the model equation are constant This does not account for the fact that cell activity may switch between different metabolic pathways during a fermentation life cycle

Despite these problems, a variety of control techniques have emerged [7] that concentrate on more effective use of those measurements which are already

available It will be the purpose of this thesis to outline how control using self tuning techniques would apply to a fed batch fermentation process

1 3 MOTIVATION FOR RESEARCH

The research undertaken and the efforts to design a adaptive/self tuning based controller for a fermentation system which are described in this disseratation have been motivated primarily by the upsurge in engineering interest in adaptive/self tuning regulators Engineering interest in adaptive control originated primarly with aerospace problems It was found that the use of classical linear controllers in aircraft auto pilots did not always give satisfactory control of the altitude of high performance aircraft The changing characterstics of a fermentation process also necessitates a more sophisticated controller which would automatically adapt itself to the process Hence this project was initiated in anticipation of the applicability of a self tuning regultor to a fermentation system

The research was undertaken at the Control Technology Research Unit (CTRU) at Dublin City University in collaboration with the School of Biological Sciences

1 4 THESIS STRUCTURE

The research work undertaken in this project which investigates possible solutions to the monitoring and control of biotechnological processes is presented as follows

Chapter 2 presents the basic mathematical models used to describe the kinetics of fermation processes In particular, the specific microbial growth rate is presented

and the variety of ways available to express its dependence on environmental factors

Chapter 3 concentrates on the on–line identification of the fermentation parameters that influence growth during a fermentation cycle

Chapter 4 outlines the general state estimation problem and its associated theory and outlines the application of an Extended Kalman Filter to estimate biomass and substrate concentrations from measurements of the concentration of carbon dioxide in the exhaust gas

Chapter 5 is concerned with the adaptive control of the fermentation process with control law formulation being based on pole placement by state feedback.

Chapter 6 presents experimental results from the pilot plant This chapter presents comprehensive model validation results and off-line parameter and state estimation using experimental results

Chapter 7 comments and concludes on the overall research and highlights areas that need further work

CHAPTER 2

MODELLING AND SIMULATION OF FERMENTATION PROCESSES

A fermentation model is an abstracted and generalised description of relevant aspects of a fermentation process In fermentation, as in other processes, an accurate mathematical model is a prerequisite for the simulation, control and optimisation of the process Process models used in control systems vary in form yet have the unifying feature that they predict process outputs for a given set of inputs The final choice of model must be a calculated comprimise between the degree of simplicity that will allow good control and the equally important desire to represent all the important aspects of the process accurately In the case under consideration, the model presented is intended for use in simulation studies where the model structure will eventually be utilised by a self tuning controller implemented on a digital computer It is with the development, uses and limitations of mathematical models of fermentation kinetics and transport that this chapter is concerned Various fundamentals of a biological system are first outlined followed by a detailed analysis of the kinetics and transport as applied to a fermentation system

2 1 BIOCHEMICAL FUNDAMENTALS

The science of *biochemistry* underlines all mathematical treatment of fermentation processes, particularly *kinetics* which is at the core of all models of bioreactors Biochemistry is concerned with the particular types of chemical reactions found in all living organisms, and which underly all biological processes The challenge in learning biochemical engineering is to understand and analyze the processes of biotechnology so that we can design and operate them in a rational way To reach this goal however, a basic working knowledge of cell growth and function is required [8,Ch 5][9,Ch 4]

Microorganisms grow by converting *substrates* (e g glucose) present in the liquid medium into cell mass (e g yeast) and possibly products such as alcohol and carbon-dioxide Growth, which is characterised by an increase in cell mass occurs only where certain chemical amd physical conditions are satisfied, such as acceptable temperature and pH as well as the availability of required nutrients For the development of this model the influence of temperature and pH are neglected because they are assumed constant and controlled during a fermentation run.

2 1 1 Bioreactor Techniques

A *bioreactor* is a vessel designed to facilitate biological reactions A fermentor is a type of bioreactor, designed to facilitate fermentation processes There are various types of fermentors [10], e g bubble column reactors and tower reactors However the most widely used is the stirred tank reactor As the name suggests, this reactor consists of a vessel within which an agitator or impeller stirs the liquid broth as outlined in Appendix A There are three basic fermentation techniques

a)*Batch* The liquid, microorganisms and substrates are put into the vessel at the beginning of the batch run and no further additions are made Only environemental variables such as temperature, pH and air–flow rate are manipulated during the batch run

b)*Fed-Batch* This employs the same technique as batch, except that substrates are fed continuously into the fermentor during the run.

c)*Continuous* With this method, liquid, substrates, and microorganisms are continuously fed into and siphoned off the vessel The aim is to keep these varibles in a steady state The total concentration of products, substrates and microbes fermentor are kept constant.

Of these techniques, fed-batch poses the greatest challenge to the control engineer Batch fermentation allows only trivial setpoint control of temperature and

pH etc, while continuous fermentations tries to keep the variables in a steady state However, in fed-batch the control engineer must devise an algorithm to obtain an optimal substrate feed-rate for a given control objective In fed batch fermentation the variables directly controlled are usually substrate feed rate, agitator feed rate and aeration rate Measrurements are made of the composition of exit gas from the fermentor (partial fractions of carbon dioxide and oxygen) and dissolved oxygen concentration Note that none of the primary variables which concern the control engineer (cell growth rate and concentration of products in the liquid phase) are mentioned above This again highlights the non–availibility of sensors which are capable of accurately measuring these variables Thus the secondary measurements of exit gases need to be augmented by mathematical relations between secondary and primary process variables to obtain pseudo measurements of the main states

2 1 2 Metabolism of Bakers Yeast

This section outlines the fundamentals of reaction that occur during fermentation Figure 2 1 gives a diagrammatic representation of the principle metabolic pathways within the organism under consideration, *Saccharomyces Cerevisiae* [11,Ch 3] The metabolism is very similiar to metabolisms within other organisms It is important to remember that every step in the metabolic conversion process is controlled by enzymes and to also realise that in a series chain of reactions, the slowest reaction determines the overall rate Figure 2 2 gives a very basic scheme of the same metabolism

The main substances supplied by the organism to effect metabolic conversions are Adenosine diphosphate (ATP) and Nicotinamide adenine dinucleoide (NADH) These substances supply much of the energy required to carry out the conversions At the beginning of the metabolism, the substrate glucose (a type of sugar) is absorbed into the cell from the surrounding environment With the aid of ATP, the glucose is converted into glucose-E-phosphate This substance can enter two

pathways One which recycles the substance, the other leads to its conversion into pyruvate At this stage, two important branches in the metabolism appear, both of which eventually lead to the production of Acetyl-Coenzyme-A

As can be seen the intermediate and final pathways are important in the determination of the final product Pathways lead to the production of ethanol, a type of alcohol and CO_2, which are released into the environment. Generally, in the presence of plentiful glucose, a large amount of pyruvate is formed This in turn leads to saturation of the pathway leading to acetyl-CoA production and drives the excess pyruvate into production of large amounts of ethanol The net result is that in the presence of excess glucose, ethanol accumulates in the environment

If glucose levels are brought down, the amount of pyruvate also decreases This means that the cell looks to ethanol to produce the Acetyl-CoA needed by the metabolism Thus in the absence of glucose the available ethanol is consumed However, since the first part of the metabolism is inactive in this mode, it is less efficient in promoting growth. Also in the presence of excess glucose, the production of ethanol means that much of the glucose has been inefficiently converted to alcohol instead of cell mass

The Acetyl-CoA enters a cycle called TAC, the details of which are unimportant save that CO_2 and NADH are produced. The NADH then enters into the so called Respiratory Chain. In this chain O_2 is taken up and ATP and water released In the absence of oxygen the respiratory chain deactivates and since this chain is in series with the other main metabolic reactions the oxygen level becomes growth rate limiting This leads to an effect similiar to the deficiency of glucose

Overall, the metabolism takes in glucose and oxygen to produce cell growth, CO_2, ethanol and H_2O

2.2 MODELLING OF KINETICS

Kinetics, in chemistry, deals with the behaviour of chemical systems when *reactants* come together and give rise to products Since these reactions are the fundamental activities by which changes in biochemical systems occur, the laws governing the kinetics of biochemical reactions form the basis of all mathematical models of bioreactors, including fermentors From knowledge of the metabolism of *Saccharomyces Cerevisiae* already outlined, a mathematical description of the uptake of substrates and their utilization within the cell will be developed Aerobic bakers-yeast fermentation also utilises oxygen dissolved in the liquid to enable growth and a model of the usage of dissolved oxygen will be developed The modelling and utilisation of products such as alcohol and carbon dioxide will also be condsidered The model developed here is for a fed-batch fermentation process

2.2.1 Cell Growth.

In the initial attempts to model and understand cell population kinetics we shall first present models in which only cell mass or number concentrations will be employed to characterise the biophase The nett rate of cell mass growth r_X, is often written as [12],

$$r_X = \mu(t)\, X(t) \qquad (2\ 1)$$

where X(t) is the cell mass per unit culture volume and μ, which has units of reciprocal time, is the *specific growth rate* of the cells For a perfectly mixed fed batch fermentor in which the culture is being diluted at a rate D (hr^{-1}) then a mass balance using the above equation gives,

$$\frac{dX}{dt} = [\mu(t) - D(t)]X(t) \qquad (2\ 2)$$

$$X(t_0) = x_0 \qquad (2\ 3)$$

$$D(t) = \frac{F(t)}{V(t)} \qquad (2\ 4)$$

where F(t) is the volumetric feed flowrate of input substrate (g/l hr) and V(t) is the culture volume Section 2 2 6 deals with the growth rate μ in more detail

2.2.2 Substrate Utilisation.

Microorganisms require substrates to synthesise new cellular and extracellular products and also to provide the energy necessary to drive the reactions Thus growth and substrate utilisation are both closely related A consumption rate for the substrate may be expressed as,

$$r_S = \frac{-\mu(t)X(t)}{Y_{X\ S}} \qquad (2\ 5)$$

where $Y_{X\ S}$ is the yield of biomass per unit substrate

For a fed-batch reactor to which a substrate concentration of S_1 (g/l), defined as the input feed concentration is added a mass balance of the above gives,

$$\frac{dS}{dt} = \frac{-\mu(t)X(t)}{Y_{X\ S}} + D(t)[S_1(t) - S(t)] \qquad (2\ 6)$$

There is no guarantee that the yield factor, an empiraclly defined, apparent *stoichiometric ratio* is a constant for a given organism in a given medium [13] However if a yield factor is approximately constant for a particular cell cultivation system it provides useful knowledge of the cell mass and substrate concentration

2.2 3 Dissolved Oxygen Utilisation

Absorption of oxygen from air into a fermentation broth for use by the microorganisms is critical to the process of growth Only oxygen dissolved in the liquid may be used by the cells The rate at which oxygen is taken up by the cells from the fluid is called the *Oxygen uptake rate* (OUR) and is proportional to the cell mass growth rate

$$OUR = \frac{-\mu X}{Y_{X\,O}} \qquad (2\ 7)$$

where $Y_{X\,O}$ is a parameter known as the yield of cell mass per gram of oxygen utilised To avoid oxygen deficiency within the vessel air must transported into the vessel by some process of aeration. This transport mechanism will be dealt with later

2.2.4 Ethanol Production and Consumption

To examine the ethanol production and consumption effects within a reactor, the metabolism is divided into two stages The first stage from the adsorption of glucose to the production of alcohol and the second stage from the consumption of alcohol to the production of H_2O

In the first stage, ethanol is produced when excess substrate causes one branch of the metabolism to be saturated and the branch which produces ethanol to activate The production of excess ethanol is known as the Crabtree Effect [8,Ch 10][11,Ch 5]] The rate at which ethanol is produced depends on the level of glucose as well as on the cell mass The *Ethanol production rate* (EPR) if no ethanol is already present is described by,

$$EPR_1 = \frac{\tau_{max}\ S\ X}{k_S + S} = \tau\ X \qquad (2\ 8)$$

where τ is the ethanol growth rate per unit biomass, τ_{max} is the maximum value of τ and k_S a rate limiting constant.

However,the presence of ethanol in the medium inhibits the further production of ethanol At low concentrations, this effect is neligible but at higher concentrations inhibition becomes significant. This effect can be in incorporated in

an overall ethanol production rate equation by,

$$EPR = \frac{EPR_1}{1 + E/k_e} \qquad (2\ 9)$$

with E is the ethanol concentration and k_e a rate limiting constant for ethanol

In the second part, ethanol consumption occurs when ethanol acts as a substrate, cutting out the metabolism that acts on glucose Thus the consumption rate depends on ethanol concentration and also on dissolved oxygen in the liquid It can be shown that when two substrates are rate limiting in a single enzyme-controlled reaction series, then the overall rate is the product of the individual rates Thus the *ethanol consumption rate* (ECR) may be written as,

$$ECR = \frac{\zeta_{max}\ E\ O}{(k_{O2}+O)(k_e+E)}\ X \quad = \zeta\ X \qquad (2\ 10)$$

where ζ is the ethanol consumption rate per unit biomass, ζ_{max} is the maximum value of ζ and k_e is a rate limiting constant for ethanol and k_{O_2} the saturation constant for dissolved oxygen

Thus the overall ethanol concentration is described by

$$\frac{dE}{dt} = ECR - EPR \qquad (2\ 11)$$

$$\frac{dE}{dt} = \left(\frac{\tau_{max}\ S}{(1+E/k_e)(k_S+S)} - \frac{\zeta_{max}\ E\ O}{(k_{O2}+O)(k_e+E)} \right) X \qquad (2\ 13)$$

2.2.5 Carbon Dioxide Production

Carbon dioxide (CO_2) is produced or evolved by the cell during the growth cycle The carbon dioxide is secreted by the cell and becomes dissolved in the fluid and may exist in the liquid phase in any of the four forms CO_2, H_2CO_3, HCO_3^- and CO_3^{--} CO_2 is produced at two stages in the metabolism cycle, firstly,

when ethanol is produced and secondly, after the TAC cycle

In the first case the carbon-dioxide produced is proportional to the ethanol produced and in the second case it is proportional to the cell mass produced (growth rate) Thus the *carbon dioxide evolution rate* (CER) is described by,

$$CER = k_{C1} EPR + k_{C2} \mu X \qquad (2\ 14)$$

where k_{C1} and k_{C1} are constants of proportionally for ethanol and cell mass production respectively

Overall the level of dissolved CO_2 is described by,

$$\frac{dC}{dt} = CER + CTR \qquad (2\ 15)$$

where CTR is the rate at which CO_2 is transported across the gas liquid interface Only the dissolved CO_2 molecule is transported across the gas liquid interface and this transport phenomena will be presented in detail in Section 2 3

It is important to model the amount of dissolved CO_2 even though it does not directly affect the growth rate This is because measurements of exhaust CO_2 can be related to dissolved oxygen concentration and hence growth rate via equation (2 14)

2.2.6 Models of the Specific Growth Rate μ

The general goal in making a good medium is to support good growth of biomass and/or high rates of product synthesis such as alcohol production depending on the type of fermentation in progress This does not mean that all nutrients should be supplied in graet excess For one thing, excessive concentrations of a nutrient can inhibit or poison cell growth Moreover, if the cell grows too extensively their accumulated metabolic end product will often disrupt the normal biochemical processes of the cell Consequently it is common practice to limit

total growth by limiting the amount of one nutrient in the medium

A functional relationship between the specific growth μ and an essential compound's concentration was proposed by Monod [14] This specific growth rate model which expresses the dependence of μ on the substrate concentration S as follows

$$\mu = \mu_{max} \frac{S}{k_S+S} X \qquad (2\ 16)$$

where μ_{max} is the maximum growth rate and k_S is the "Michaelis–Menten" parameter

The biomass growth is often presumed to slow down at high biomass concentrations A possible model to accomodate this situation is the following specific growth rate depending on both S and X,

$$\mu = \mu_{max} \frac{S}{k_C X+S} \qquad (2\ 17)$$

with k_C a constant which was proposed by Contois [15]

Aerobic fermentation are processes where the microorganisms need oxygen to develop properly In such cases, dissolved oxygen (DO) in the culture medium can be considered an additional substrate If two substrates (DO and S) are rate limiting in a single enzyme controlled reaction series, then the overall rate is the product of the individual rates This law which has Monod similarities is often referred to as the Ollson model for specific growth rate μ,

$$\mu = \mu_{max} \frac{S}{k_S+S} \frac{O}{k_{O_2}+O} \qquad (2\ 18)$$

where k_{O_2} is the saturation constant and O is the dissolved oxygen concentration

The effect of ethanol in promoting cell growth can be understood by referring to Figure 2 1 This shows that the two substances, glucose and ethanol, act in parallel to promote cell growth Thus, unlike series rates which are multiplicative, parallel rates add together to determine the overall rate Thus on the whole, if taken in conjuction with the Ollson model, three rate limiting substrates are involved the first two, ethanol and glucose rates, are in parallel and add together This resultant rate is in series with the oxygen reaction and thus the oxygen rate is multiplied by the resultant to give the overall rate This growth rate model referred to as the Comprehensive model may be described as,

$$\mu = \left(\mu_{max} \frac{S}{k_S+S} + \nu_{max} \frac{E}{k_e+E}\right) \frac{O}{k_{O_2}+O} \qquad (2\ 19)$$

where ν_{max} is the maximum rate of product formation

2 3 MODELLING OF TRANSPORT

While kinetics deals with how substances interact to form products, another aspect of the system that must be modelled is the mechanism by which the substances come together in order to facilitate reaction [16] Whether transport rates becomes important depends on the magnitude of the rate of transport compared to the rate of reaction If the rate at which some substance is transferred to the area of interaction is of similiar or lesser magnitude than the rate at which the substance is taken up by the reaction then the transport mechanism becomes rate limiting in the overall reaction. If, however, the transport rate is faster than the rate of reaction then there will always be substances available for reaction

The purpose of aeration in fermenatation is to supply oxygen to and at the same time to remove carbon dioxide suspended in the culture broth after being evolved by the microbial cells Mixing in the gas and liquid phases affect the

aeration characteristics of a fermentor Liquid phase mixing also influences the residence time distribution of the broth and thereby yields of microbial mass and products In the sparged stirrer fermentor which we will deal with, air is sparged into the broth which is continuously mechanically agitated Dispersion of gas bubbles is done mainly by the mechanical force of the impeller

Glucose fed into the fluid becomes dissolved immediately, unlike gases which are held in air bubbles before dissolving In this model the transport of glucose is ignored This leaves the transport of gases as the important features in the overall model of transport in agitated systems This is particulary true of oxygen as it may have a growth limiting effect The importance of carbon dioxide is that primary variables may be inferred from exhaust gas analysis In this section a comprehensive model of the transport of oxygen and carbon dioxide will be developed

2 3 1 Oxygen Transfer

In section 2 2 3 the term *oxygen transport rate* (OTR) was introduced into the kinetics model The rate of transfer of oxygen from air bubbles to the dissolved state is vitally important to keeping a good supply of oxygen as demanded by aerobic fermentations The oxygen must cross the gas-liquid interface to be of use to the cells This mechanism is controlled by the liquid phase mass transfer resistance It is sufficient to state from previous investigators [8,Ch 8][17,Ch 9] that the rate of oxygen transfer can be stated as,

$$OTR = k_l a \ (O^* - O) \qquad (2\ 20)$$

where k_l is the liquid phase mass transfer coefficient (cm/hr) and a is the bubble surface area per unit volume of liquid (cm^2/cm^3), O^* is the saturation concentration of dissolved oxygen and O is the dissolved oxygen concentration in

the liquid The lumped $k_{\ell}a$ term is usually referred to as the volumetric transfer coefficient (hr^{-1})

2.3.2 Carbon Dioxide Transfer

Carbon dioxide transfer can be developed in exactly the same way as oxygen transfer This implies that we can write a similiar equation for the *carbon dioxide transfer rate* (CTR) as for oxygen

$$CTR = K_d \, K_{\ell}a(C^* - C) \qquad (2.21)$$

where C^* is the saturated concentration of CO_2 in the liquid, C is the liquid concentration of dissolved CO_2 and K_d is the factor by which the volumetric absorption coefficient for oxygen is greater than that of CO_2

Equations (2.20) and (2.21) both contain $k_{\ell}a$, the volumetric absorption coefficient for oxygen and, in principle, this term is variable depending on certain factors including aeration of the vessel and agitation rate The next section analyses this term in more detail

2.3.3 Absorption Coefficient

The volumetric absorption coefficient is composed of two terms as already outlined The first term k_{ℓ} is the rate of mass transfer across the gas liquid interface and the second term a is the interfacial area per unit volume The first term k_{ℓ} is "conductance" of the gas–liquid membrane , i e it is a measure of the ease with which mass crosses the gas liquid interface The local mass flux at the gas liquid interface for a bubble is given by [8,Ch 8]

$$\text{Mass flux} = - D_{O_2} \left. \frac{\delta \Omega}{\delta z} \right|_{z=0}$$

$$= k_\ell(O^* - O) \qquad (2\ 22)$$

where D_{O_2} is the diffusion coefficient = P_m/L where P_m is the permeability of the membrane and L is the membrane thickness and z is the coordinate measure from gas into liquid phase, with its origin at the gas liquid interface

The Sherwood number Sh is defined [9] by

$$Sh = \frac{k_\ell\ d_1}{D_{O_2}} \qquad (2\ 23)$$

where d_1 is the impeller diameter for agitated systems

Now, k_ℓ is proportional to the average fluid velocity u_{rms}, since an increase in fluid velocity will increase the density difference between gas and liquid phase This average fluid velocity is, in turn, proportional to the power input per unit volume by an impeller in an agitated system according to

$$u_{rms} = k\ \frac{(d_b\ P_i)^{1/3}}{(\rho_c V)^{1/3}} \qquad (2\ 24)$$

with d_b being the bubble diameter, P_i the power input to the agitator, V the volume of the fluid, ρ_c the continuous phase density and k a scaling constant

If we define the Reynolds and Schmidt numbers [8] for stirred systems as,

$$Re = \rho_\ell N_s D_s^{\,2}/\mu_c \qquad (2\ 25)$$

$$Sc = \mu_c/\rho D_{O_2} \qquad (2\ 26)$$

with μ_c being the fluid viscosity, ρ_ℓ the fluid density, N_s the stirrer rotation speed and D_s the stirrer diameter, then it can be shown that Sh = g(Re,Sc) with g( ) some function of Re and Sc According to data presented by Calderbank [18] and Richards [19] the correlation,

$$Sh = 0\ 13\ Sc^{1/2}\ Re^{3/4} \qquad (2\ 27)$$

is accurate for systems with turbulent aeration Combining (2 23)-(2 27) gives

$$\frac{k_\ell d_t}{D_{O_2}} = 0\ 13\ \frac{(\rho_\ell N_s D_s)^{1/2}}{\mu_c^{1/2}}\ \frac{\mu_c^{3/4}}{(\rho_\ell D_{O_2})^{3/4}} \qquad (2\ 28)$$

If μ_c, ρ_ℓ and D_{O_2} are considered constant then

$$k_\ell = 0\ 13 N_s^{1/2} \qquad (2\ 29)$$

The value of the interfacial area, a, in an aerated and agitated system depends on agitator power input. The shear tip of the stirrer tends to cause small bubbles to be formed, which increases the interfacial area per unit volume In addition, bubbles have only a limited lifespan from the time they enter the fluid until they disperse Since the amount of bubbles entering the fluid is dependent on the air flow rate, then the number of bubbles in the fluid is also dependent on the air flow rate According to Calderbank [18], the value of the interfacial area is given by

$$a \propto \frac{(P_g/V)^{2/5}\ \rho_\ell^{1/5}\ (v_s/v_b)^{1/2}}{\delta^{3/5}} \qquad (2\ 30)$$

with P_g the agitator power requirement for an aerated system, v_s the average linear velocity of air per cross sectional area in the vessel, v_b the ascending bubble velocity, δ the surface density of the fluid and V the liquid volume Overall assuming v_b and δ are constant then combining (2 29) and (2 30) gives the following volumetric coefficient,

$$k_\ell a = 0\ 13\ (P_g/V)^{2/5}\ v_s^{1/2}\ N_t^{1/2} \qquad (2\ 31)$$

It is important to have $k_\ell a$ modelled with potential control inputs N_t or P_g for control stge consideration and implementation.

2.3 4 Gas Phase Concentrations

From the oxygen and carbon dioxide transport equations given in Section (2 3 1) and Section (2 3 2) and using standard thermodynamic and gas laws we will

now develop equations for the concentration of O_2 and CO_2 in the exhaust gas of a fermentor In order to derive such equations, we first make use of a fundamental gas law called Dalton's Law which states that the sum of the mole fractions of all substances in a gas is unity,

$$\sum_{i=1}^{n} x_i = 1 \qquad (2\ 32)$$

where x_1 x_n are the molal concentrations of the constitutent gases Also the *mole fraction* of a gas is defined as

$$x_g = p_g/P = N_G\ R\ T/P \qquad (2\ 33)$$

where p_g is the partial pressure of the gas and P the pressure of the overall solution N_G is the *mole concentration* of the gas, R the universal gas constant and T the temperature

Henry's Law states that,

$$O^* = p_O/H \qquad (2\ 34)$$

where p_O is the partial pressure of oxygen m the gas phase and H is the Henry's law constant.

The gas phase of the fermentor is made up of CO_2, O_2 and N_2 (if the very low concentrations of H_2O are ignored) It is assumed that N_2 is an inert gas, i e that it does not react Thus the molar conventration of N_2 does not change The difference between inflowing (*i*) and outgoing (*o*) oxygen mass flow (Q) relative to the liquid volume can be calculated [20] as

$$\frac{Q^i_{O_2} - Q^o_{O_2}}{Q^i_{O_2}} = \frac{[1-x^o_{CO_2}]\ x^i_{O_2} - [1-x^i_{CO_2}]\ x^o_{O_2}}{x^i_{O_2}\ [1-x^o_{O_2}-x^o_{CO_2}]} \qquad (2\ 35)$$

Likewise the rate of change of molal oxygen concentration in the gas phase may

be calculated as,

$$\frac{dO_g}{dt} = \frac{(Q_{O_2} - OTR)V}{V_g M_{O_2}} \qquad (2\ 36)$$

where V_g is the volume of the gas phase and M_{O_2} is the molecular weight of oxygen

We now assume that the molar fractions in the exit gas are the same as those in the gas phase of the fermentor (i e $x^0_{O_2} = x_{O_2}$ etc) Then using (2 33) to convert (2 36) to a mole fraction quantity and substitution of (2 35) the following differential equation for the oxygen mole fraction in the gas phase results

$$\frac{dx_{O_2}}{dt} = \frac{F^i}{\epsilon_g V}\left[\frac{[1-x_{CO_2}]\ x^i_{O_2} - [1-x^i_{CO_2}]\ x_{O_2}}{[1-x_{O_2}-x_{CO}]}\right] - \frac{R\ T\ \epsilon_f}{P\ \epsilon_g}\ OTR \qquad (2\ 37)$$

By similiar arguments to above derivation of balance equations for carbon dioxide yields the following differential equation,

$$\frac{dx_{CO_2}}{dt} = \frac{F^i}{\epsilon_g V}\left[\frac{[1-x_{O_2}]\ x^i_{CO_2} - [1-x^i_{O_2}]\ x_{CO_2}}{[1-x_{O_2}-x_{CO}]}\right] - \frac{R\ T\ \epsilon_f}{P\ \epsilon_g}\ CTR \qquad (2\ 38)$$

where ϵ_f is the mean liquid holdup in the reactor = $V_f/[V_f+V_g]$ and ϵ_g is the mean relative gas holdup in the reactor = $V_g/[V_f+V_g]$

2 4 FED BATCH FERMENTER SIMULATION

In order to assess the bioreactor model's accuracy and to facilitate controller appraisal, the model was simulated in software The simulator uses a classical fourth order Runge-Kutta technique for integration, one of the more advanced and perhaps the most widely used in engineering applications for non-linear systems In

this section numerical integration techniques are addressed with particular emphasis on the Runge–Kutta technique, program structure is outlined with the help of a flowchart and the criterion for choice of numerical integration is discussed

2 4 1 Numerical Integration Methods

The essence of a numerical method is to convert a differential equation into an equivalent model composed of difference equations In this form the model can be programmed on a digital computer Numerical algorithms differ mostly as a result of the specific procedure used to obtain the difference equations In general, as the accuracy of the approximation is increased, so too is the complexity of the programming involved Here we discuss why the Runge Kutta integration method was chosen in preference to other available methods

The principle of all numerical integration methods is to estimate the system states at time (t+h) given the states at time t where h is the sampling period [21] For a general equation of the form,

$$\dot{x} = f(x,u,t) \qquad (2\ 39)$$

At each step computations are done by some formula normally based upon the Taylor series,

$$x(t+h) = x(t) + hx(t) + \frac{h^2}{2!}\ x(t) \qquad (2\ 40)$$

If h is chosen to be sufficiently small and if sufficient higher order derivatives of x and powers of of x are taken then the value x(t+h) can be perfectly found The simplest method, called the Euler method, only takes the first power of h into account assuming the terms in h^n (n>1) are very small compared to h This is valid only if $h \ll 1$ The Euler method has the form,

$$x(t+h) = x(t) + hf(x,u,t) \qquad (2\ 41)$$

The Euler method is of limited practical use due to it's large truncation error per step of order h^2 This is exaggerated when a large step length h is used If it was possible to use a very small step h and if round off error did not occur in the calculations then the Euler method would satisfy most requirements However, the overall solution for Euler, even when small values of the sampling period h are used, remains strongly dependant upon the sample period.

The Runge Kutta derivation [22,Ch 8] follows the same pattern as Euler except terms up to h^4 are retained in equation (2 40) Again for a general equation of the form,

$$x = f(x,u,t) \qquad (2\ 42)$$

the formula for advancing the solution step is

$$x_1 = x_0 + \frac{h}{6}(K_1 + 2K_2 + 2K_3 + K_4) \qquad (2\ 43)$$

where

$$K_1 = f(x_0,y_0) \qquad (2\ 44)$$
$$K_2 = f(x_0 + h/2,\ y_0 + hK_1/2) \qquad (2\ 45)$$
$$K_3 = f(x_0 + h/2,\ y_0 + hK_2/2) \qquad (2\ 46)$$
$$K_4 = f(x_0 + h,\ y_0 + hK_3) \qquad (2\ 47)$$

The Runge Kutta algorithm does not require calculation of the higher derivatives of x as is indicated in the Taylor series method Instead, the algorithm utilizes the computation of $f(x,u)$ at various points Also since the fourth order numerical integration method incorporates the first four derivatives of the Taylor series the truncation error is of the order h^5

2 4 2 Simulation Program Structure

Figure 2 3 shows the outline flowchart for the simulation program The Runge Kutta routine is called periodically from the main C program at times determined by the integration interval An integration interval of 0 005 (18sec) hours was used

and the value of each state was printed out to a data file at periods of 0 1 hours The twenty hour run time of the simulation was typical of a real system Figure 2 4 and Figure 2 5 outline the structure of the two main functions in the simulation program

2.5 SUMMARY

In this chapter the basic fundamentals of a fermentation system were outlined A comprehensive model for a fed batch bakers yeast fermentation was then presented The modelling section was divided into two stages

Modelling of kinetics

Modelling of transport

The Runge-Kutta numerical integration technique used to simulate the model on a digital computer were then presented complete with the structue of the simulation program This model structure and simulation studies defined the starting point and basis for the development of the self tuning control strategy to be applied to the bioreactor

CHAPTER 3

PARAMAMETERIZATION AND IDENTIFICATION OF THE FERMENTATION PROCESS

3 1 INTRODUCTION

Self–tuning controller may be divided into two types, implicit and explicit The implicit self tuner schemes incorporate the controller parameters into the identification procedure thus removing the requirement to identify the plant seperately The explicit self tuning controller used in this research exhibits the following two features,

1 . A parameter estimator that monitors the inputs and outputs of the fermentation process and hence computes dynamic estimates of the process in terms of a set of parameters in a predefined mathematical description of the process Models for such an exercise will be presented in this section.

2 A control design algonthm that accepts data from the parameter estimator to calculate the required control signal using a control law This will be presented in chapter five

Most parameter identification techniques have had their greatest sucess with linear systems Biological systems are inherently non–linear and in the presence of such non–linearities the process equations must be structured in a suitable linear form for use in a parameter identification proceedure Processes which are non–linear and time variant may therefore be sucessfully controlled most notably because of the the self tuning controller's ability to track time varying parameters

A key factor in the self–tuner is the structuring of the model used by the parameter estimator Based on the various models for the specific growth rate μ

outlined in Chapter 2 different identification models will be presented ranging from a simple model which has no structure on growth rate μ to a comprehensive structure which incorporates ethanol and dissolved oxygen terms in the expression for growth rate

3.2 LEAST SQUARES IDENTIFICATION

The goal in process identification is to infer a model (and estimates of the model parameters) given a process input/output data record This activity can be carried out in an "off-line" manner, in which all data is analysed at once (Classical Least Squares), or by using "on-line" techniques where the addition of a new data point is employed to update the model parameters (Recursive Least Squares) In self tuning control sequential updating of the model parameters is more appropiate than non-sequential processing of the input-output data Algorithms which are suited to real time usage and are based on sucessive updating of the model parameters are called "recursive" There are a large number of recursive identification algorithms described in the literature [23,24], the most popular of which is Recursive Least Squares (RLS)

3.2.1 Recursive Least Squares

If we consider a dynamical system with input sysytem u(t) and output signal y(t) Suppose that these signals are sampled in discrete time at t=1,2,3 and that the sampled data values can be related through the following linear difference equation,

$$y(t) + a_1 y(t-1) + \ + a_n y(t-n) = b_1 u(t-1) + \ + b_m u(t-1) \qquad (3\ 1)$$

This may be written in the form

$$y(t) = \theta^T(t)\ \Phi(t) \qquad (3\ 2)$$

where $\Phi(t)$ and $\Theta(t)$ are the regressor and parameter vectors respectively,

$$\theta^T(t) = \{ a_1 \quad a_n \quad b_1 \quad b_m \} \tag{3 3}$$

$$\phi^T(t) = \{ -y(t-1), \quad -y(t-n) \quad u(t-1), \quad u(t-m) \} \tag{3 4}$$

One way to obtain estimates of $\Theta(t)$ is to try and minimise the prediction error using the following criterion and minimising with respect to $\Theta(t)$

$$J_N(\theta) = \sum_{t=1}^{N} [y(t) - \theta^T(t)\Phi(t)]^2 \tag{3 5}$$

Minimisation of J_N w r t Θ gives the estimate of Θ as,

$$\theta(N) = \left[\sum_{t=1}^{N} \Phi(t)\Phi^T(t) \right]^{-1} \sum_{t=1}^{N} \Phi(t)y(t) \tag{3 6}$$

For real time applications it is possible to rewrite (3 6) in a recursive fashion as

$$\theta(t) = \theta(t-1) + L(t)[y(t) - \theta^T(t-1)\Phi(t)] \tag{3 7}$$

$$L(t) = \frac{P(t-1)\Phi(t)}{1 + \Phi(t)P(t-1)\Phi(t)} \tag{3 8}$$

$$P(t) = P(t-1) - \frac{P(t-1)\Phi(t)\Phi^T(t)P(t-1)}{1 + \Phi^T(t)P(t-1)\Phi(t)} \tag{3 9}$$

3 3 2 RLS for Time Varying Systems

The RLS algorithm can be modified to maintain its sensitivity to process parameter variations This may be done by introducing an exponential weighting factor, called a forgetting factor [25,Ch 13], in the performance index,

$$J_N(\theta) = \sum_{t=1}^{N} \lambda^{N-t} [y(t) - \theta^T(t)\Phi(t)]^2 \tag{3 10}$$

where λ is the exponential forgetting factor, $0 < \lambda \leq 1$ The forgetting factor is a measure of how fast old data is forgotten For $\lambda < 1$, more weight is placed on recent measurements than on older measurments The following modified RLS for time varying systems results,

$$\theta(t) = \theta(t-1) + L(t)[y(t) - \theta^T(t-1)\Phi(t)] \qquad (3\ 11)$$

$$L(t) = \frac{P(t-1)\varphi(t)}{\lambda + \Phi(t)P(t-1)\Phi(t)} \qquad (3\ 12)$$

$$P(t) = \frac{1}{\lambda}\left[P(t-1) - \frac{P(t-1)\varphi(t)\varphi^T(t)P(t-1)}{1 + \Phi^T(t)P(t-1)\Phi(t)} \right] \qquad (3\ 13)$$

In the simulation results that follow a variable forgetting factor approach is sometimes taken based on the nature of the expected parameter variations [26] The exponential forgetting factor $\lambda=\lambda^{N-t}$ where N is the total number of data points and t the current data or iteration point is commonly used

Much of the theory on self tuning control is based on the requirement of "persistent excitation" Parameter estimation will be sucessful only when the energy level of the input , both in amplitude and in spectral content, is above a certain threshold For a fed batch process Lozano [27] has shown that a pseudo random binary sequence (PRBS) with magnitude equal to 10% of the input feed concentration added to the feed concentration satisfies thie above condition.

Also in the simulation, a suitable choice of the initial covariance matrix P(0) must be made For P(0), a diagonal matrix with large elements (e g 10^4 or larger) implies that the users confidence in the initial set of parameter estimates is poor, while small values fotr the diagonal elements implies good initial estimates In the simulation results presented a large value of P(0) is chosen (10^3) that will initially cause rapid changes in the parameter estimates via equations (3 11) and and (3 12)

3 3 IDENTIFICATION MODELS

This section covers the topics of model selection and the parameterization of these models It is assumed that measurements of the various states of biomass, substrate, dissolved oxygen and ethanol are available where applicable

3 3 1 Unstructured model

If we reproduce equations (2 2) and (2 6) which describe the rate of change of biomass and substrate in a fed batch fermentor and impose no predefined structure on μ the growth rate

$$\frac{dX}{dt} = (\mu(t) - D(t))X(t) \qquad (2\ 2)$$

$$\frac{dS}{dt} = -\frac{\mu(t).X(t)}{Yx\ s} + D(t)[S_1(t)-S(t)] \qquad (2\ 6)$$

$$\mu(t)= \mu \qquad (3\ 14)$$

A discrete time model can be obtained by a first order Euler approximation of the derivative as

$$\frac{dX(t)}{dt} = \frac{X(t)-X(t-1)}{h} \qquad (3\ 15)$$

where X(t) denotes the biomass concentration and h is the sampling period All identification models presented use a Euler approximation for discretization. Identification models based on a fourth order Runge–Kutta dicretization methods proved too complex for practical use

Substituting eqt (3 15) into (3 12) and (3 13) gives

$$X(t) = X(t-1) + h\mu X(t-1) - hD(t-1)X(t-1) \qquad (3\ 16)$$

$$S(t) = S(t-1) + hD(t-1)[S_1(t)-S(t)] - \frac{\mu(t-1)X(t-1)}{Y_{X\ S}} \qquad (3\ 17)$$

To use recursive least squares type identification algorithms we must first obtain expressions for the system which are linear in the parameters This sset of equations for all the models to be outlined will consist of a known measurement vectors y(t), a known regressor $\Phi(t)$ and an unknown parameter vector $\Theta(t)$ It is the function of the RLS routine to identify the elements of the parameter vector given a set of process input and output measurments

Thus equation (3 16) may be written as,

$$y(t) = \theta^T(t)\ \Phi(t) \qquad (3\ 18)$$

where

$$y(t) = \{\ X(t)-X(t-1)+hD(t-1)X(t-1)\ \} \qquad (3\ 19)$$

$$\Phi^T(t) = \{\ hX(t-1)\ \} \qquad (3\ 20)$$

$$\theta^T(t) = \{\ \mu\ \} \qquad (3\ 21)$$

Similarly, by discretization of (3 17) the parameter $Y_{X\,S}$ may be identified,

$$Y_{X\ S}[S(t-1)-S(t)-hD(t-1)S_1(t-1)-hD(t-1)S(t-1)] = h\mu(t-1)X(t-1) \qquad (3\ 22)$$

Substitution of eqt (3 16) into the rhs of (3 17) gives a direct estimate of the yield coefficient $Y_{X\,S}$

$$Y_{X\ S} = \frac{[X(t)-X(t-1)-hD(t-1)X(t-1)]}{[S(t-1)-S(t)-hD(t-1)S_1(t-1)-hD(t-1)S(t-1)]} \qquad (3\ 23)$$

The expression for the identification of the parameter $Y_{X\,S}$ shows it to be independent of the model of the growth structure This may also be represented in the same least squares format as before,

$$y(t) = \theta^T(t)\ \Phi(t) \qquad (3\ 24)$$

where

$$y(t) = \{\ X(t)-X(t-1)-hD(t-1)X(t-1)\ \} \qquad (3\ 25)$$

$$\Phi^T(t) = \{\ S(t-1)-S(t)-hD(t-1)S_1(t-1)-hD(t-1)S(t-1)\ \} \qquad (3\ 26)$$

$$\theta^T(t) = \{\ Y_{X\ S}\ \} \qquad (3\ 27)$$

3 3 2 Monod Model

For this second model we impose the following Monod-like structure on the growth rate,

$$\mu(t) = \frac{\mu_{max}\ S(t)}{k_S+S(t)} \qquad (3\ 28)$$

Using a similiar procedure as before, the discretized equations for biomass and substrate become,

$$X(t) = X(t-1) + \frac{h\mu S(t-1)X(t-1)}{k_S+S(t-1)} - hD(t-1)X(t-1) \qquad (3\ 29)$$

$$S(t) = S(t-1) + hD(t-1)[S_1(t)-S(t)] - \frac{h\mu_{max}S(t-1)X(t-1)}{Y_{X\ S}[k_{S+}S(t-1)]} \qquad (3\ 30)$$

The recursive least squares structure for (3 29) is,

$$y(t) = \theta^T(t)\ \Phi(t) \qquad (3\ 31)$$

where

$$y(t) = \{\ X(t)-X(t-1)+hD(t-1)X(t-1)\ \}S(t-1) \qquad (3\ 32)$$

$$\Phi^T(t) = \{\ hS(t-1)x(t-1),\ X(t-1)-X(t)-hD(t-1)X(t-1)\ \} \qquad (3\ 33)$$

$$\theta^T(t) = \{ \mu_{max}, k_S \} \qquad (3\ 34)$$

The derivation of a direct estimate or least squares estimate of $Y_{X\,S}$ follows the same procedure as outlined in Section 3 3 1 does not differ from (3 23) or (3 24)–(3 27)

3 3 3 Ollson Model

A third identification model may be derived from imposing an Ollson like structure on the growth rate μ

$$\mu(t) = \frac{u_m\ S(t)}{k_S+S(t)} \quad \frac{O(t)}{k_{O2}+O(t)} \qquad (3\ 35)$$

The discretized equations for biomass and substrate become,

$$X(t) = X(t-1)+ \frac{h\mu_{max}S(t-1)O(t-1)X(t-1)}{[k_S+S(t-1)][k_{O2}+O(t-1)]} - hD(t-1)X(t-1) \qquad (3\ 36)$$

$$S(t)= S(t-1)+ hD(t-1)[S_1(t)-S(t)] - \frac{h\mu_{max}S(t-1)X(t-1)O(t-1)}{Y_{X\,S}[k_{S+}S(t-1)][k_{O2}+O(t-1)]} \qquad (3\ 37)$$

An RLS structure linear in the parameters gives,

$$y(t)=\theta^T(t)\ \Phi(t) \qquad (3\ 38)$$

where

$$y(t) = \{ X(t)-X(t-1)+hD(t-1)x(t-1) \}O(t-1)S(t-1) \qquad (3\ 39)$$

$$\phi^T(t) = \{\ hX(t-1)S(t-1)O(t-1),\ -O(t-1)\Omega,\ S(t-1)\Omega,\ -\Omega\ \} \quad (3\ 40)$$

$$\theta^T(t) = \{\ \mu_{max},\ k_S,\ k_{02},\ k_S k_{02}\ \} \quad (3\ 41)$$

$$\Omega = \{\ X(t)-X(t-1)+hD(t-1)X(t-1)\ \} \quad (3\ 42)$$

Again the estimate for $Y_{X\,S}$ is as equation (3 23) and (3 24)-(3 27)

3 3 4 Comprehensive Model

Using the comprehensive structure of growth rate μ a fourth identification model is derived

$$\mu(t) = \left(\frac{\mu_{max}\ S(t)}{k_S+S(t)} + \frac{\upsilon_{max}\ E(t)}{k_e+E(t)} \right) \frac{O(t)}{k_{02}+O(t)} \quad (3\ 43)$$

The discretized equations for the two main state variables biomass and substrate concentration become,

$$X(t) = X(t-1) + \frac{h\mu_{max}S(t-1)O(t-1)X(t-1)}{[k_S+S(t-1)][k_{02}+O(t-1)]} - hD(t-1)X(t-1) + \frac{h\upsilon_{max}E(t-1)O(t-1)X(t-1)}{[k_e+E(t-1)][k_{02}+O(t-1)]} \quad (3\ 44)$$

$$S(t) = S(t-1) + hD(t-1)[S_1(t)-S(t)] - \left[\frac{\mu_{max}S(t-1)}{[k_S+S(t-1)]} + \frac{\upsilon_{max}E(t-1)}{k_e+E(t-1)} \right] \frac{hX(t-1)O(t-1)}{Y_{X\,S}[k_{02}+O(t-1)]} \quad (3\ 45)$$

An RLS structure linear in the parameters may be extracted giving

$$y(t) = \theta^T(t)\ \Phi(t) \qquad (3\ 46)$$

where

$$y(t) = \{\ X(t)-X(t-1)+hD(t-1)x(t-1)\ \}E(t-1)O(t-1)S(t-1) \qquad (3\ 47)$$

$$\begin{aligned}\Phi^T(t) = \{\ & hX(t-1)S(t-1)O(t-1)E(t-1),\ -O(t-1)E(t-1)\Omega,\\ & -E(t-1)S(t-1)\Omega,\ -O(t-1)S(t-1)\Omega,\\ & hS(t-1)O(t-1)X(t-1),\\ & hE(t-1)O(t-1)X(t-1),\ -S(t-1)\Omega,\ -O(t-1)\Omega,\\ & -E(t-1)\Omega,\ -\Omega\ \}\end{aligned} \qquad (3\ 48)$$

and

$$\begin{aligned}\theta^T(t) = \{\ & (\mu_{max}+\upsilon_{max}),\ k_S,\ k_{O2},\ k_e,\ k_e\mu_{max},\ k_S\upsilon_{max},\\ & k_{O2}k_e,\ k_Sk_{O2},\ k_ek_{O2}k_S\ \}\end{aligned} \qquad (3\ 49)$$

$$\Omega = \{\ X(t)-X(t-1)+hD(t-1)X(t-1)\ \} \qquad (3\ 50)$$

In this identification scheme many lumped parameters are identified Identification of parameters k_e and k_S is used to get estimates of μ_{max} from the lumped parameter $k_e\mu_{max}$ and similarly k_S is used to identify $k_{S\mu}$max

Again the estimate for $Y_{X\,S}$ is as eqt (3 23) and (3 24)-(3 27)

3 4 SIMULATION RESULTS

This section will outline identification results for the models presented above with use of the following parameters and inputs,

μ_{max} = 0 3	k_{O2} = 0 0006	$Y_{X\,S}$ = 0 5
k_S = 0 22	k_e = 0 5	υ_{max} = 0 15
$Y_{X\,S}$ = 0 5	D = 0 2	

Table 3 1

In these identification studies a constant forgetting factor refers to simulations in which λ is kept constant (e g λ=0 99) An exponential forgetting factor refers to using $\lambda=\lambda^{N-i}$ where N is the total number of data points and i the current iteration or data point. Fig 3 1 and Fig 3 2 identify a time varying growth. This is equivalent to tracking the unstructured growth rate in Section 3 3 1 Results are presented which compare the tracking properties of a constant forgetting factor (Fig 3 1) and exponential forgetting factor (Fig 3 2) Both of the above simulations try to identify an overall growth rate from a Monod simulation in which the k_S parameter has been changed to a value of 5 to increase the overall time variance of μ

Fig 3 3 presents the results for the identification of the Monod parameters of Section 3 3 2 The results again compare the convergence properties of the constant (Fig 3 3) and exponential (Fig 3 4) forgetting factor The yield parameter $Y_{X S}$ is estimated using the direct estimate of equation (3 23)

The convergence of Ollson model parameters are shown in Fig 3 5a and 3 5b The convergence is aided by an exponential forgetting factor Fig 3 5a is scaled to show two of the Ollson parameters, μ_{max} and k_S while Fig 3 5b shows the k_{O_2} parameter and the lumped parameter $k_S k_{O_2}$ Table 3 2 compares actual and identified parameters

parameter	actual value	estimated value
μ_{max}	0 3	0 3
k_S	0 22	0 22
k_{O_2}	0 0006	0 00598
$k_S k_{O_2}$	1 32x10^{-4}	1 44x10^{-4}

Table 3 2

The identification of the parameters of the comprehensive model of Section 3.3.4 is shown in Fig 3.6a and 3.6b. Fig 3.6a is scaled to show the following parameters, $\mu_{max}+\upsilon_{max}$, k_s, k_e, $k_e\mu_{max}$ and k_sk_e while Fig 3.6b shows the remaining parameters of equation (3.49).

parameter	actual value	estimated value
$\mu_{max}+\upsilon_{max}$	0.45	0.45
k_s	0.22	0.2198
k_e	0.50	0.4979
$k_e\mu_{max}$	0.15	0.1491
k_sk_e	0.11	0.1105
k_{o_2}	0.0006	0.0059
$k_s\upsilon_{max}$	0.0330	0.0329
$k_{o_2}k_e$	0.0003	0.00038
$k_{o_2}k_s$	1.32×10^{-4}	2.9×10^{-4}
$k_ek_{o_2}k_s$	6.6×10^{-5}	2.21×10^{-4}

Table 3.4

3.5 DISCUSSION

It is obvious that the popular estimation technique of recursive least squares will exhibit good convergence when properly applied. Based on the results presented above there are several conclusions that can be drawn about the the features of a sucessful estimation scheme for a fermentation system.

It has been shown in the literature [6] many times that the tracking of time varying parameters requires the use of a variable forgetting factor. A comparsion of the convergence properties of Fig 3.1 and Fig 3.2 shows a marked improvement with the use of a variable forgetting factor over that of a constant forgetting factor for tracking the time varying specific growth rate μ. The effect of the forgetting factor can be seen from equation (3.13),

$$P(t) = \frac{1}{\lambda}\left[P(t-1) - \frac{P(t-1)\varphi(t)\varphi^T(t)P(t-1)}{1+\Phi^T(t)P(t-1)\Phi(t)}\right] \qquad (3.13)$$

The forgetting factor λ, prevents the elements of P from becoming too small. This

maintains the sensitivity of the RLS algorithm and allows new data to continue to effect the parameter estimates

The convergence of the Monod parameters are presented in Fig 3 3 and Fig 3 4 Again the use of an exponential forgetting factor improves parameter convergence (Fig 3 4) over that of a constant forgetting factor

The Ollson parameters of Fig 3 5a and 3 5b show that two of the parameters (μ_{max} and k_S) converge while the parameters k_{O_2} and $k_{O_2} k_S$ although they converge have very small values Only in a self tuning environment could the controller sensitivity to these parameters be tested

The Comprehensive Model parameters shown in Fig 3 6a and Fig 3 6b show six significant parameters $\mu_{max}+\upsilon_{max}$, k_S, k_e, $k_e\mu_{max}$, k_sk_e and $k_S\upsilon_{max}$ (Fig3 6a) with the rest converging to their respective values in Fig 3 6b-d Both the Ollson and Comprehensive structures utilise an exponential forgetting factor It remains to be seen if the Comprehensive growth rate structure was used as part of an identification scheme in a self tuning controller whether the controller performance would be adversely affected by neglecting some or all of the small parameter values

3.5 SUMMARY

Chapter 3 has outlined various model structures that may be used in the identification of fermentation systems Four models have been presented and their respective simulation results show good parameter identification The type of model structure chosen for the parameter estimation algorithm will ultimately depend on the type of fermentation run in operation. The presentation of the various models attempts to cover all metabolic pathways that yeast can take during the process of fermentation

CHAPTER 4

STATE ESTIMATION TECHNIQUES FOR BIOREACTORS

4 1 INTRODUCTION

It will be instructive to define at the outset of this chapter several terms which will be used repeatedly in the context of estimation techniques in a bioreactor system It should be recognised at this point that besides temperature and pH which are always among the *state variables,* the other components of the state vector depend on the nature of the model of the biological system considered In fermentation systems one is mainly interested in biomass and substrate concentration and also the level of dissolved oxygen concentration because it affects the rate of microbial growth *Culture parameters* or *growth parameters* are the parameters that describe the state of growth of micro-organisms, such parameters then will be the specific growth rate μ, the various yields, Y, and the mass transfer rates of O_2 and CO_2 in the liquid phase and others

The importance of on-line estimation may be seen in the fact that presently the majority of fermentation processes are interfaced with various types of instruments for exhaust gas analysis Such instruments are becoming an integral part of standard bioreactor instrumentation With the introduction of computers mainly for data acquisition and logging a few measurements are recorded as received and occasionaly some additional parameters (respiratory quotient) requiring simple calculations are included in the computer printout of the process The main point of the estimation studies to be presented is that there is a great deal of additional information that may be obtained from the available measurements This information,primarily in the form of estimated state variables and culture parameters, requires little additional effort and can be employed on-line in the systems that already employ dedicated computing capabilities Important information

such as the level of cell biomass, specific growth rates, yields and concentration of products may be obtained at various operating points and as complexity increases additional correlations may be introduced to provide for indeterminable parameters

Needless to say the on–line estimation of various states and parameters facilitates greatly the study of the performance of a microbial culture Not only does it provide for an extended array of parameters that can be monitored, thus describing more completely the biolgical process, but it also yields information at short sampling intervals compared to the process dynamics, thus eliminating the uncertainityand speculation about the events that took place between two consecutive samples Finally, the filtering of measurements, which is part of the estimation process, eliminates any random noises and yields smooth reliable estimates

The primary variable that is desirable to control in a fermentation process is cell growth Thus, it is necessary to be able to both measure this variable or alternatively measure the cell concentration, from which cell growth rate can be determined However, no reliable or accurate instrumentation is available which allows direct on–line measurement of these variables

In spite of recent developments in optical, ion selective and enzyme sensors most of the concentration variables in the fermenter liquid phase cannot be measured on-line Sensors measuring the biomass and substrate concentrations would be most advantageous but as yet there are no such comercially available sensors suitable for industrial applications The monitoring of physiological and biochemical parameters in fermentation processes has not significantly advanced and almost universally pH, dissolved oxygen and redox potential are the only states that can be monitored for control puroposes [28] More recently, the monitoring of dissolved carbon dioxide and the exploitation of developments in lower cost mass spectrometry to replace and extend infrared gas phase monitoring [29], has received

attention Today's measurement technology covers only a small fraction of the desirable information needed to improve microbial growth and production Maintaining maximum production is difficult because of unpredictable changes in process parameters in batch and fed-batch fermentation and lack of on-line information concerning the process states

With digital set-point control gaining popularity and increasing use of digital computers, for example in programmed start up procedures, automated variations of set points to implement optimal policies and also predetermined response to various pertubation, clearly the determination of a new set point will rely on accurate knowledge of the bioreactor state and state estimates will be indispensible for this purpose Some methods use differential equations expressing the time rate of change of state variables as a function of the operating and culture parameters to give a structured self contained set of equations while other techniques are more model independent. The presentation of various general frameworks which achieve the state estimation objective by utilizing various macroscopic and elemental balances and appropriate estimation techniques will be the subject of the following chapter

4.2 OBSERVERVABILITY OF A NON-LINEAR SYSTEM

In linear control theory there are methods for the design of observers which converge exponentially to true state values [30,Ch 9] For non-linear systems , there are very few works dealing with this subject and the applications are not numerous For a fermenter system Monod-type formulas are widely used to describe cell growth limited by a single substrate The model equations are,

$$\dot{X} = (\mu - D)X \qquad (4\ 1)$$

$$\dot{S} = D[S_1 - S] - \frac{\mu X}{Y_{X\ S}} \qquad (4\ 2)$$

$$\mu = \frac{\mu_m S}{k_S + S} \qquad (4\ 3)$$

where X and S are the biomass and substrate concentration respectively, D is the dilution rate, S_1 is the feed substrate concentration and μ_m, $Y_{X\,S}$, and k_S are characterstic parameters of the process

A system is observable if, for each pair of initial states $x_1(0)$, $x_2(0)$, we can find an input variable $u(t)$ such that x_1, x_2, are distinguishable by observations of the corresponding output variables $y_1(t)$ and $y_2(t)$ There are some works dealing with theoretical aspects of observers for non–linear systems and we firstly present a theorem about the observervability of non-linear systems The theorem presented by Gallegos [31] is an extension af a lemma given by Willamson [32] and deals with the observablity of a nonlinear system

Theorem

A necessary and sufficient condition for the system

$$\mathbf{x} = \mathbf{f}(\mathbf{x}) + \sum_{i=1}^{m} \mathbf{g}_i(\mathbf{x})\, u_i, \qquad \mathbf{u}=(u_1, \ldots, u_m)^T \in \mathbf{R}^m \qquad (4\ 4)$$

$$y = h(\mathbf{x}) \qquad \mathbf{x}\in\mathbf{R}^n,\ y\in\mathbf{R} \qquad (4\ 5)$$

to be completely ,uniformly, locally, observable is that there exists a system of local coordinates on $\mathbf{R}^n$ such that (4 4) is of the form

$$\mathbf{x} = \begin{bmatrix} x_1 \\ \vdots \\ x_n \\ F(x) \end{bmatrix} + \sum_{i=1}^{m} \begin{bmatrix} g_{1\,1}(x_1) \\ g_{1\,2}(x_1, x_2) \\ \vdots \\ g_{1n}(x_1, \ldots, x_n) \end{bmatrix} u_1 \qquad (4\ 6)$$

$$y = x_1 \qquad (4\ 7)$$

From (4 6) and (4 7), it is possible to estimate the state vector through successive derivatives of the output and input variables This theorem will be applied to a fermentation system in the following section

4 3 STATE ESTIMATION

The central control objective of any bioreactor is to provide optimal growth conditions for biomasss growth. General variables such as temperature and pH can be sucessfully controlled by conventional loops However, other important process variables such as biomass, product and substrate utilization are rarely measured on–line These important process variables can be estimated using available standard measurements in conjuction with mathematical relationships Frequently, the parameters of the system must be determined before the predictions of the model become available for design or control purposes Their values can be determined from correlations, simple experiments or linear regression ideas as outlined in the Chapter 3 The joint development of modern control theory and microprocessors has seen the introduction of techniques, such as Kalman filtering which may be organised for parameter and state estimation. In order to determine whether a system is performing properly and ultimately to control the system performence the designer must know the states of the system The technique of determining the states of a system from noisy measurements of states (auxiliary or otherwise) is called Kalman filtering

Stephanopoulos and San [35] utilize measurements of O_2 and CO_2 in the gas stream and employ proper macroscopic material and elemental balances to measure the total growth rate and yield With these measurements available an extended Kalman Filter is employed to produce estimates of the state variables Dekkers [36] outlines an indirect estimation method for on–line determination of the biomass concentration, the specific growth rate, the substrate utilization rate and the ethanol concentrationof a fed batch bakers yeast fermentation. Dekkers derives a measurement model from stochiometric considerations These equations and a simple state model for the biomass and the biomass production rate are used in an extended Kalman filter for estimation of the process variables

In this section three types of algorithms for the estimation of state variables such as substrate and biomass will be outlined Two non-adaptive algorithms for state estimation are presented [33,34] In section 4 4 adaptive algorithms will be presented The word "adaptive" is used for state estimation schemes since the algorithms are designed to continuously adapt the structure of the observer to the variations of the growth parameters The general estimation problem and its associated theory will then be outlined with particular reference to the application of a Kalman filter to the state estimation problem in a fermentation process

4 3 1 Non-linear Observer

In this section we will make use of the theorem in Section 4 2 to estimate the state vector of the model equations of the fermentor Equations (4 1)-(4 3) have the form given by (4 6) and (4 7) with,

$$f(x)=\begin{bmatrix} \mu x \\ -\frac{\mu x}{Y_{x\,s}} \end{bmatrix}, \quad g_1(x)=\begin{bmatrix} -x \\ \\ -s \end{bmatrix}, \quad g_2(x)=\begin{bmatrix} 0 \\ \\ 1 \end{bmatrix} \qquad (4\ 8)$$

and $u_1=D$, $u_2=DS_1$ The system is therefore observable and the fermentation model may be expressed as the following model,

$$\begin{bmatrix} z_1 \\ \\ z_1 \end{bmatrix} = \begin{bmatrix} z_2 \\ \\ F(z) \end{bmatrix} + \begin{bmatrix} g_{11}(z_1) \\ \\ g_{12}(z_1,z_2) \end{bmatrix} u_1 + \begin{bmatrix} g_{21}(z_1) \\ \\ g_{22}(z_1,z_2) \end{bmatrix} u_2 \qquad (4\ 9)$$

$$y = z_1 \qquad (4\ 10)$$

with

$$z_1 = x \qquad (4\ 11)$$

$$z_2 = \mu x \qquad (4\ 12)$$

$$g_{11}(z_1) = -z_1 \qquad (4\ 13)$$

$$g_{12}(z_1,z_2) = z_2 \left(\frac{z_2}{\mu_m z_1} - 2\right) \qquad (4\ 14)$$

$$g_{21}(z_1) = 0 \qquad (4\ 15)$$

$$g_{22}(z_1, z_2) = \frac{(\mu_m z_1 - z_2)^2}{\mu_m k_S z_1} \qquad (4\ 16)$$

$$F(z) = \frac{z_1}{z_2}\left[z_2 - \frac{(\mu_m z_1 - z_2)^2}{\mu_m k_S Y_{X\ S}} \right] \qquad (4\ 17)$$

From equtation (4 9) it is possible to estimate the state vector since,

$$z_2 = z_1 - g_{11}(z_{11})D = y + Dy \qquad (4\ 18)$$

In this way, if the biomass concentration x is measured (unfortunately Gallegos [31] makes this restrictive assumption), it will only be necessary to estimate the substrate concentration S The following estimate for S results,

$$\hat{S} = \frac{k_S z_2}{\mu_m z_1 - z_2} \qquad (4\ 19)$$

From equation (4 9) we see the need for having the derivative of the process output However using an Euler approximation we may write,

$$\dot{y}(t) \approx \frac{y(t) - y(t-T)}{T} \qquad (4\ 20)$$

with T small compared to the process dynamics From (4 11) we have in discrete form

$$\hat{S}(k) = \frac{k_S a\ [y(k) - y(k-1) + TDy(k)]}{\mu_m y(k) - a(\ y(k) - y(k-1) + TDy(k)\ )} \qquad (4\ 21)$$

where a=1/T

4.3.2 Non-adaptive Observer

When the substrate concentration S(t) (or biomass concentration X(t)) is measured on-line and the yield coefficient is known a simple algorithm can be implemented to estimate X(t) (or S(t)) If we rewrite the model equations (4.1-4.3) and let k_1 be the yield coefficient.

$$\dot{X} = (\mu - D)X \qquad (4.1)$$

$$\dot{S} = D[S_1 - S] - k_1 \mu X \qquad (4.4)$$

$$\mu = \frac{\mu_m S}{k_S + S} \qquad (4.3)$$

The basic derivation of the estimation algorithm is based on the fact that in microbial growth, the rate of biomass production is proportional to the rate of substrate consumption Assuming that X(t) is available for on-line measurement an auxiliary state variable Z(t) is defined by the following equation,

$$\frac{dZ(t)}{dt} = D(t)[S_1(t) - Z(t)] \qquad (4.22)$$

The motivation for the introduction of Z(t) may be seen from the fact that if we define $Y = k_1 X$, then from (4.1-4.3),

$$\frac{d[Y(t)+S(t)]}{dt} = D(t)[S_1(t) - (Y(t)+S(t))] \qquad (4.23)$$

Comparing (4.15) and (4.16), Z(t) can obviously be considered as an on-line estimate of Y(t) + S(t), with an estimation error

$$\epsilon(t) = Z(t) - [Y(t) - S(t)] \qquad (4.24)$$

governed by the stable dynamic equation

$$\frac{d\epsilon(t)}{dt} = -D(t)\epsilon(t) \qquad (4.25)$$

The above algorithm is stable as $D \geq 0$ and on-line estimate of S(t) can now be

computed as

$$S(t) = Z(t) - k_1 X(t) \qquad (4\ 26)$$

A simple discrete time version of this algorithm has been derived by using a first order Euler approximation for dZ/dt.

$$Z(k+1) = Z(k) + TD(k)[S_1(k) - Z(k)] \qquad (4\ 27)$$

$$\hat{S}(k) = Z(k) - k_1 X(k) \qquad (4\ 28)$$

where k is the time index and T is the sampling period

4 3 3 Extended Kalman Filter

A brief presentation of the basic features of the general state estimation problem is outlined below A linear system is first considered because exact solutions are available for such systems The non–linear case is then discussed

In a biochemical reactor system, as is often the case with state estimation problems, the state of the system is not directly measurable but is observable through the measurement of outputs of the system, such as exhaust gas concentrations If the state x of a dynamical system satisfies the linear equation of (4 29) then the state estimation problem can generally be stated as follows,

$$x = Ax + Bu + \zeta(t) \qquad (4\ 29)$$

The linear equation is forced by the non–random control input u and the random disturbance $\zeta(t)$ One must develop an algorithm for determining the state x(t) at time t from the observations of an output y(t) of the system, contaminated by the random errors $\xi(t)$ and related to the state x by,

$$y = Hx + \xi(t) \qquad (4\ 30)$$

Because of the errors ξ in the measurement, x, the true state cannot be found - only an estimate for x is possible Therefore in the presence of the random noises $\zeta(t)$ and $\xi(t)$ the estimation problem is understood in the sense of finding an estimate of the state x such that the uncertainty, or variance, of the estimation error is minimised [37,Ch 5] If the noises $\zeta(t)$ and $\xi(t)$ can be modelled by a white noise process then the estimate x can be found as the solution of the following filter equation,

$$\hat{x} = A\hat{x} + Bu + K[y - H\hat{x}] \qquad (4\ 31)$$

with K, the filter gain given by,

$$K = PH^{T}R^{-1} \qquad (4\ 32)$$

and the variance of the estimation error (a measure of the uncertainty in the estimate of x), $P = E[(x-x)(x-x)^{T}]$, given by

$$P = AP + PA^{T} + Q - PH^{T}R^{-1}HP \qquad (4\ 33)$$

The matrices Q and R (positive semi-definite) are measures of the intensity of the noises ξ and ζ, respectively with $Q\delta(t) = E[\zeta(t)\zeta^{T}(t)]$ and $R\delta(t) = E[\xi(t)\xi^{T}(t)]$

The above equations describe the evolution of the estimate of x and its variance P with time for a linear system Most systems of practical interest , however, are non–linear and of the general form,

$$x = f(x) + \zeta(t) \qquad y = h(x) + \xi(t) \qquad (4\ 34)$$

For such systems, a variety of filtering algorithms have been devised, one of which is the Kalman filter, obtained by linearzing the non–linear equations around the current estimate and applying (4 1-4 5) to the linearized equations,

$$\hat{\dot{x}} = f(\hat{x}) + K[y - h(\hat{x})] \qquad (4\ 35)$$

$$K = Ph^{T}(\hat{x})R^{-1} \qquad (4\ 36)$$

$$\dot{P} = f(\hat{x})P + Pf^{T}(\hat{x}) + Q - Ph^{T}(\hat{x})R^{-1}h(\hat{x})P \qquad (4\ 37)$$

The above equations apply to the case when the measurements are taken continuously in time If we consider a continuous non–linear stochastic model of micro-organism growth and substrate consumption dynamics in a batch fermentation process and output model that consists of measurement of the *carbon dioxide evolution rate*,

$$\dot{x}(t) = F(x(t)) + \zeta(t) \qquad (4\ 38)$$

$$y(t) = H(x(t)) + \xi(t) \qquad (4\ 39)$$

where x(t) is the state vector consisting of biomass (x_1) and substrate concentrations (x_2) and the components of F(x) are,

$$f_1(x(t)) = \frac{\mu_m\, x_1\, x_2}{k_S + x_2} \qquad (4\ 40)$$

$$f_2(x(t)) = \frac{\mu_m\, x_1\, x_2}{Y_{X\,S}(k_S + x_2)} \qquad (4\ 41)$$

y(t) is the *carbon dioxide evolution rate* which is related to the state vector by the non-linear function H(x(t)) where,

$$H(x(t)) = \frac{1}{Y_{X\,C}} \frac{\mu_{max}\, x_1\, x_2}{k_S + x_2} \qquad (4\ 42)$$

where $Y_{X\,C}$ is yield of carbon dioxide on biomass

In our model equations (4 9-4 10) state and measurement noise with covariance

$$E[\zeta(t)\zeta(t)^T] = Q\delta_{ij} \qquad (4\ 43)$$

$$\delta_{ij} = 1 \text{ for } i = j$$

$$0 \text{ for } i \neq j$$

and

$$E[\xi(t)\xi(t)^T] = R\delta_{ij} \qquad (4\ 44)$$

The initial state of the model is to be assumed normally distributed stochastic variable with mean $E[x(o)] = \hat{x}(o)$

and covariance

$$E[x(o) - \hat{x}(o))(x(o) - \hat{x}(o))^T] = P \qquad (4\ 45)$$

Since the state vector x(t) is unmeasurable on–line and in the presence of state and observation noise the problem posed is how to find an on–line estimation algorithm based on available measurement of carbon dioxide evolution rate The extendedKalman filter application is presented as a technique for on–line estimation of state variables based on the model process equations (4 38-4 45) The configuration of such an estimation scheme is shown in Figure 4 1

Applying a simple Euler approximation to the above continuous model, we can derive the following discrete non–linear stochastic model of micro–organism growth and substrate consumption for the batch fermentation process as

$$x(k+1) = g(x(k),T) + \zeta(k) \qquad (4\ 46)$$

$$y(k) = H(x(k)) + \xi(k) \qquad (4\ 47)$$

where $g(x(k),T) = x(k) + T\,F(x(k))$ and T is the sampling interval The extended Kalman filter equations may be written as follows

$$\hat{x}(k+1/k+1) = \hat{x}(k+1/k) + K(k+1)[y(k+1) - H\,\hat{x}(k+1/k) \qquad (4\ 48)$$

$$\hat{x}(k+1/k) = g(\hat{x}(k/k),T) \qquad (4\ 49)$$

$$K(k+1) = P^*(k+1)\,H^T\,[HP^*(k+1)H^T + R]^{-1} \qquad (4\ 50)$$

$$P^*(k+1) = \Phi(k)P(k)\Phi(k) + Q \qquad (4\ 51)$$

$$P(k+1) = [I - K(k)H]P^*(k) \qquad (4\ 52)$$

where

$x(k+1/k+1)$ is the optimal state estimate at time k+1

$x(k+1/k)$ is the state estimate at time k+1 based on estimate $x(k/k)$ at time k (prediction)

$y(k+1)$ is the output observation vector

H is the linearized observation matrix

$K(k+1)$ is the Kalman gain matrix.

$K(k+1)[y(k+1) - H\,x(k+1/k)]$ is a correction sequence

P(k) is a symmetric error filtering matrix.

$P^*(k+1)$ is a symmetric error prediction covariance matrix

$\Phi(k)$ is the transition matrix of the linearised model evaluated at time k for estimate $x(k/k)$

Q is the state noise covariance

R is the output noise covariance

The transition matrix $\Phi(k)$ can be obtained by linearization of the non-linear discrete model around estimate $x(k)$, where $\Phi(k) = I + T J_{|x(k)}$ The Jacobian matrix of the model equations is described as,

$$J_{11} = \frac{\delta f_1(x(t))}{\delta x_1(t)}_{|x(k/k)} = \frac{\mu_m x_2(k/k)}{k_S + x_2(k/k)} \qquad (4\ 53)$$

$$J_{12} = \frac{\delta f_1(x(t))}{\delta x_2(t)}_{|x(k/k)} = \frac{k_S \mu_m x_1(k/k)}{[k_S + x_2(k/k)]^2} \qquad (4\ 54)$$

$$J_{21} = \frac{\delta f_2(x(t))}{\delta x_1(t)}_{|x(k/k)} = \frac{-\mu_m x_2(k/k)}{Y_{X\ S}[k_S + x_2(k/k)]} \qquad (4\ 55)$$

$$J_{22} = \frac{\delta f_2(x(t))}{\delta x_1(t)}_{|x(k/k)} = \frac{\mu_m k_S x_1(k/k)}{Y_{X\ S}[k_S + x_2(k/k)]^2} \qquad (4\ 56)$$

and the linearized observation matrix becomes,

$$H_{11} = \frac{\delta H(x(t))}{\delta x_1(t)}\Big|_{x(k/k)} = \frac{\mu_m x_2(k/k)}{Y_{X\,C}[k_S + x_2(k/k)]} \qquad (4\ 57)$$

$$H_{12} = \frac{\delta H(x(t))}{\delta x_2(t)}\Big|_{x(k/k)} = \frac{k_S \mu_m x_1(k/k)}{Y_{X\,C}[k_S + x_2(k/k)]^2} \qquad (4\ 58)$$

4 4 COMBINED STATE AND PARAMETER ESTIMATION

The algorithms presented in Section 4 3 rely on the availibilty of measurements of one or more states and the knowledge of the parameters Algorithms which are configured to allow state *and* parameter estimation are outlined in the following sections

4 4 1 Partially Adaptive Observer

In this section a state estimation algorithm is presented that is referred to as a "partially adaptive observer" We assume that the specific growth rate $\mu(t)$ is the only unknown parameter and that the yield coefficients are known. Considering the problems with availability of reliable on-line sensors for the measurement of substrate and biomass, the case of the estimation of the biomass concentration X(t) from the disolved oxygen concentration O(t) is considered Augmenting eqts (4 1-4 3) to include an equation for the dissolved oxygen concentration we have,

$$\frac{dO(t)}{dt} = k_l a(O(t)^* - O(t)) - \frac{\mu(t).X(t)}{Y_{X\,O}} \qquad (4\ 59)$$

where $k_l a$ is the mass transfer coefficient (hr^{-1}),

$O(t)^*$ is the concentration of oxygen that would exist in

the bulk liquid phase if it were in thermodynamic equilibrium

with the gas phase (g/l),

O(t) is the actual concentration of oxygen in the liquid phase,

Y_{XO} is the yield of biomass on oxygen (g/g)

If we consider a bioreactor described by equations (4.1-4.3) and (4.31) and we assume that the dissolved oxygen concentration O(t) is measured on-line. Then the following adaptive observer can be used to estimate on-line the biomass concentration X(t)

$$\frac{d\hat{O}(t)}{dt} = k_1 a[O(t)^* - O(t)]W(t) - D(t)O(t) - a\hat{R}(t) - bX(t) + C_1[O(t) - \hat{O}(t)] \qquad (4.60)$$

$$\frac{d\hat{X}(t)}{dt} = \hat{R}(t) - D(t)\hat{X}(t) + C_2[O(t) - \hat{O}(t)] \qquad (4.61)$$

$$\frac{d\hat{R}(t)}{dt} = -C_3[O(t) - \hat{O}(t)] \qquad (4.62)$$

where again C_1–C_3 are design parameters which are at the disposal of the user to control the speed of convergence, while a and b fixed constants and R(t) is an on-line estimate of the total growth rate R(t),

$$\hat{R}(t) = \mu(t)\, X(t) \qquad (4.63)$$

4.4.2 Fully Adaptive Observer

In this section a "fully adaptive observer" will be outlined which does not require any prior knowledge of the yield parameters or growth rate μ, that is they will be assumed to be unknown. If we again consider the bioreactor described by (4.1-4.3) and assume that the biomass concentration X(t) is measured on-line. If

we define the auxiliary time varying parameters

$$\theta_1(t) = S(t) - \mu(t) \tag{4 64}$$

$$\theta_2(t) = k_1\mu(t) \tag{4 65}$$

Then the following state space representation is equivalent to (4 1-4 3)

$$\frac{dX(t)}{dt} = -\theta_1(t)X(t) + X(t)S(t) - D(t)X(t) \tag{4 66}$$

$$\frac{dS(t)}{dt} = -\theta_2(t)X(t) + D(t)S_1(t) - D(t)S(t) \tag{4 67}$$

The following fully adaptive observer can be derived from the above to estimate on–line the substrate concentration S(t)

$$\frac{d\hat{X}(t)}{dt} = -\hat{\theta}_1(t)X(t) + X(t)\hat{S}(t) - D(t)X(t) + C_1[X(t) - \hat{X}(t)] \tag{4 68}$$

$$\frac{d\hat{S}(t)}{dt} = -\hat{\theta}_2(t)X(t) - D(t)\hat{S}(t) + D(t)S_1(t) + [C_2 + C_3X(t)V(t)^2][X(t) - \hat{X}(t)] \tag{4 69}$$

$$\frac{dV(t)}{dt} = -D(t)V(t) + X(t) \tag{4 70}$$

$$\frac{d\hat{\theta}_1(t)}{dt} = -C_3X(t)[X(t) - \hat{X}(t)] \tag{4 71}$$

$$\frac{d\hat{\theta}_2(t)}{dt} = -C_3X(t)V(t)[X(t) - \hat{X}(t)] \tag{4 72}$$

where V(t) is an auxiliary filtered value of X(t) and C_1–C_3 are the design parameters These parameters are at the disposal of the user in order to control the speed of convergence [33]

4.5 SIMULATION RESULTS

Simulation results are first presented for the estimation of substrate S(t) using the non-linear observer of Section 4.3.1. As the discrete form of the observer in equation (4.21) uses the Euler method to estimate the rate of change of biomass at the output the effect the changing of the integration interval has on the estimate of substrate is shown in Fig 4.2a-c for h=0.5hr, 0.05hr and 0.025hr. Each simulations use the following paramater values

μ_{max} = 0.8 $Y_{X/S}$ = 0.5 S_i = 90 S(0) = 12.0

k_S = 0.5 D = 0.42 X(0)= 0.3

Table 4.1

It may also be observed that the estimate of substrate in equation (4.20) depends on the process parameters μ_{max} and k_S. However, for fermentation processes, these parameters change frequently and an estimation error will be produced. Fig 4.3 illustrates this problem when from t=5hr to t=5.5hr the parameter μ_{max} is varied 15% about its nominal value.

The non–adaptive observer of Section 4.3.2 exhibits varying degrees of sucess when applied in simulation. Initially the estimation of S(t) was carried out on the same simulated process as indicated by Table 4.1. Results for the estimation of S(t) are shown in Figure 4.4. The convergence of the state estimate was slow and as equation (4.25) relates the rate of convergence of the estimate to the dilution rate it was deemed necessary to vary the input dilution rate, D. Figure 4.5 illustrate the convergence of the estimate for a process with D=0.75hr^{-1} and Fig 4.6 shows the convergence of the estimate for a batch fermentation. In the above simulation the initial value of the auxiliary variable was Z(0)=12.0.

The Extended Kalman Filter outlined in Section 4.3.3 is based on the

available measurement of the carbon dioxide evolution rate (CER) The simulated CER in mol/ℓ hr corrupted by a 10% pseudo randon binary sequence for estimation purposes is shown in Fig 4 7 The filter shows excellent estimates of Biomass in Fig 4 8 and also Substrate in Fig 4 9 when given the correct initial conditions, an initial value of P=0 for the estimate error covarience matrix and a 10% corruption on the CER measurment at each sampling interval However, performance of the filter suffers when incorrect initial conditions are given as is shown for Biomass in Fig 4 10 and for Substrate in Fig 4 11 This is a significant problem because in a real fermentation plants correct initial values of states are seldom available

4 6 DISCUSSION

Some modern techniques have been applied in this chapter to solve the problem of state estimation in a fermentation context. The convergence of the state estimates in the first method of a non–linear observer proves to be very dependent on the sampling interval Fig 4 2a-c shows how the error in the substrate estimate deceases as the sampling rate increases Overall this estimation scheme proves to be "rigid" and unable to cope with paramater variations as shown in Fig 4 3 The non-adaptive schemes would therefore be of little practical use

The non-adaptive observer has a major drawback in that the speed of convergence is completly determined by the experimental conditions through the dilution rate D(t) This leads to poor results especially in batch operations (Fig 4 6) and furtheremore there is a bias on the estimate of S(t) if there is an initial error on Z(t) This technique of state estimation shows better convergence as the dilution rate increases Convergence for a dilution rate of $D=0\,75hr^{-1}$ is shown in Fig 4 5 but such increases in dilution rate have the physical signifance of producing large increases in biomass concentration X(t)

The Extended Kalman Filter proved to be the most sucessful technique of state estimation as shown in Fig 4 8 and Fig 4 9 Unfortunately as with the rest of the estimation schemes it is very sensitive to incorrect initial state estimates and the filter fails to recover from this initial bias as outlined in Fig 4 10 and Fig 4 11 One solution to this may be the use of an iterative Kalman Filter where iterations of the output equations at each sampling interval could help to reduce the estimation error

4 7 SUMMARY

This chapter has attempted to demonstrate how accurate biomass and substrate estimation may take place under standard fermentation conditions The numerical results show that the Extended Kalman Filter give satisfactory results during computer simulation while the non-linear and adaptive observer are two restrictive in their assumptions about the availability of measurements of biomass and substrate Such measurements are not available on line via sensors and this assumption coupled with the fixed parameter approach of the observer leaves such observer ill equipped for on-line usage

CHAPTER 5

SELF TUNING CONTROL OF FERMENTATION PROCESSES

5 1 INTRODUCTION

A variety of control schemes have been applied recently to fermentation systems The techniques involved controlling several process parameters including dissolved oxygen tension, respiratory qoutient, oxygen uptake rate, biomass and temperature In 1975 , Miskiewicz et al [38] described a control system to control the nutrient supply to the system on the basis of dissolved oxygen concentration An alternative scheme, for maintaining dissolved oxygen concentration, is to control the oxygen air or sparge rate and/or agitation speed, Kobayashi et al [39]

The control of respiratory quotient (RQ) has also been a popular approach Aiba et al [40] controlled RQ in the range 1 0 to 1 2 by step changes in the feed rate to prevent substrate acculumation. The control of oxygen uptake rate (OUR) in conjuction with RQ has been proposed by Perigner and Blachere [41] and Raimerez at al [42] The technioque involves step changes in the substrate feed rate dependant on the values of RQ and OUR Woehrer et al [43] utilised both RQ and ethanol to control the glucose medium addition.

The technique of material balancing has been implemented by Cooney et al [44] and Wang et al [45] to estimate biomass and control a bakers yeast fermentation It was also applied to penicillin fermentation in 1982 by Wang [46] The optimal operation of a fed-batch reactor for maximal biomass productivity was presented by Weigand uet al [47] using the maximum principle by manipulation of the substrate feed rate Similiar optimal control strategies have also been described by Constantinidies [48] and by Blanch and Rogers [49] The application of a classical proporotional and integral (P+I) controller and multivariable control

by a non-interacting controller has been described by Takamatsu et al [50]

Although it is generally recognised that the conventional PID regulator is remarkably effective in practice, its initial tuning and the maintenance of good tuning on a plant with many control loops can be a time consuming activity, particulary if the process dynamics are slow The PID regulator really only exhibits good performance for dominant second order plants with fixed parameters Self tuning control is one approach to the automatic tuning problem for a system with time varying parameters As outlined previously a self tuning controller consists of two main elements Firstly, a recursive parameter estimator that computes estimates of plant dynamics in terms of a set of parameters in a structured model and secondly a control design algorithm as outlined in Figure 5 1 The self tuning regulator is very flexible with respect to the design method Self tuners based on pole placement, minimum–varience control and LQG control have been considered [51] Multivariable adaptive/self tuning control of fermentation processes has also been presented by Yousefpour [52] and by Williams [53]

A self tuning regulator based on pole placement via state feedback will be considered in this chapter An algorithm is called self tuning, if, as the number of input and output samples tend to infinity the control signal generated becomes that which would be produced by the corresponding feedback law designed on the basis of known process dynamics - the principle of certainty equivalence Self tuners are performance oriented, whereby, the engineer specifies a desired closed loop performance, despite unknown plant parameters or drift. Compare this to PID where the user specifies coefficients K, T_I, T_d to try to obtain good performance at current plant conditions despite the fact that this control may deteriorate at a later stage if the parameters change

In this chapter we will introduce the the idea of self tuning control as applied to a fermentation process We will first outline the concept of linearization

as we will linearize the non-linear fermentation process for control purposes The controller will be designed using state feedback and we will look at the single input single output (SISO) case followed by the multi input multi output (MIMO) case The parameter estimation algorithm (RLS) and the Extended Kalman Filter will then be introduced into the overall self tuning controller as outlined in Figure 5 2

5.2 PROCESS MODEL

If we reproduce the discretized equations for our two-state fed batch model with a Monod structure on the specific growth rate μ

$$X(k) = X(k-1) + \frac{h\mu S(k-1)X(k-1)}{k_s+S(k-1)} - hD(k-1)X(k-1) \qquad (5\ 1)$$

$$S(k) = S(k-1) + hD(k-1)[S_1(k)-S(k)] - \frac{h\mu_m S(k-1)X(k-1)}{Y_{X\ S}[k_s+S(k-1)]} \qquad (5\ 2)$$

where h is the sampling period in hours

An equivalent discretized non-linear state space representation of the process may be obtained,

$$x(k) = A(k-1)x(k-1) + B(k-1)u(k-1) \qquad (5\ 3)$$

where

$$x(k) = (X(k)\ \ S(k))^T \qquad (5\ 4)$$

$$u(k-1) = D(k-1) \qquad (5\ 5)$$

and the components of the A and B are respectively,

$$a_{11} = 1 + \frac{h\mu_m S(k-1)}{[k_s+S(k-1)]}, \quad a_{12} = 0 \qquad (5\ 6, 5\ 7)$$

$$a_{21} = \frac{-h\mu_m S(k-1)}{Y_{X\,S}[k_{S+}S(k-1)]} \quad , \quad a_{22} = 1 \qquad (5\ 8, 5\ 9)$$

and

$$b_{11} = -hX(k-1) \qquad (5\ 10)$$

$$b_{12} = h(S_1(k)-S(k-1)) \qquad (5\ 11)$$

5 3 PROCESS MODEL LINEARISATION

We will first limit our analysis of the process to obtaining linear dynamics of the system This may seem incompatible with the fact that most of the bioengineering processes are modelled by non-linear equations However, linear techniques are valuable because there is no general theory for the analytical solution of non–linear differential equations and consequently no comprehensive analysisof non-linear dynamic systems Also a non-linear system may be adequately approximated by a linear system near some operating conditions Significant advances in the linear control theory permit the synthesis and design of very effective controllers even for non-linear processes Fundamental, therefore , is the concept of linearization and the procedure for approximating non-linear systems by linear systems

The following equations represent general non–linear and time varying dynamics

$$x(k+1) = f(x(k),u(k),k) \qquad (5\ 12)$$

$$y(k) = g(x(k),u(k),k) \qquad (5\ 13)$$

where

x(k) is the state vector, u(k) is the input vector, y(k) is the the output vector , and the vector functions f and g specify the non-linear systenm dynamics

The first step in the linearization process is to find the equilibrium point(s) of the system when inputs assume their constant or steady values For any system we

say that x_0 is an equilibrium state if it does not change under constant u_0

For discrete time systems, x_0 is the solution of the equation

$$x(k+1)-x(k) = f(x(k),u_0) = 0 \qquad (5\ 14)$$

We can then use Taylor series to expand these equations about the equilibrium point (x_0,u_0), the linear terms of a Taylor series expansion of (5 1) and (5 2) retaining only first order terms are given by,

$$x(k+1) = f(x_0,u_0) + \frac{\delta f}{\delta x|_{x_0,u_0}}(x-x_0) + \frac{\delta f}{\delta u|_{x_0,u_0}}(u-u_0) \qquad (5\ 15)$$

A similiar expansion of (5 13) will yield,

$$y(k+1) = g(x_0,u_0) + \frac{\delta g}{\delta x|_{x_0,u_0}}(x-x_0) + \frac{\delta g}{\delta u|_{x_0,u_0}}(u-u_0) \qquad (5\ 16)$$

If we define the incremental variables $\delta x=x-x_0$, $\delta u=u-u_0$ and $\delta y=y-y_0$, then the resulting linearized equations become,

$$\delta x(k+1) = A^* \delta x(k) + B^* \delta u(k) \qquad (5\ 17)$$

$$\delta y(k) = C^* \delta x(k) + D^* \delta u(k) \qquad (5\ 18)$$

where the matrix,

$$A^* = \frac{\delta f}{\delta x}(x_0,u_0), \qquad B^* = \frac{\delta f(x_0,u_0)}{\delta x} \qquad (5\ 19,5\ 20)$$

$$C^* = \frac{\delta g}{\delta x}(x_0,u_0), \qquad D^* = \frac{\delta g}{\delta x}(x_0,u_0) \qquad (5\ 21,5\ 22)$$

5 3 1 Linearized State Space Mdel- Single-Input Single-Output (SISO)

Using (4 17-4 20) we obtain the following linear variational model for the plant,

$$\delta x(k+1) = A^* \delta x(k) + B^* \delta u(k) \qquad (5\ 25)$$

where

$$\delta x(k) = [x(k)-x_0,\ s(k)-s_0]^T \qquad (5\ 26)$$

$$\delta u(k) = [D(k)-D_0] \qquad (5\ 27)$$

and the components of the A^* and B^* are respectively,

$$a^*_{11} = 1 + \frac{h\mu_m S_0}{[k_S+S_0]} - hD_0 \ , \quad a^*_{12} = \frac{hk_S\mu_m X_0}{[k_S+S_0]^2} \qquad (5\ 28, 5\ 29)$$

$$a^*_{21} = \frac{-h\mu_m S_0}{Y_{X\ S}[k_S+S_0]} \ , \quad a^*_{22} = 1 - \frac{h\mu_m X_0 k_S}{Y_{X\ S}(k_S+S_0)^2} - hD_0 \qquad (5\ 30, 5\ 31)$$

and

$$b^*_{11} = -hX_0 \qquad (5\ 32)$$

$$b^*_{12} = h(S_1(k)-S_0) \qquad (5\ 33)$$

Imposing the conditions expressed in (4 12) on equations (3 16) and (3 17) gives the following *equilibrium points* for biomass and substrate

$$S_0 = \frac{k_S D_0}{\mu_{max}-D_0} \ , \qquad X_0 = Y_{X\ S}\left(S_1 - \frac{k_S D_0}{\mu_{max}-D_0}\right) \qquad (5\ 34, 5\ 35)$$

5 3 2 Linearised State Space Model - Multi-Input Multi-Output (MIMO)

Using (4 17-4 20) we obtain the following multi-input multi-output linear variational model for the plant,

$$\delta x(k+1) = A^*\ \delta x(k) + B^*\ \delta u(k) \qquad (5\ 36)$$

where

$$\delta x(k) = [x(k)-x_0,\ s(k)-s_0]^T \qquad (5\ 37)$$

$$\delta u(k) = [u_1(k)-u_{10}(k),\ u_2(k)-u_{20}(k)]^T \qquad (5\ 38)$$

with $u_1(k) = D(k)$ (5 39)

and $u_2(k) = D(k)S_1(k)$ (5 40)

and the components of the A^* and B^* are respectively,

$$a^*_{11} = 1 + \frac{h\mu_m S_0}{[k_S+S_0]} - hu_{10}, \quad a^*_{12} = \frac{hk_S\mu_m X_0}{[k_S+S_0]^2} \qquad (5\ 41,5\ 42)$$

$$a^*_{21} = \frac{-h\mu_m S_0}{Y_{X\ S}[k_S+S_0]}, \quad a^*_{22} = 1 - \frac{h\mu_m k_S}{Y_{X\ S}(k_S+S_0)^2} - hu_{10} \qquad (5\ 43,5\ 44)$$

and

$$b^*_{11} = -hX_0, \quad b_{12} = 0 \qquad (5\ 45)$$

$$b^*_{12} = h(S_1(k)-S_0), \quad b_{22} = h \qquad (5\ 46)$$

Imposing the conditions expressed in (4 12) on equations (3 16) and (3 17) gives the following *equilibrium points* for biomass and substrate of the MIMO system,

$$S_0 = \frac{k_S u_{10}}{\mu_{max}-u_{10}}, \quad X_0 = Y_{X\ S}[(u_{20}/u_{10}) - S_0] \qquad (5\ 47,5\ 48)$$

5 3 3 Controllability

If we consider the discrete time system that uses the following statee space model

$$x(k) = Ax(k-1) + Bu(k-1) \qquad (5\ 49)$$

$$y(k) = Cx(k) \qquad (5\ 50)$$

The system is controllable if it is possible to find a control sequence such

that an arbitrary state can be reached from any initial state in finite time If we define the controllability matrix [30,Ch 5] as,

$$W_C = [\ B\ AB\ \ \ A^{n-1}B\ ] \qquad (5\ 51)$$

if W_C has rank n, then it is possible to find n equations from which the control signal can be found such that the initial state is transferred to the desired final state x(k) and the system is deemed controllable

The controllability of the SISO and MIMO systems may be analysed by taking the parameter values of Table 3 1 with an equilibrium input $D_0 = 0\ 2\ hr^{-1}$ and input feed concentration of 9g/l

The controllability matrix of the SISO linearized system becomes,

$$W_C = \begin{bmatrix} -2\ 39 & -0\ 659 \\ 4\ 78 & 1\ 318 \end{bmatrix} \qquad (5\ 52)$$

This matrix is not full rank and Ackermans formula [30,Ch 9] states that W_C^{-1} must exist for SISO state feedback design (or any other feedback structure that gives closed–loop poles specified by some polynominal P(z)=0)

For the MIMO case the controllability matrix becomes,

$$W_C = \begin{bmatrix} -2\ 39 & 0 & -2\ 469 & -0\ 181 \\ 0\ 22 & -0\ 5 & 0\ 417 & -0\ 137 \end{bmatrix} \qquad (5\ 53)$$

This matrix has rank=2 and is controllable It is with the design of a state feedback controller for the MIMO model that the remainder of this chapter will deal Therefore it is worthwhile to examine the accuracy of the linearisation procedure outlined in Section 5 3 To use a linearised model of a non-linear plant it is desirable that the magnitude of the higher order derivatives in the Taylor

series expansion of equation (5 15) tend towards zero A comparsion of the matrices A^* with A^*_1 and B^* with B^*_1 should validate this idea where,

$$A^* = \frac{\delta f}{\delta x}(x_0,u_0) , \qquad B^* = \frac{\delta f}{\delta x}(x_0,u_0) \qquad (5\ 19,5\ 20)$$

$$A^*_1 = \frac{\delta^2 f}{\delta x^2}(x_0,u_0) , \qquad B^*_1 = \frac{\delta^2 f}{\delta x^2}(x_0,u_0) \qquad (5\ 54,5\ 55)$$

For plant parameters of μ_{max}=0 8, $Y_{X\,S}$=0 5, k_S=0 5 and equilibrium inputs of $u_{1\,0}$=0 685714 and $u_{2\,0}$=4 8 the following matrices result,

$$A^* = \begin{bmatrix} 0 & 0\ 0653 \\ -1\ 37 & -0\ 5551 \end{bmatrix} \qquad B^* = \begin{bmatrix} 2 & 0 \\ -3 & 1 \end{bmatrix} \qquad (5\ 56,5\ 57)$$

$$A^*_1 = \begin{bmatrix} 0 & -0\ 0373 \\ 0 & 0\ 0746 \end{bmatrix} \qquad B^*_1 = \begin{bmatrix} 0 & 0 \\ 0 & 0 \end{bmatrix} \qquad (5\ 58,5\ 59)$$

The above, relatively small, values of the second derivatives would imply that the linearised model should be a good approximation of the non–linear model when operating about the equilibrium inputs $u_{1\,0}$ and $u_{2\,0}$

5 4 REGULATION BASED ON POLE PLACEMENT BY STATE FEEDBACK

The regulation problem is discussed in this section with the fundamental design method of pole placement being developed The purpose is to arrange a feedback structure so that all poles of the closed loop system assume prescribed values The problem is initally solved under the restrictive assumption (for fermentation systems) that all state variables can be measured directly [19] Any linear system may be represented as,

$$x(k+1) = A(k-1)x(k-1) + B(k-1)u(k-1) \qquad (5\ 60)$$

Because feedback solutions are desired, it is necessary to specify the information available for generating the control signal Because the properties of the system are specified by the closed loop poles, the closed loop system must be linear The feedback must also be linear so the admissible controls for the fermentor model can be expressed as a linear feedback

$$u(k) = L\ x(k) = -l_1X(k) - l_2S(k) \qquad (5\ 61)$$

With this feedback the closed loop system becomes

$$x(k+1) = [A(k)-B(k)L(k)]x(k) = A_C(k)x(k) \qquad (5\ 62)$$

where

$$A_C = \begin{bmatrix} a_{11}-b_{11}l_1 & a_{12}-b_{11}l_2 \\ a_{21}-b_{21}l_1 & a_{22}-b_{21}l_2 \end{bmatrix} \qquad (5\ 63)$$

Equating the characteristic equation of $A_C(k)$ to the following desired characteristic equation

$$z^2 + p_1z + p_2 = 0 \qquad (5\ 64)$$

where p_1 and p_2 are the desired pole locations and solving for the two state

feedback gains l_1 and l_2 (APPENDIX A) we get,

$$l_1 = (t + l_2 u)/v \quad (5\ 65)$$

$$l_2 = (vp_1p_2 - vq - rt)/(ru + v) \quad (5\ 66)$$

where

$$t = p_1 + p_2 - a_{11} - a_{22} \quad (5\ 67)$$

$$u = b_{21} + b_{22} \quad (5\ 68)$$

$$v = -(b_{11} + b_{12}) \quad (5\ 69)$$

$$q = a_{11}a_{22} - a_{12}a_{21} \quad (5\ 70)$$

$$r = a_{12}b_{21} + b_{22}a_{12} - a_{22}b_{11} - a_{22}b_{12} \quad (5\ 71)$$

$$s = a_{21}b_{11} + a_{21}b_{12} - a_{11}b_{21} - a_{11}b_{22} \quad (5\ 72)$$

The pole placement problem had been solved explicitly and in the following the section simulation results will be presented for a self tuning state feedback controller

5.5 SIMULATION RESULTS

The simulation results that follow will be divided into section as follows Firstly, simulation studies will be presented that compare the linearised and nonlinear models of the fermentation process Then the operation of a fixed parameter state feedback controller will be outlined followed by a self tuning state feedback controller Both the above controllers assume the availibility of measurements of the output states, this is not true of the real plant and hence the need to introduce a self tuning Extended Kalman filter This is based on output measurements of carbon dioxide from the fermenter and provides estimates of the states (biomass and substrate) A sampling period of h=0 05hr (3 min) will be used in the simulation studies to follow

5.5.1 Non-Linear and Linearised Plant Comparsion

In the comparative studies between the non-linear and linearised plant the following parameters and inputs are used

μ_{max}=0.8	k_S =0.22	$Y_{X/S}$=0.5
u_{10} =0.42	u_{20}=4.97	

Table 5.1

These inputs and parameters give equilibrium state values of X_0=4.22g/l and S_0=0.552g/l. Figure 5.3 shows a comparsion between the linearised and non-linear plant when operating from an initial state vector (X,S) of x = (2,4). The results in Figure 5.4 highlight the problem of moving the operating conditions of the plant further away from the equilibrium states. Figure 5.4 shows linear and non-linear models operating with an initial state vector of x = (0.5,8), far removed from the equilibrium states. This situation is not ideal as in the real plant the initial states will be far removed from the equilibrium states of the plant. This problem may be solved by updating the equilibrium model at each sampling interval. The new linearised model is calculated using the previous states of the non-linear model as,

$$u_{10} = \frac{\mu_{max} * S_0}{k_S + S_0} \qquad u_{20} = [\,(X_0/Y_{X/S}) + S_0\,] * u_{10} \qquad (5.73, 5.74)$$

Figure 5.5 shows the good approximation between the linearised and non-linear for the updated equilibrium point. The idea of an updated equilibrium point will be used in a control structure later.

5.5.2 Fixed Parameter Controller

The block diagram of a state feedback controller for a fermentation plant is shown in Fig 5.6. The controller feedback gains are designed using the current A^* and B^* of the linearised model. The control inputs to the plant in the MIMO

model are defined as u1 the dilution rate, D, and u2 the product of the dilution rate and the input feed substrate ($u2=D*S_i$) The reference state trajectories (X,S) must therefore be multiplied by the inverse steady state gain matrix G_{SS} where,

$$G_{SS} = B^{*-1} [I-(A^{*}- B^{*} L)] \qquad (5\ 75)$$

where L is the feedback gain matrix and I the identity matrix Results for this control structure will now be presented

Figure 5 7 shows results for state deviations of (2,3) → (2 4,3 8) The plant was linearised around its initial conditions and the closed loop poles were chosen as $p_1=p_2 = 0\ 8$ Figure 5 7 shows the critically damped plant response (non-oscillatory) for these pole locations Figure 5 8 shows the control inputs for these state deviations and Figure 5 9 isolates the control input u1 (dilution rate) to show that it is a realistic input for the *actual* plant, u2 is a constant times the dilution rate as previously outlined Figure 5 9 shows the initial correction needed in the control input as the equilibrium model is based on the inverse relationship outlined in equations (5 73) and (5 74) At t=0 the plant is assumed to be in equilibrium with equilibrium states equal to the initial conditions and equilibrium control inputs solved via the inverse relationship outlined above

As expected when the setpoints are moved away from the current equilibrium point (the initial conditions) the control performance suffers Figure 5 10 shows the controller performance for the same closed loop poles of 0 8 but with larger state deviations than previously, (2,3) → (4 5,4) The plant outputs attain their respective setpoints but not in the desired critically damped reponse The control inputs in Figure 5 11 are unrealistic for the *actual* plant Hence this control structure is limited in its application

Two alternatives may be considered Firstly, a linearised model about the setpoint could be used and secondly, for large deviation intermediate setpoints could be chosen to give plant outputs that go from their initial conditions to their

respective setpoints in a piecewise manner with intermediate updating of the linearised model

For a linearised model about the setpoint we use the state trajectories of (2,3) → (2 4,3 8) Fig 5 12 shows the plant output for this approach and 5 13 shows the input dilution rate The plant i/o values are similiar to the results for linearizing about the initial conditions For initial conditions far removed from the setpoint the plant does not show a critically damped response either but does show different control inputs Figure 5 14 shows the plant o/p for linearising about the set points and large deviations of states The profile is smoother than that shown in Figure 5 10 but again not critically damped Of the control inputs in Figure 5 15 the dilution rate shows an unrealistic value for the actual plant

The second alternative, as mentioned earlier, is to implement a method of piecewise linearisation, whereby an intermediate setpoint is defined and the equilibrium model updated once this point is reached Updating the equilibrium model at each sampling interval was not possible as the large correction in the control input as shown in Fig 5 9 occured at each sampling interval and negative values of equilibrium states resulted Results are shown in Figure 5 16 when the piecewise update technique is used The control inputs are shown in Figure 5 17 This method provides better scope as the plant can be driven from its initial conditions to some remote value in a piecewise fashion.

5.5 3 Self Tuning Controller

The schematic diagram of a self tuning state feedback controller for a fermenter is shown in Figure 5 18 The non-linear plant is simulated with a Monod growth structure and the parameter identification model of Section 3 3 2 is used in the Recursive Least Squares (RLS) identification technique The non-linear plant is simulated with the following parameter values,

μ_{max}=0 8 k_S =0 22 $Y_{X\ S}$=0 5

Table 5 2

The plant outputs are shown in Figure 5 19 for state trajectories of (2,3) → (2 4,3 8), these trajectories will be used throughout the remainder of the simulation studies as will closed loop pole locations of $p_1 = p_2$ =0 8 The convergence of the plant parameters is shown in Figure 5 20 The yield parameter $Y_{X\,S}$ has been identified using the direct estimate technique of Chapter 3 The parameters μ_{max} and k_S were identified using an RLS subroutine Initial parameters estimates of μ_{max} =0 1 and k_S=0 05 and $Y_{X\,S}$=0 1 were used in all simulations Clearly the parameters of Figure 5 20 begin to converge after 0 01hr A forgetting factor of λ=0 95 and initial covariance matrix P=10^5 were used The control action of Figure 5 21 although severe at first, due to the bad initial estimates of parameters and an inverse equilibrium calculation based on these estimates, improves as the parameters converge

The performance of the self tuning controller is now investigated for a changing plant parameter At t=0 7hr the plant parameter μ_{max} is changed by 10% around its nominal value to μ_{max}=0 88 Again λ=0 95 and P=10^5 apply Simulation results are shown in Figures 5 22-5 24 The plant outputs are shown in Figure 5 22 and despite the disturbed parameter value the set points are reached at t=4 55hr Even with this disturbed parameter the control inputs in Figure 5 24 are acceptable for an actual plant. The identified plant parameters of Figure 5 23 show slow recovery after the μ_{max} is disturbed It was decided to change the forgetting factor to λ=0 9 and investigate the effects on parameter convergence when μ_{max} is disturbed Simulation results for the plant outputs, parameter convergence and control inputs are shown in Figures 5 25-5 27 The parameter convergence properties are improved the setpoints are reached in 2 85hr compared to 4 55hr in the previous case As expected the control action, shown in Figure 5 27, associated with such an improvement in performance is severe and in fact not suited for an actual plant.

5 6 CONCLUSIONS

This chapter on self tuning control of fermentation processes has attempted to join together much of the work and ideas outlined in the previous chapters The self tuning controller used incorporated the procedures outlined in Chapter 3 regarding the identification of plant parameters and the effect of continual updating of these parameters Detailed studies of the controller performances over a range of conditions has been outlined Some work remains especially that of the introduction of a self tuning Kalman Filter into the overall control loop This aside the self tuner showed encouraging results The main merit of the self tuner is its ability to track time varying parmeters and coupled with the process of linearisation it may be possible to improve the control of an actual fermentation process However, in some of the simulation studies outlined initial control signal and parameter variations are unacceptable In a real system the view of the self tuner as a black box device which can be connected to a system and left to look after itself may be somewhat of a myth Care would be needed in setting limits on the control signal and on parameter variations Perhaps a self tuner used as part of a control system would be more beneficial The application of the self tuner to a real plant is necessary and looks feasible with the introduction of an Extended Kalman Filter

CHAPTER 6

EXPERIMENTAL RESULTS AND MODEL VALIDATION

This chapter will present experimental results from a pilot scale fermentor The process instrumentation and measurements techniques are outlined for the system Model validation, identification of model parameters and an on–line method of state estimation is investigated for a batch process Finally, the validity of the experimental results is discussed

6 1 PROCESS INSTRUMENTATION

This section will discuss the instrumentation employed for the fermentation of bakers yeast on on 10-litre pilot plant fermentor, as outlined in Appendix A The fermentation vessel used was a New Brunswick SF-116 fermentor This stainless steel vessel is steam sterilisable and the vessel contents were typically sterilised at 120°C and 15psig for 45-60 minutes before innoculation The vessel is equipped with an agitator and during fermentation process the medium is agitated at 300-400 rpm A sampling port which must be steam sterilised prior to each sample facilites off–line analysis

A New Brunswick Scientific Series 900 polarographic dissolved oxygen electrode was used to measure dissolved oxygen levels A New Brunswick Scientific dissolved oxygen transmitter (Model DO-50) with a 0-10mV analog output corresponding to 0-100% saturation was used in conjunction with the electrode

An important feature of any fermentation instrumentation are the gas analysers

An Analytical Development Company analyser, type SS206, was used to monitor CO_2 levels in the exhaust gas stream The exhaust gas for carbon dioxide measurment was first passed through a drying column containing calcium chloride to remove excess moisture before entering the infra-red analyser The analyser gives 0-5v output for 0-10% CO_2 A Servomex 570A analyser was used to measure oxygen levels in the exhaust gas Again prior to analysis the gas was dried by passing through a column of silica gel The paramagnetic oxygen analyser outputs a linear 0-1V for 0-100% oxygen

A calibration routine preceeded each fermentation run. The carbon dioxide analyser was set to zero using air as normal air content is 0 003% CO_2 while the span of the instrument was set using a 5% CO_2 gas supply Zero on the oxygen analyser was set using a nitrogen gas supply and the span of the instrument was set using air as normal air content is 21% The saturation level of the dissolved oxygen probe was set by bubbling air through the medium in the vessel at 12 l/min air input and 300rpm agitator speed (the operating conditions) The zero set on the dissolved oxygen instrument was obtained by bubbling nitrogen through the medium

The various instrumentation signals were signal conditioned and interfaced to a IBM compatible 386 based Personal Computer via Metrabyte DASH16 and DDA06 input/output cards The DASH16 provides timers and D/A facilities and uses an industry standard (HI-674) 12 bit successive approximation converter with a 12µs conversion time All instrumentation signals were filtered and interfaced in differential configuration which provided 90db common mode rejection and ±10v common mode range The DDA06 provides 6 independent 12 bit D/A converters and 24 bits of digital I/O and are TTL/CMOS compatable The exhaust gas was channeled to the CO_2 and O_2 analysers using 24V solenoids. The solenoids were "thrown" by Darlington Drivers triggered by the digital output lines The exhaust gases were sampled every 5 min (0 083 hr) with a 30 sec delay from triggering of

the solenoid to sampling (i e the solenoids were thrown at 4 5 min intervals) This was necessary to to allow the exhaust gas to stream through the drying columns and register the respective analyser At 5 min intervals the recorded value of CO_2, O_2 or DO was the mean value over 100 consecutive samples

6.2 MATERIALS AND METHOD

The preparation for a fermentation was in two stages The first stage involved the preparatation of a yeast innoculum and the second the preparation of the growth medium The innoculum was used to seed a production medium batch and incubated over 20hrs The actual production batch stage was the stirred aerated fermentation process and was run in the New Brunswick pilot-plant fermenter Following the fermentation the yeast was harvested by continuous centrifugation.

6.2.1 Innoculum Preparation

Cane molasses -40g/l

$(NH_4)_2SO_4$ - 5g/l

pH 5 0-5 2 before sterilization (121°C, 20 min)

pH 4 7-4 9 before inoculation

A flask containing 400ml concentrates was innoculated with 2-4ml of a yeast cell suspension (*Saccharomyces Cerevisiae)* The flasks was incubated on a shaker table at 30°C for 24h

6.2 2 Medium Preparation

Eight litres of medium was prepared according to the following recipe,

Cane molasses - 20g/l

$(NH_4)_2SO_4$ - 5g/l

Antifoam - 50ml

(poloxyethyleneglycol-ppg)

pH 5 0-5 2 before sterilization (121°C, 45min)

pH 4 7-4 9 before inoculation

The medium in the vessel was sterilised at 121°C for 45 min with constant agitation The production medium was inoculated with a 10% voulme of the seed culture and incubated at 30°C, 300rpm and 1 2 v/v/min During the production fermentation samples were taken at t_0 and every two hours thereafter to determine sugar levels and dry weight of yeast.

6 3 PRODUCTION OF LABORATORY RESULTS

To validate the model for the system it was necessary to obtain accurate measurments of the two main state variables in an off–line fashion as there are no avaliable sensors for on line measurement Measurements of biomass (g/l) were obtained using the technique of dry weights and levels of glucose were found using a sugar reducing test.

6 3 1 Wet Cell Weight/Dry Yeast Weight

The process of obtaining dry yeast weight measurements was initiated by preweighing 10ml centrifuge tubes Then 10ml of yeast culture was pipetted into the centrifuge tube and spun in a Sorval RC SB high speed centrifuge at 10,000 rpm for 10 mins The supernatant was poured off and saved for the sugar determination experiment to follow The weight of the pellet and the tube was recorded The wet cell or sludge weight was calculated in units of g/l To obtain dry yeast weight measurements the pellet was resuspended in 5ml of distilled water and the contents placed in a heated oven (120°C) for 24hr on preweighed trays Upon removal and weighing dry yeast weights per 10ml may be calculated This

can then be scaled to a reading of g/l

6 3 2 Sugar Level Determination

Sugar levels during the fermentation may be monitored using a method called DNS for the estimation of reducing sugars By addition of of *3,5 Dinitro Salicyclic acid* (DNS) to a broth sample a reaction occurs which causes a colouremetric change in the broth. This coloremetric change may be detected at a wavelength of 540nm

A stock solution of 1% glucose was prepared in a volumetric flask and solutions of 0 1% (1mg/ml) were prepared from them as required. Dilutions of samples were prepared usmg distilled water A set of glucose standards in the range 0-1 mg/ml was also prepared which consists of reading of optical density versus glocose concentration A 2ml sample of standard was placed in a tube and 2 ml of DNS reagent added

The tubes were covered and boiled for 10 mins After removing and immediate cooling, 10 ml distilled water was added to all tubes The optical density of the sample solution at 540nm was measured with a Pye Unicam SP6-550 spectrophotometer The standard curve of optical density versus glucose concentration then allowed calculation of the glucose concentration of the fermenter samples in g/l

6 4 MODEL VALIDATION

The following model validation section will be divided into three parts In the first part, a comparitive study between experimental and simulated results for the main states (biomass and substrate) will be presented The second will validate the dissolved oxygen measurements and in the third the exhaust gas levels will be studied Where applicable in the following sections the different specific growth rate models outlined in Chapter 2 will be used and a study of parameter variations and their effects will take place

6 4 1 Validation of Biomass and Substrate Measurements

To validate the primary states we considered the fermentation run to be substrate limiting and the following sections outline the fitting of a Monod growth rate structure to the experimental results Fig 6 1 and Fig 6 2 shows a comparative test between experimental and simulation with the following parameters,

$\mu_{max} = 0\ 3 \quad k_S = 4\ 0 \quad Y_{X\ S} = 0\ 16$

Table 6 1

The profiles show encouraging results for biomass in Fig 6 1 The concentration of glucose shown in Fig 6 2 does not decay fast enough in comparsion with the experimental results so it was deemed necessary to increase the rate of activity μ_{max} The results of various increases in μ_{max} is shown for biomass and substrate in Fig 6 3 and Fig 6 4 respectively A value of μ_{max}=0 35hr^{-1} would seem to be most suitable for validation of the biomass and substrate measurements

6 4 2 Validation of Dissolved Oxygen Measurements

The dissolved oxygen measurements from the New Brunswick Probe outputs a saturation level of dissolved oxygen concentration of between 0-100% For comparsion with simulation values, 100% saturation in the broth was taken as 0 04 g/l of dissolved oxygen [8,Ch 8] This is the saturation level of dissolved oxygen in distilled water at 30°C A comparasion between experimental and simulation values of dissolved oxygen for varying μ_{max} is shown in Fig 6 5 with use of the following parameter values,

$k_S = 4\ 0 \quad Y_{X\ S} = 0\ 16 \quad Y_{X\ O} = 1\ 2$

Table 6 2

and $k_{\ell}a$ = 300hr^{-1} Fig 6 6 shows profiles of dissolved oxygen when operating with the parameters of Table 6 2 (μ_{max} = 0 3) and varying the value of the adsorption coefficient $k_{\ell}a$ A value of μ_{max}=0 3hr^{-1} and $k_{\ell}a$=330hr^{-1} was deemed a best fit for dissolved oxygen validation.

6 4 3 Validation of Gas Analysis

The results from the carbon dioxide analyser are shown in Fig 6 7 with the mole fraction concentration of carbon dioxide in the exhaust gas reaching a maximun of 1 5% The results from the Servomex oxygen analyser is shown in Fig 6 8 The accuracy of this Servomex oxygen analyser proved to be the issue of most concern throughout many fed–batch runs While a decrease in oxygen levels from the normal 21% is seen at the output the instruments minimum value of 20 3% is quite dissappointing A comparative study of experimental and simulated results of exhaust CO_2 and O_2 for changing μ_{max} is shown in Fig 6 9 and Fig 6 10 respectively

6.5 IDENTIFICATION USING EXPERIMENTAL RESULTS

As was pointed out in Section 6 3 the measurements of biomass and substrate were achieved off-line for the purpose of model validation Initially parameter estimates were found using a classical least squares structure Ten data points were taken due corresponding to the 2hr sampling interval during the 20hr run As a Monod growth rate structure proved most sucessful in Section 6 4 the data was formatted to identify the Monod parameters as in Section 3 3 2 Classical Least squares returned the following Monod parameters, μ_{max}=0 147, k_S=-0 529 and $Y_{X\,S}$=0 092 It will be seen later that these values differ fro the RLS results as the Classical Least Squares method identifies one set of parameters that suit over the whole fermentation run

For use in a recursive least squares identification package, as would be the case in an on-line self tuning controller, it is necessary to obtain more data points of substrate and biomass than the ten that were achieved during the 20hr run Three methods of data interpolation were tried initially to obtain sufficient data points for the recursive least squares technique These are presented in Section 6 5 1 to estimate the parameters of an unstructured growth rate model and the most sucessful interpolation technique is then used for the parameter estimation of the Monod and Ollson models in Section 6 5 2

6.5 1 Unstructured Growth Rate Model

The first method of interpolation used was a polynominal fit to the experimental biomass and substrate profiles The polynominal fit for biomass and substrate is shown in Fig 6 11 and Fig 6 12 respectively Data points were now extracted at intervals of 0 05hr and inputted to the RLS routine Results are displayed in Fig 6 13

The second method took a straight line fit between each of the ten data

points in a piecewise fashion and again extracted data points at intervald of 0 05hrs Results are displayed in Fig 6 14

The third method of interpolation strove to fit french curves between the data points This was done manually and hence data points were read at 0 5hr intervals Results are displayed in Fig 6 15

Thepiecewise fit, discussed later, was deemed the most suitable for identification purposes and was then used to estimate the parameters of a Monod and Ollson model

6.5 2 Monod and Ollson Growth Rate Models

In this section we assume a Monod dependent growth rate and using the piecewise data fit and sampling interval of h=0 05 results for a Monod parameter estimation is shown in Fig 6 16 and Fig 6 17 Results for the Monod parameters show reasonable correlation with thoses used in the experimental validation The yield parameter is identified as 0 12 (0 16 in validation), while μ_{max} is identified as 0 22hr^{-1} (0 35hr^{-1} in the validation) The k_S parameter shows the biggest variation from the validation values A time varying parameter with a minimum value of -3 2 was identified (Fig 6 17) but a value of 4 0 used in validation These variations will be discussed in the next section

For an Ollson growth rate structure we include the measured values of dissolved ,oxygen. The dissolved oxygen samples were taken every 5min (0 083hr) and equivalently the sampling interval on the piecewise fits of biomass and substrate was changed to 0 083hr Results are presented in Fig 6 18

6 6 DISCUSSION

6 6 1 Model Validation

In the analysis and design of any control system it is necessary to have a mathematical model of the given plant. Such a mathematical model must describe thesystem dynamics as completely as possible The model validation and identification studies presented above provide some interesting insights into the dynamics of a batch fermentor

The validation of biomass and substrate results proved to be the most sucessful The results of Fig 6 3 and Fig 6 4 provided acceptable fits for both primary states but variations in μ_{max} affect not only biomass and substrate results but also dissolved oxygen Having neglected the effects which μ_{max} had on the other states it was through validation of the dissolved oxygen measurement that the complex dynamics and interdependence of many states and parameters could be seen for fermentation processes

In Fig 6 5 it may be seen that the rate of uptake of oxygen from the dissolved state by the yeast cells is strongly dependent on the growth rate At higher values of μ_{max} the uptake of oxygen by the cells, is greater than the rate at which oxygen is being dissolved into the broth. In fact at μ_{max}=0 35 the broth becomes deficient in dissolved oxygen. Manipulation of the adsorption coefficient $k_{\ell}a$ was then considered to increase the rate of oxygen transport into the system It is evident in Fig 6 6 that increasing the value of $k_{\ell}a$ prevents a deficiency in dissolved oxygen We also see that under conditions of constant μ_{max} variations in the value of $k_{\ell}a$ changes the minimum concentration of dissolved oxygen but not what point in time at which this minimum occurs

As with any control system the accuracy of the instruments used must be

investigated The galvanic dissolved oxygen probe used provided a continuous concentration measurement in solution of oxygen partial pressure in percent of oxygen An oxygen permeable membrane seperates the cathode and anode electrode internals from the medium fluid Reactions at the electrode surfaces produce small amounts of current to provide voltage measurement which is correlated to the oxygen flux through the membrane In early batch runs it was found that the normal membrane did not withstand the rigirous sterilization and agitation procedure The new membrane left the instrument less sensitive and thereafter span sets (100%) in the calibration routine took the order of 8 minutes

Another issue that must be addressed with regard to the DO probe is its loss of calibration over a 20hr batch run The instrument fails to recover 100% saturation even when relative activity in the vessel has ceased This may be explained by either of the following Firstly, the probe was calibrated in the medium outlined in Section 6 2 2 with high substrate and low biomass concentrations The solubility of oxygen in the resulting medium of 20hr later with high biomass, low substrate concentration and secondary products may only be 40% of initial reading as the probe indicates Secondly, accumulation of various bodies on and around the membrane over the 20 hrs would have an adverse effect on the permeability of the membrane The answer is most likely a combination of the two because when the probe was removed at the end of the run and placed in saturated distilled water it only attained readings in the 70-90% range

It was thought that in the batch run presented that the broth became deficient in oxygen and this could have had an effect on DO, O_2 and CO_2 measurements At t=10hr the air input was increased from 12l/min to 14l/min. The dissolved oxygen level of the broth (Fig 6 5) and the O_2 level in the exhaust gas (Fig 6 8) shows increased concentrations and the carbon dioxide exhaust (Fog 6 7) the expected decrease at t=10hr This would imply that the dissolved oxygen state was in equilibrium and that the rate of consumption was equal to the rate of transport.

It can only be assumed that the fermentation may have been oxygen limiting at some time between t=7hr and t=10hr If the system was oxygen limiting it may explain the slightly lower than expected exhaust CO_2 output. A typical "trough" shaped dissolved oxygen concentration of Fig 6 6 may have pushed the experimental and simulation values of CO_2 in Fig 6 9 closer

The Servomex 570A oxygen analyser measures the paramagnetic susceptibility of the oxygen and has a quoted accuracy of ±0 1% and a response time of less than 7 5 seconds with an inlet pressure of 10psig Unfortunately the analyser did not display such accuracy during any of the batch runs and definetly for fermentation purposes a model 580A with a 0-25% range would be more appropriate than the current single 0-100% range

6 6 2 Experimental Identification of Parameters

In light of the results from the identification of parameters using experimental results we must look at the validity and the physical significance of some of the identified parameters First we will look at the results of fitting an unstructured growth model to the experimental data via the three methods of data interpolation.

The maximum rate of growth in the system occurs at t=7hr ($\mu \propto dX/dt$) The polynominal fit data fails to estimate this and returns a maximum growth rate occuring at t=1 2hr in Fig 6 13 This occurs because in the polynomianl fit the slope of the biomass and substrate profiles are changed substantially and hence the occurence of the maximum value of the parameter μ is changed

The piecewise data fit of Fig 6 14 returns a better estimate of growth with a peak at t=7hr The overall profile of μ in Fig 6 14 is not as smooth as in the polynominal fit of Fig 6 13 with the parameter changing in a piecewise fashion

However the maximum value of μ=0 35hr^{-1} compares well with the value used in the model validation section. The french curve data fit returns an peak estimate of μ=0 28 at t=7 5hr but as data points were taken at 0 5hr intervals compared with 0 05 in the above two cases this method suffers mainly because of the manual interpolation of data from the graphs

The yield paramater $Y_{X\,S}$ is defined as the yield of biomass on substrate or $\Delta X/\Delta S$ The yield of 2 2g/l (Fig 6 1) of biomass from 12g/l (Fig 6 2) of substrate implies $Y_{X\,S}$=0 18 The polynominal fit (Fig 6 13) and piecewise fit (Fig 6 14) estimate an increasing yield rate that converges to a value of 0 12 The French curve fit in Fig 6 15 estimates a poor value of $Y_{X\,S}$=0 06

From the above estimation scheme the piecewise fit proved most sucessful and was then used to fit a Monod growth structure to the data The Monod parameters μ_{max} and $Y_{X\,S}$ are shown in Fig 6 16 with the k_S parameter shown in Fig 6 17 The parameters μ_{max} and $Y_{X\,S}$ converge to expected values However the RLS estimate of k_S is poor This would seem to validate the results of Fig 6 3 and Fig 6 4 that when fitting a Monod model to the data descrepancies existes between experimental and simulated values due to model inaccuracies In an RLS framework these descrepancies manifest themselves in the identification of a time varying but incorrect k_S parameter

In Fig 6 18 an Ollson growth rate structure was fitted to the data The paramater converge to unrealistic values and prove that for the fermentation in question was substrate limiting and not double substrate limiting Therefore the growth rate for this run is best described by a Monod growth rate structure

6 7 SUMMARY

This chapter has outlined the work undertaken in a pilot plant on a 10l fermentor with details of materials, methods and process instrumentation. Using the experimental results model validation and identification studies were carried out. The results indicate that for the results presented from the pilot plant, a Monod growth rate best described the process

CHAPTER 7

CONCLUSIONS

The computer control and optimization of fermentation processes is of great economic interest to industry and has created a substantial research interest in academic institutions This thesis has outlined research undertaken into the self tuning control of fermentation processes at the Control Technology Research Unit (CTRU) at Dublin City University in collaboration with the School of Biological Sciences

The analysis of fermentation processes reveal many problems that face the designer of a self tuning controller The main hurdles in a self tuning context are the need for an accurate model structure that describes the system completely and the availability of process measurements for the purpose of on–line identification of system parameters To further complicate the control system design, bioprocesses are systems which are inherently non–linear and highly interactive This is evident from the fact that the biomass concentration is not only affected by the substrate concentration but by the dissolved oxygen concentration, stirrer speed, pH and temperature

In this thesis, a comprehensive model for a fed batch Baker's Yeast fermentation has been developed It has been demonstrated that the choice of model for a fermentation process depends largely on the the control objective, as well as on the relative importance of various transport and kinetic factors under conditions most likely to be found in the course of an actual implementation The transport model presented is applicable to any agitated and aerated reactor while the kinetic model depends on the metabolism of the specific organism

The critical importance of on-line estimation methods results from the

inaccuracy of the presently available growth models, the rather small number of measurements that presently can be made on-line and the high sensitivity that most biological systems exhibit to variations in the environmental conditions Most biosensors have not gained wide scale acceptance on industrial process with problems in the area of robustness and long term stability This problem of the availability and reliability of on-line sensors and the considerable delay that can be introduced into process measurements by off-line analysis has led to investigation into process observers such as the Kalman Filter This method of state estimation has tried to improve control techniques by moving from the off-line to the on-line domain The Kalman Filter observer is not without problems as a fixed parameter model can suffer from simplifications made in the fermentor model system The simulation results presented show that the Kalman Filter, like the non-linear and non-adaptive observers, suffers the most from inaccurate initial estimates of the process states

A Recursive Least Squares (RLS) algorithm for the identification of system parameters based on on-line measurements of the states has been presented The good agreement between simulated and experimental parameters indicates that the proposed algorithm would be very useful in a self tuning control context especially as the RLS shows good tracking of time varying parameters with a variable forgetting factor

The particular self tuning control algorithm developed provided interesting results It strove to include the various parts of the controller already developed seperately viz the identification and estimation algorithms The state feedback controller developed differed from other self tuning controllers presented in the literature in that it attempted to the control process states and not optimally control the envoirnment in which biomass could grow The results show that a self tuning controller can sucessfully be applied to a fed batch fermentation process simulated on a digital computer

The possibility of future work as a result of this study of fermentation processes lies mainly in the real time implementation of the self tuning control strategy at a pilot plant scale In this thesis an integrated approach has been presented for the on-line estimation of state variables and culture parameters The real time application of any self tuning strategy will depend on the availibility of accurate measurements of the state variables The problem of determining the states of a system from noisy measurements of exhaust gases via the technique of Kalman Filtering has shown promise but additional work is needed The current method is based on the non-linear correlation between the process states and the carbon dioxide output in the exhaust gas However, as mentioned earlier, the filter suffers from inaccurate initial state estimates and one area of future work could be the use of an iterative Kalman Filter which incorporates iterations of the output equations to reduce the estimation errors and the bias due to poor initial estimates The future availability of accurate measurements of oxygen concentration in the exhaust gas could further enhance any estimation algorithm

In future estimation schemes consideration should also be given to more complex algorithms The relatively large sampling time associated with the control of fermentation processes ensures adequate processing time is avaliable for any increase in complexity of algorithms These algorithms may consist of using a combined state and parameter estimators [52] rather than the presently seperate Recursive Least Squares and Kalman Filter techniques Consideration should also be given to cases where the state noise covariance Q and observation noise covariance R are not known a priori Algorithms are available that can be used on-line to identify the unknown covariances

Future control schemes could also revert back to the popular approach of controlling the environment in which maximum growth rates could be achieved The control of the dissolved oxygen concentration via the input air flow rate and

agitation speed is one approach that could be tried in a self tuning context

The use of modelling and optimization for on-line computer control, coupled with the increasing use of available sensors for monitoring fermentation processes will continue to be of interest to industry The progress in control techniques must be influenced in a positive manner by academic efforts and hopefully the research undertaken for this thesis will contribute to the increasingly important field of the control of biological systems

REFERENCES

1 The First European Conference on Computer Control in Fermentations *Dijon, France (1973)*

2 Arminger W, Computer Applications in Fermentation Technology *Biotechnology & Bioengineering Syposium No 9, Wiley, New York (1979)*

3 Alford J S, Evolution of the Fermentation Computer System at Eli Lilly & Co *Third International Conference on Computer Applications in Fermentation Technology, Manchester, (1981)*

4 Flynn D, Instrumentation for Fermentation Processes *IFAC Conference on Modelling and Control of Biotechnical Processes, Helsinki (1982)*

5 Schugerl K, Modelling of Biotechnical Processes *IFAC Modelling and Control of Biotechnical Processes, Conference, Noordwijkerhout (1985)*

6 Scheiding W and Hecht V, Aspects of Modelling of Microbial Growth Processes *IFAC Conference on Modelling and Control of Biotechnical Processes, Helsinki (1982)*

7 Johnson A, The Control of Fermentation Processes *IFAC Conference on Modelling and Control of Biotechnical Processes, Conference, Noordwijkerhout (1985)*

8 Bailey J E and Ollis D F, Biochemical Engineering Fundamentals *McGraw-Hill, New York, (1977)*

9 Brauer H, Biotechnology Vol 2 Fundamentals of Biochemical Engineering *VCH, (1985)*

10 Solomons, G L, Materials and Methods in Fermentation *Academic Press, London (1969)*

11 Aiba S, Humphrey A, and Millis N, Biochemical Engineering Second Edition *Academic Press (1973)*

12 Sinclair C and Kristiansen B, Fermentation Kinetics and Modelling *Open University Press (1987)*

13 Nagai S, Mass Energy Balances for Microbial Growth Kinetics *Advances in Biochemical Eng Vol 11, p53, (1979)*

14 Monod J, The Growth of Bacterial Cultures *Annual Rev Microbiology, Vol 3, p371*

15 Contois D, Kinetics of Bacterial Growth , Relationship Between Population Density and Specific Growth Rate of Continuous Cultures, *Journal of Gen Microbiology, Vol 21, p40 (1959)*

16 Vardar–Sukan F, Dynamics of Oxygen Mass Transfer in Bioreactors *Process Chemistry Vol 21, p40-44, (1986)*

17 Wang D, Cooney C and Demain A, Fermentation and Enzyme Technology *Wiley & Sons (1979)*

18 Calderbank P, Physical Rate Processes in Industrial Fermentations Part 1, The Interfacial Area in Gas Liquid Contacting with Mechanical Agitation *Trans Instn Chem Engrs Vol 36, p443 (1958)*

19 Richards J, Studies in Aeration and Aeration *Progress in Industrial Microbiology, Vol 3, p143 (1961)*

20 Bellgardt K, Kuhlmann W and Meyer H, Deterministic Growth Model of *Saccharomyces Cerevisiae*, Parameter Identification and Simulation *IFAC Conference on Modelling and Control of Biotechnical Processes Helsinki (1982)*

21 Hornbeck R, Numerical Methods, *Quantum Publishers, New York, (1975)*

22 Atkinson L, and Harley P, An Introduction to Numerical Methods with Pascal *Addison Wesley, London, (1983)*

23 Ljung L and Soderstrom, Theory and practice of Recursive Identification, *Cambridge Mass, MIT pres (1985)*

24 Isermann R, Parameter Adaptive Control Algorithms - A Tutorial, 6^{th} *IFAC Conference, Digital Computer Applications to Process Control, Dusseldorf (1980)*

25 Astrom K J and Witenmark B, Computer Control Systems, *Theory & Design, Prentice Hall (1984)*

26 Clarke D W, Implementation of Self Tuning Controllers, *Chapter 6 in Self Tuning & Adaptive Control Theory and Applications, Harris S and Billings (Eds) Peter Peregrinus Ltd (1981)*

27 Lozano R and Carillo J, Adaptive Control of a Fermentation Process, *IFAC 9th Triennial World Congress, Budapest (1984)*

28 Mor, J R, A Review of Instrumental Analysis in Fermentation Technology, *The First European Conference on Computer Control in Fermentations, Dijon, France (1973)*

29 Llyod, D et al, Mass Spectrometry in Fermentation Processes, *Trends in Biotechnology, 1,60 (1983)*

30 Astrom, K J and Wittenmark, B, Computer Controlled Systems *Prentice -Hall, 629 895 (1984)*

31 Gallegos, J A and Gallegos, J, Estimation and Control Techniques for Continuous Culture Fermentation Processes *Biotechnology and Bioengineering, Vol 16,pp 442-451 (1984)*

32 Willamson, D, Observation of Bilinear Systems with Application to Biological Control *Automatica, 13, 243-255 (1977)*

33 Dochain, D, On-line Parameter Estimation, Adaptive State Estimation, Adaptive Control of Fermentation Processes *Ph.D Thesis, University of Louvain (1986)*

34 Dochain, D and Bastin, G, Adaptive Identification and Control Algorithms for Non–Linear Bacterial Growth Systems *Automatica, 20,621-634 (1984)*

35 Stephanopoulos G and Ka–Yiu San., On–Line Estimation of Time Varying Parameters Application to Biochemical Reactors *IFAC Conference on Modelling and Control of Biotechnical Processes, (Helsinki,Finland) (1982)*

36 Dekkers R M , State Estimation of a Fed–Batch Bakers Yeast Fermentation. *IFAC Conference Modelling and Control of Biotechnical Processes, (Helsinki,Finland) (1982)*

37 Jazwinski A H , Stochastic Processes and Filtering Theory *Academic Press, New York (1970)*

38 Miskiewicz T et al, Control of Nutrient Supply in Yeast Propagation. *Biotechnology & Bioeng , 17, 1829-1832*

39 Kobayashi, T et al, Automatic Control of Dissolved Oxygen Concentration with a Microcomputer *6th International Fermentation Symposium on Advances in Biotechnology, London, Canada (1980)*

40 Aiba, S , Nagai, S , Nishizawa, Y , Fed Batch Culture of *Saccharomyces Cerevisiae* a pespective of computer to enhance the productivity in Bakers Yeast cultivation *Biotech & Bioeng ,18, 1001-1016 (1976)*

41 Perinnger, P , Blachers, H T , Modelling and Optimal Control of Bakers Yeast Production in Repeated Fed-Batch Culture *Proc 2nd Int Conf on Computer Appl in Ferm Tech , Univ of Pennsylvania, Philadelphia*

42 Raimerez, A , et al, Optimization of Fermentation Plants *Biotechnology Letters, 3,(10), 205-560*

43 Wohrer, W , et al, Ethanol and RQ Based Computer Control in Fed Batch Cultures of Bakers Yeast. *6th International Fermentation Symposium on Advances in Biotechnology, London, Canada (1980)*

44 Cooney, C , Wang, H , Wang, D , Computer Control of Bakers Yeast Processes *Biotechnology & Bioeng , 19, 55-67 (1977)*

45 Wang, H , Wang, D , Cooney, C, Computer Aided Penicillin Fermentation. *Biotechnology & Bioeng , 19, 69-86, (1977)*

46 Wang, H , Wang, D , Cooney, C, Computer Aided Penicillin Fermentation. *Biotechnology & Bioeng , 21 975-995, (1979)*

47 Weigand, W et al, Optimal Productivity in a Fed-Batch Reactor, *Biotech & Bioeng Symp No 9, 335-348 (1979)*

48 Constatnunides, A et al, Optimization of a Fed-Batch Fermentation Process Part 1, Development of Mathematical Models for Batch Penicillin *Biotech & Bioeng, 12, 803-830 (1970)*

49 Blanch, H and Rogers, P, Computer Control and Optimisation of Microbial Production. *Biotech & Bioeng, 14, 151-171 (1972)*

50 Takamatasu, T, Shioya, S, Shiota, M ,Kitabata, T, Theory and Practice of Optimal Control in Continuous Fermentation Processes *Biotechnology & Bioeng Symp No 9, 283-301 (1979)*

51 Yousefpour, P, Williams, P, Control of a Fermentation Process Using an Adaptive Technique *Biotechnology Letters 3(9), 519-524 (1981)*

52 Moir, T J and Grimble, M J, Optimal Self Tuning Filtering , Prediction and Smoothing for Discrete Multivariable Processes *IEEE Trans on Auto Contr, Vol AC-29, No 2,pp 128-137, Feb (1984)*

FIGURES

FIG 2.1 METABOLIC SCHEME FOR SACCHAROMYCES CEREVISIAE

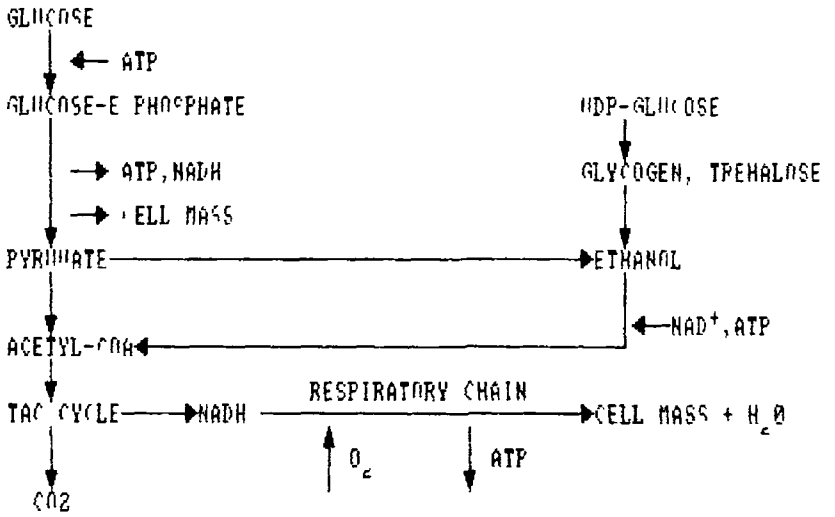

FIG 2.2 SIMPLIFIED SCHEME OF THE METABOLISM OF S. CEREVISIAE

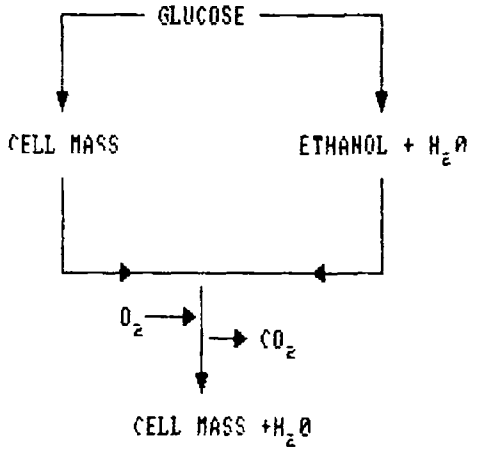

FIG 2.3 OUTLINE FLOWCHART OF SIMULATION PROGRAM.

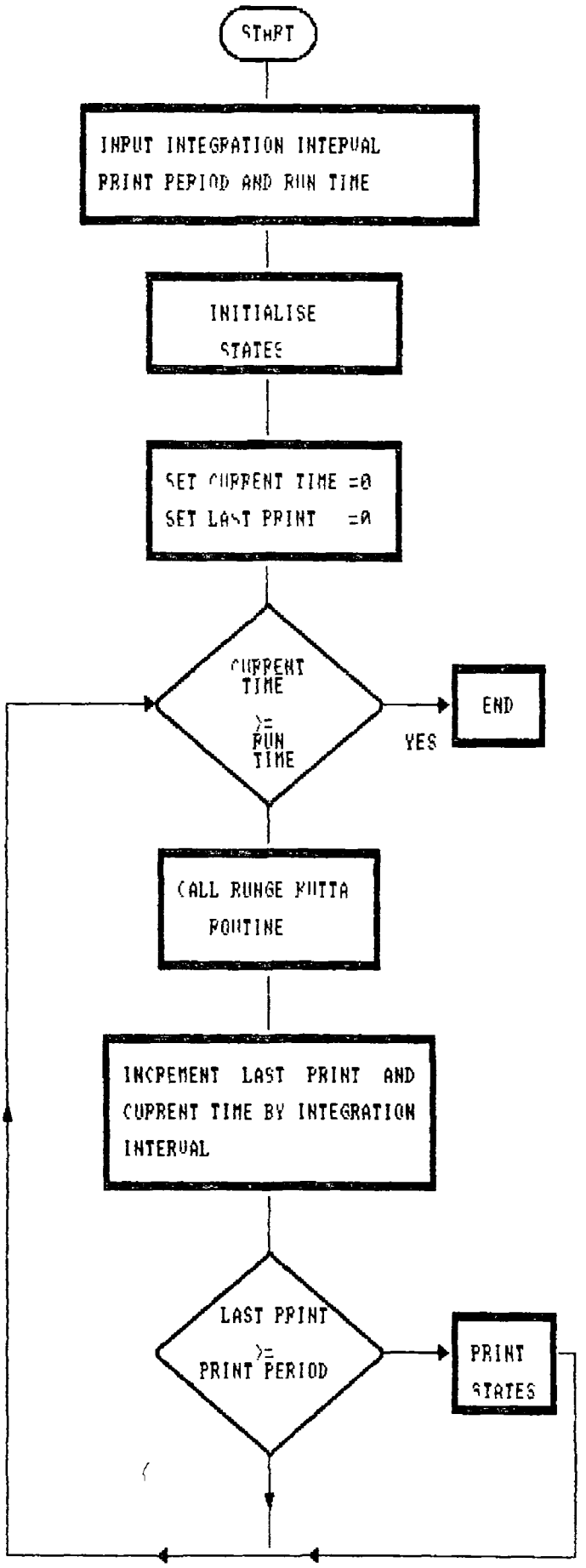

FIG 2.4 FLOWCHART OF RUNGE-KUTTA SUBROUTINE

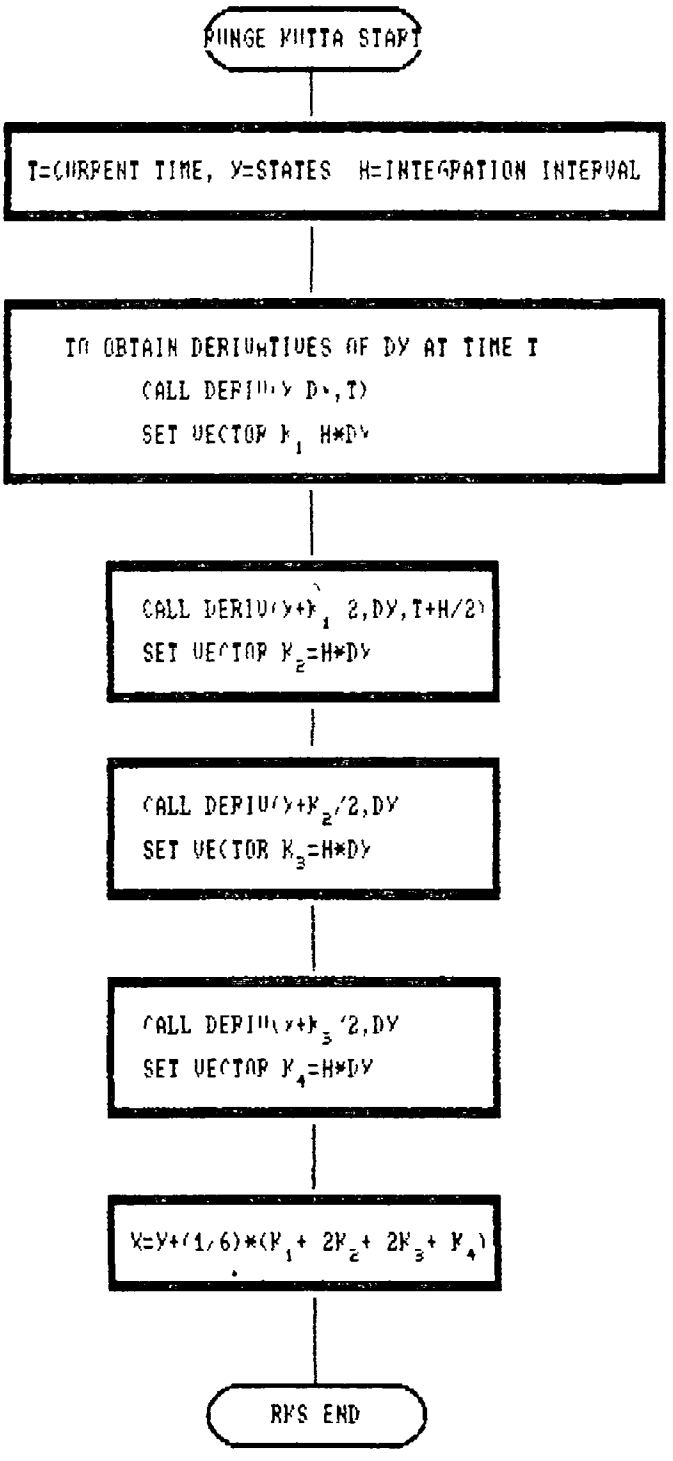

FIG 2.5 OUTLINE FLOWCHART OF SUBROUTINE WITH DIFFERENTIAL EQTS. OF THE MODEL

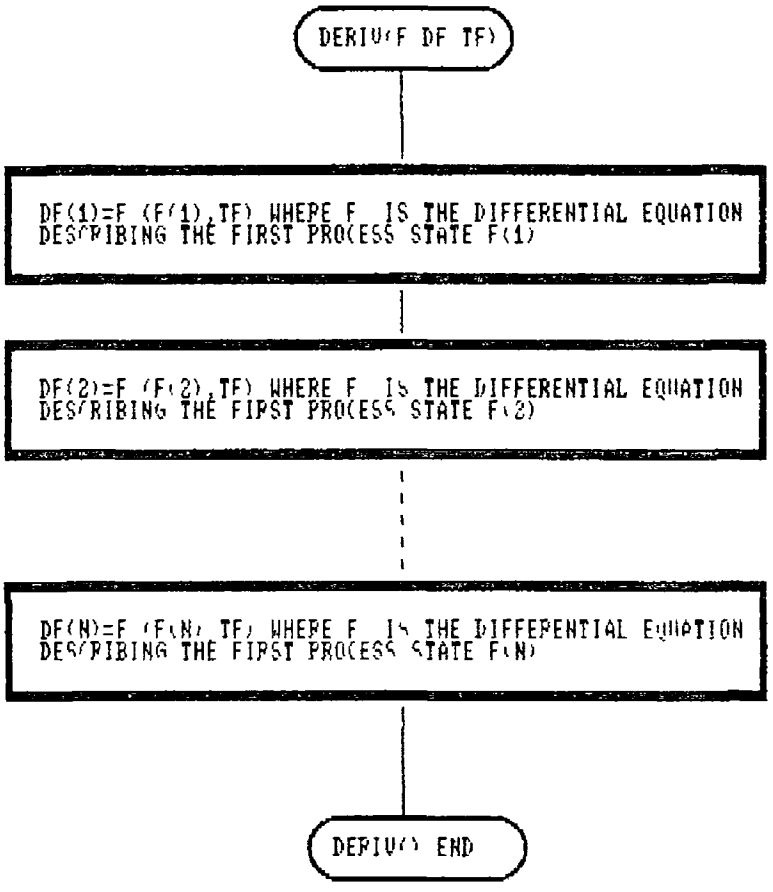

Fig 3.1 Growth Rate,lambda=0.99

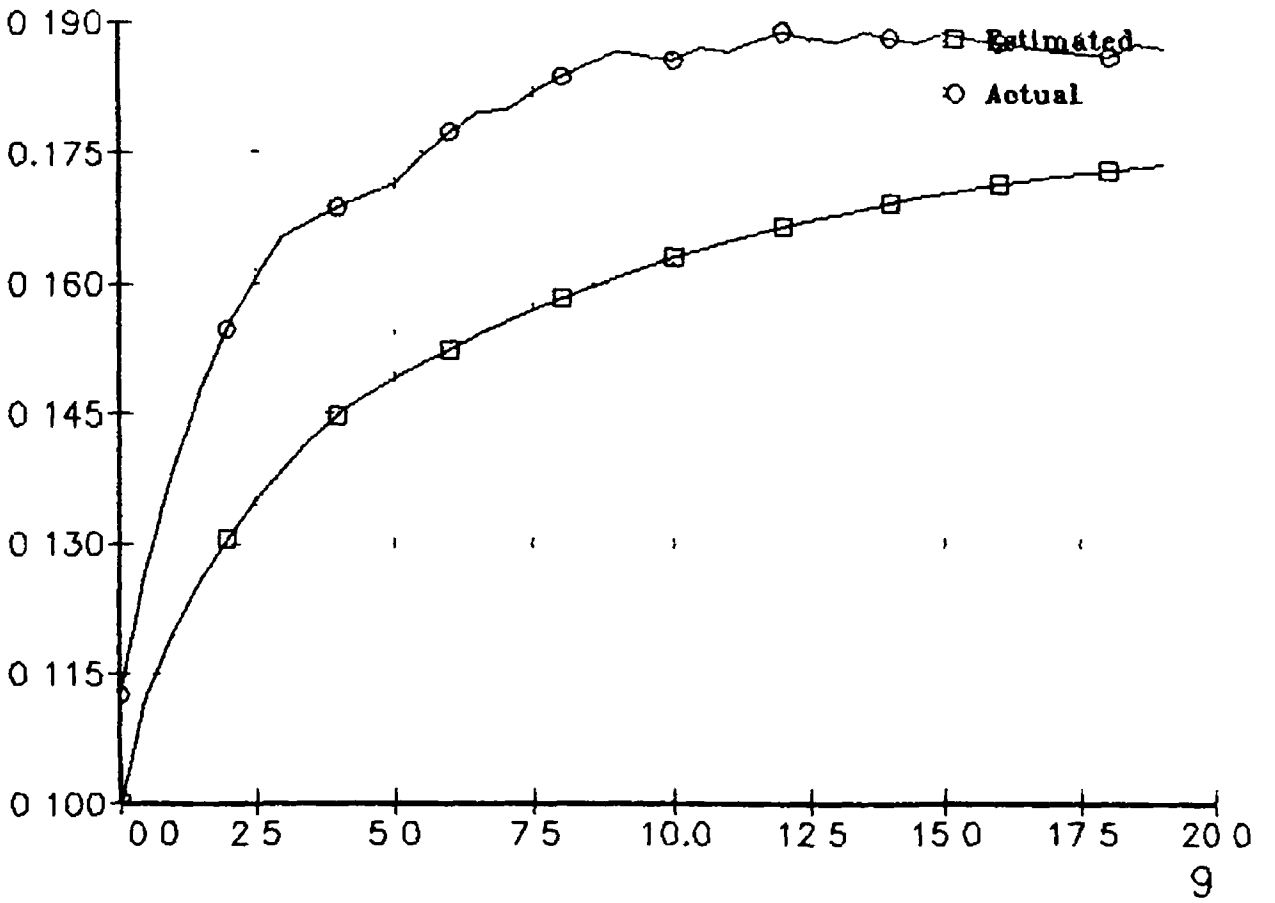

Fig 3.2 Growth Rate,lambda=exp

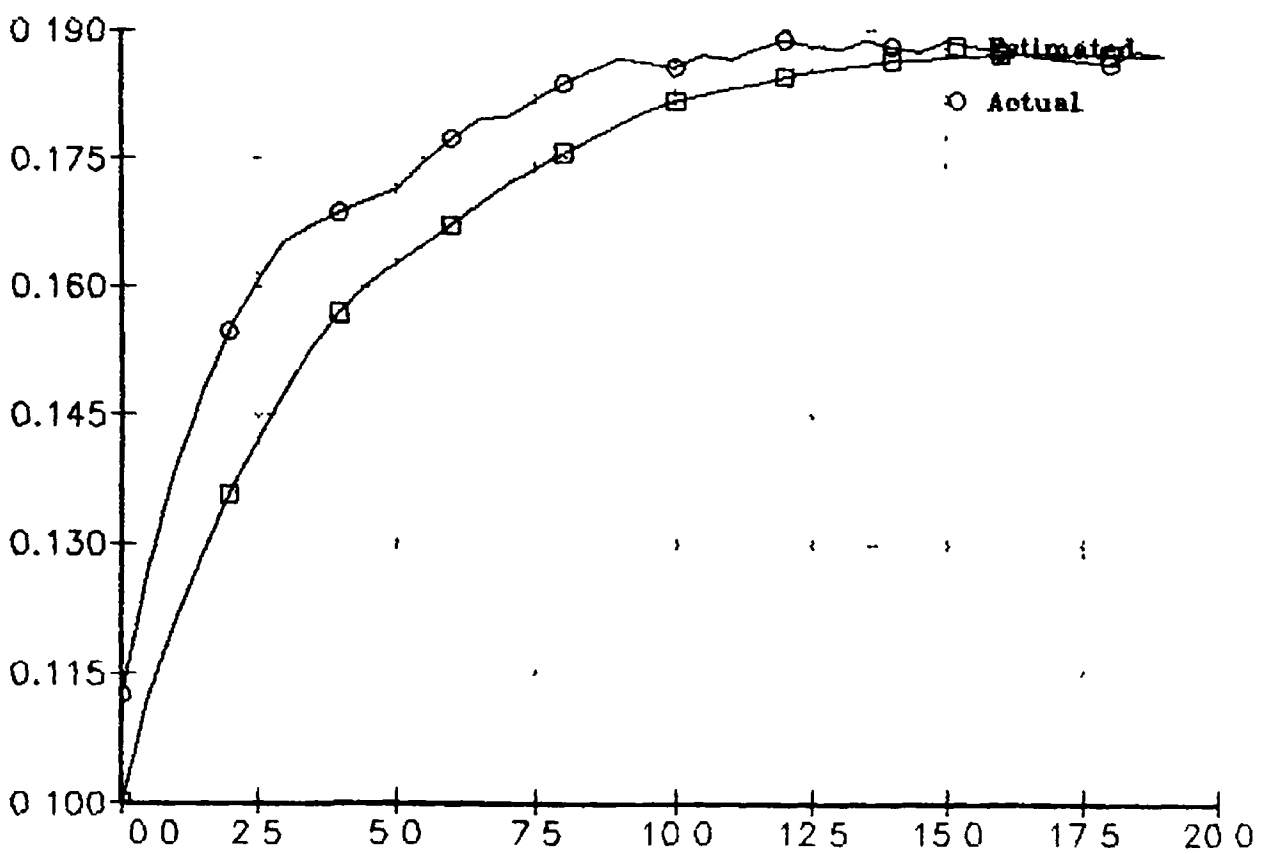

Fig 3.3 Monod,lambda=0.99

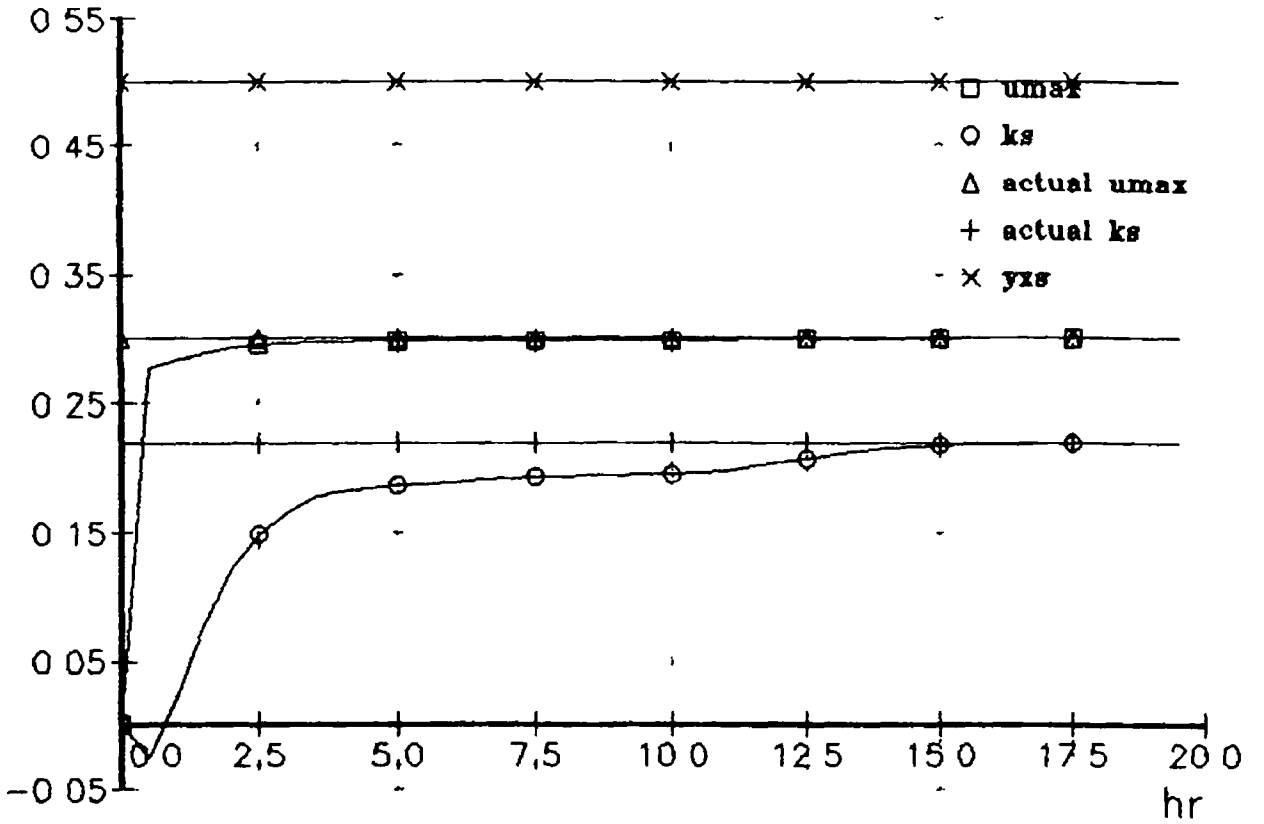

Fig 3.4 Monod,lambda=exp

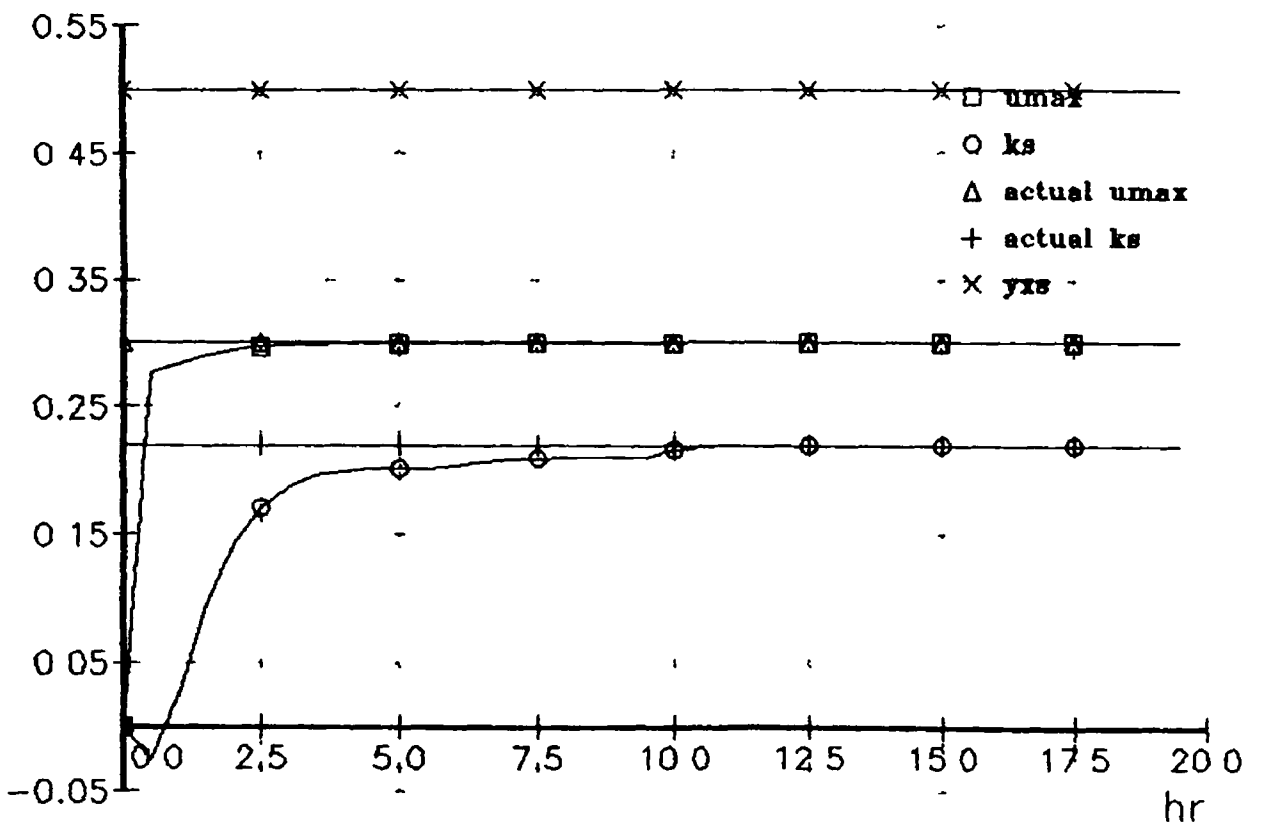

Fig 3.5a Ollson Parameters

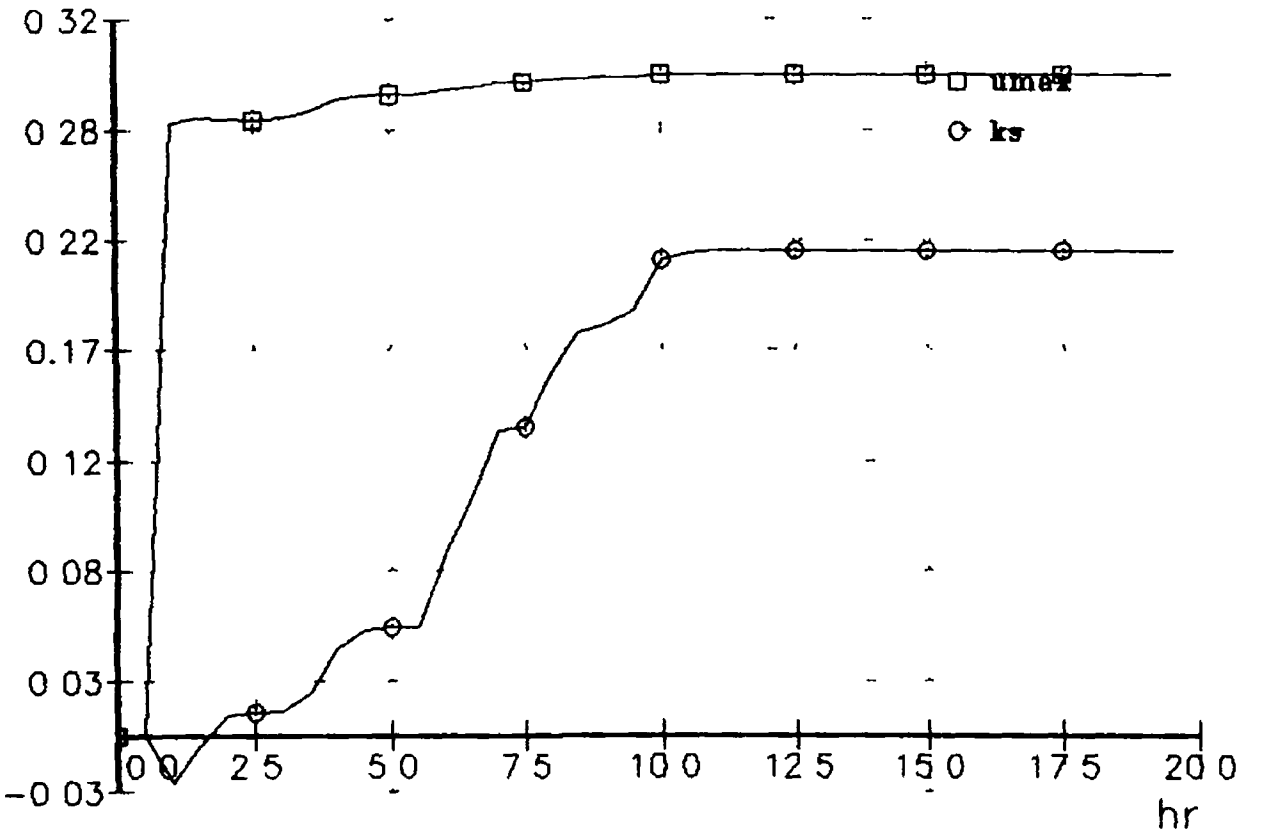

Fig 3.5b Ollson Parameters

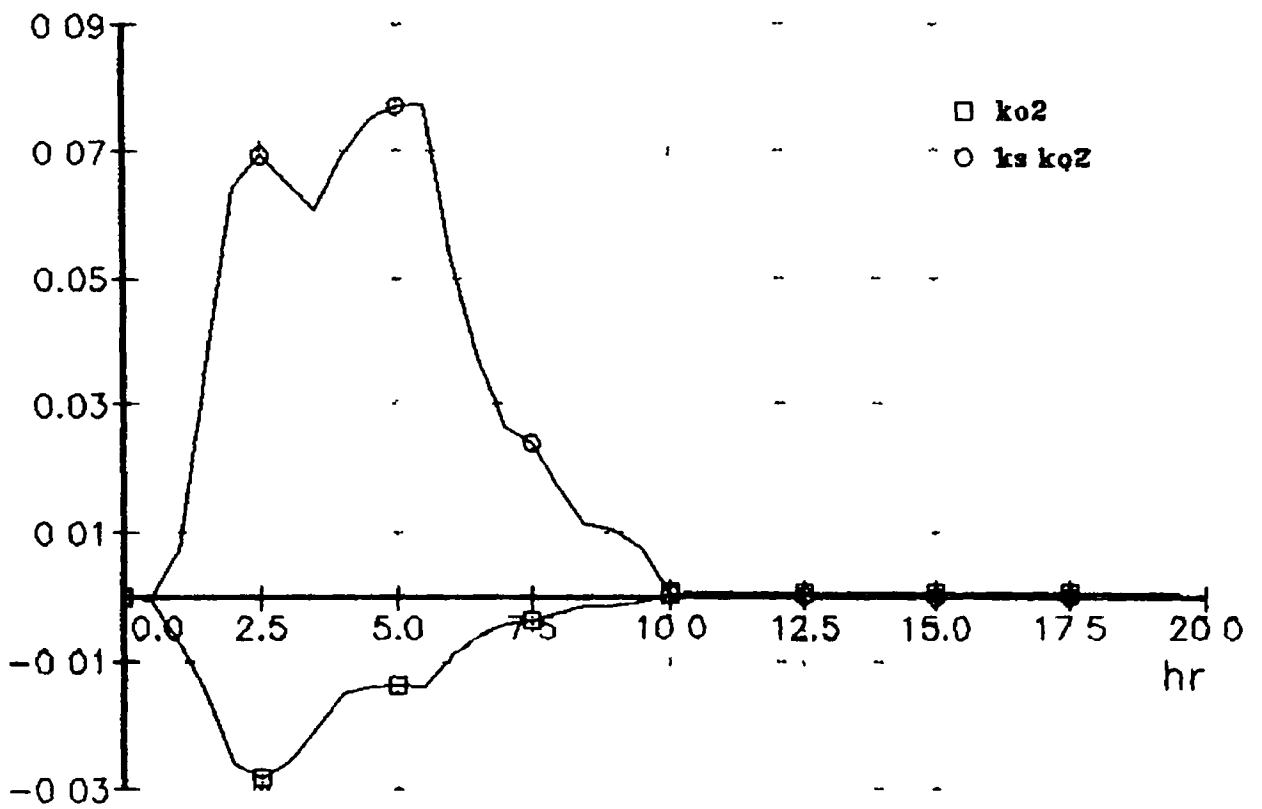

Fig 3.6a Comprehensive Model

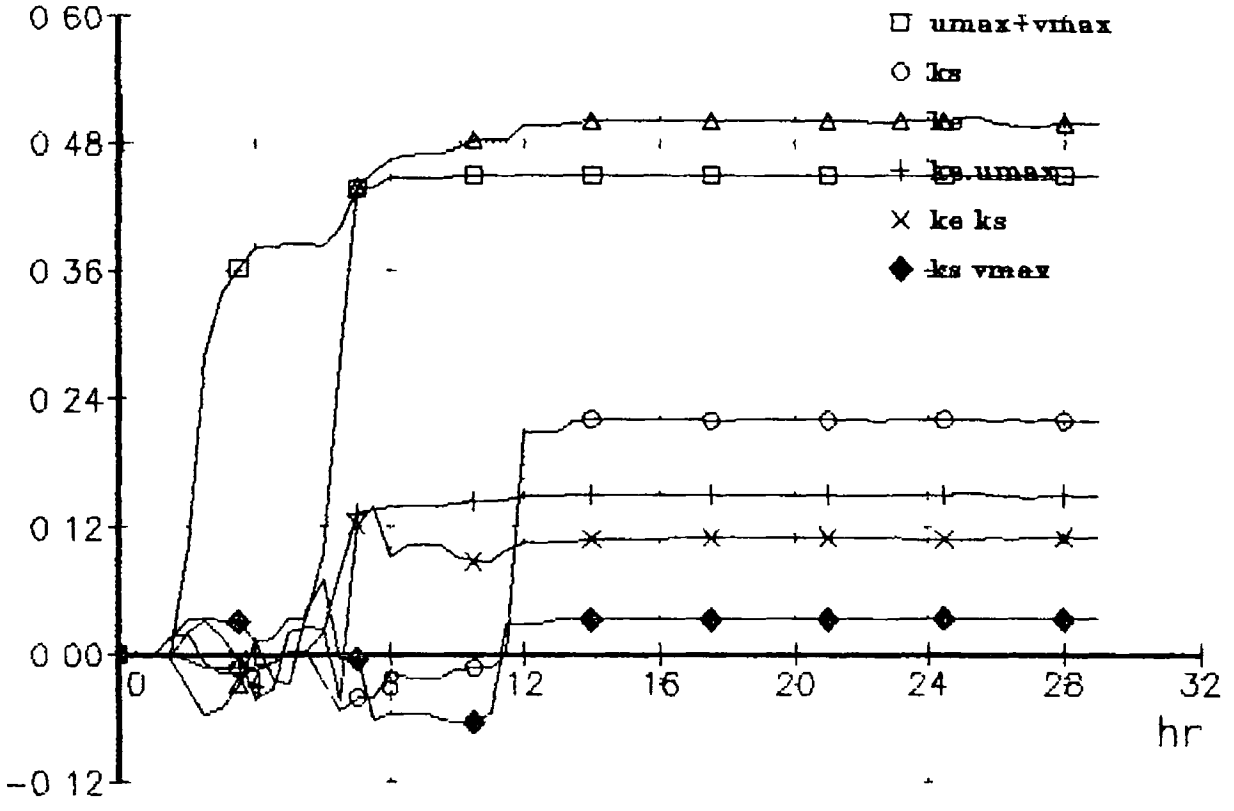

Fig 3.6b Comprehensive Model

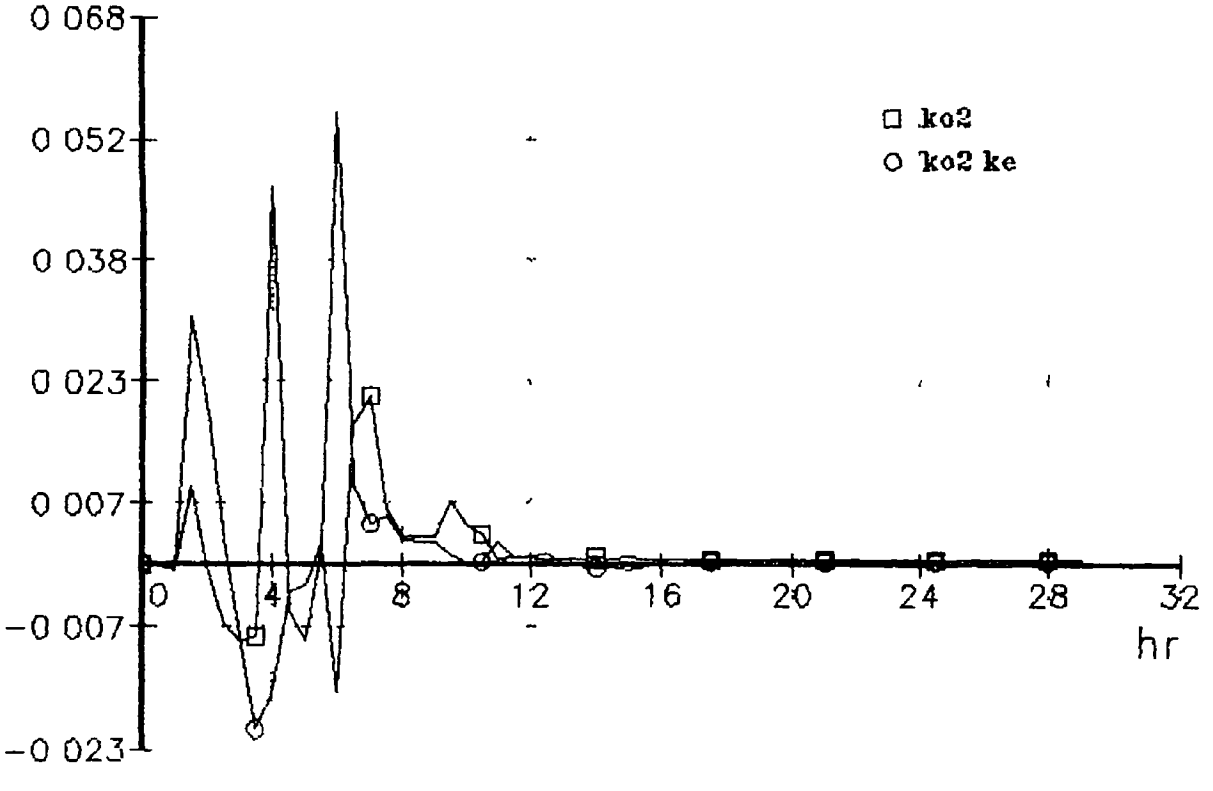

Fig 3.6c Comprehensive Model

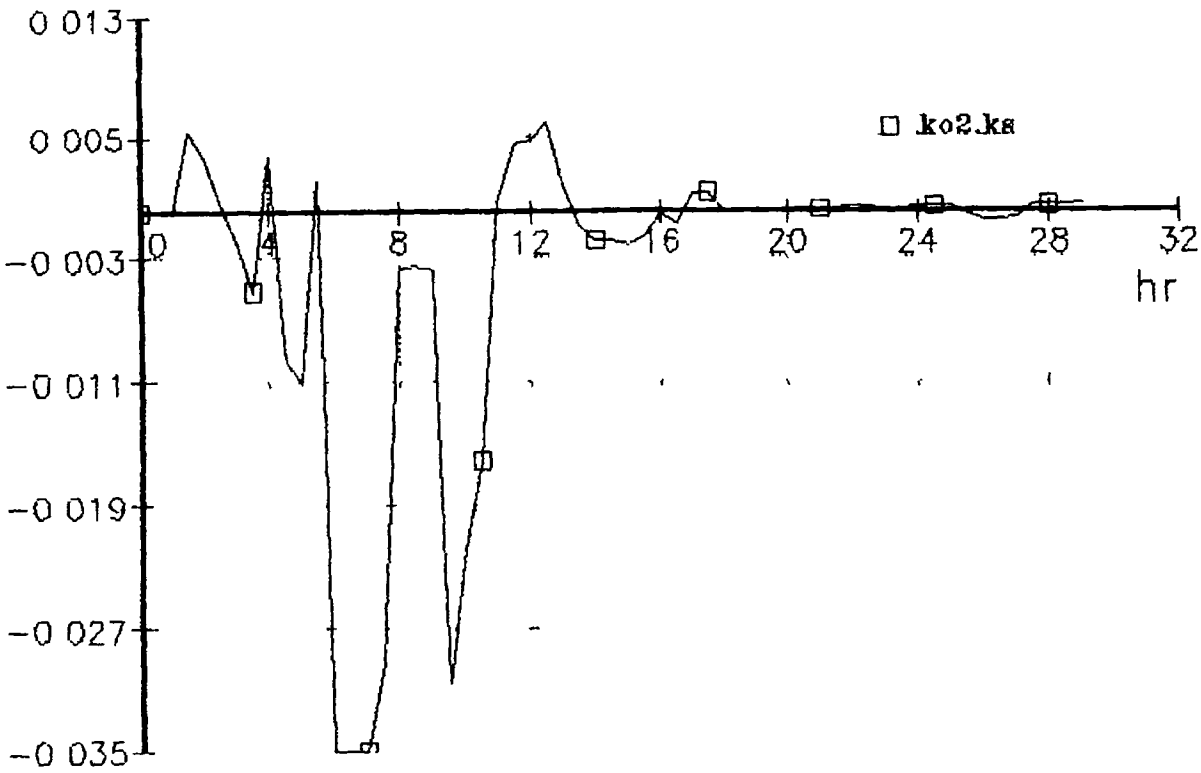

Fig 6.3d Comprehensive Model

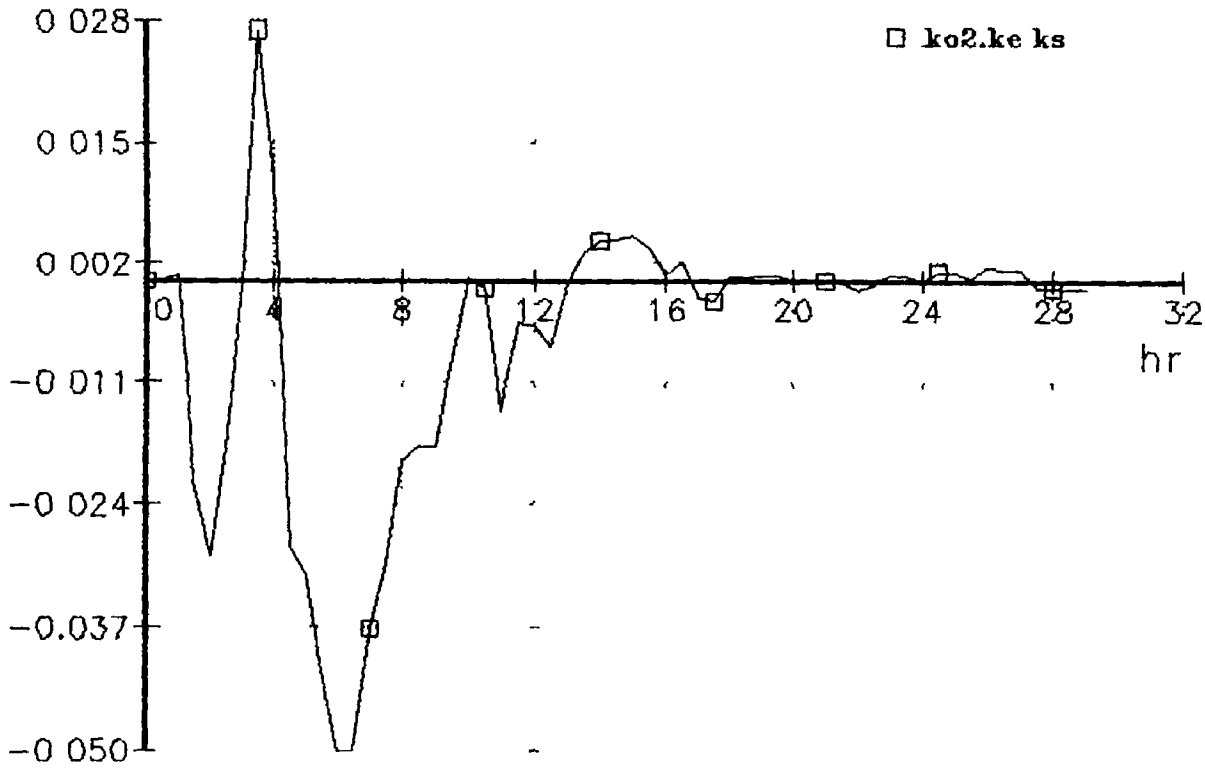

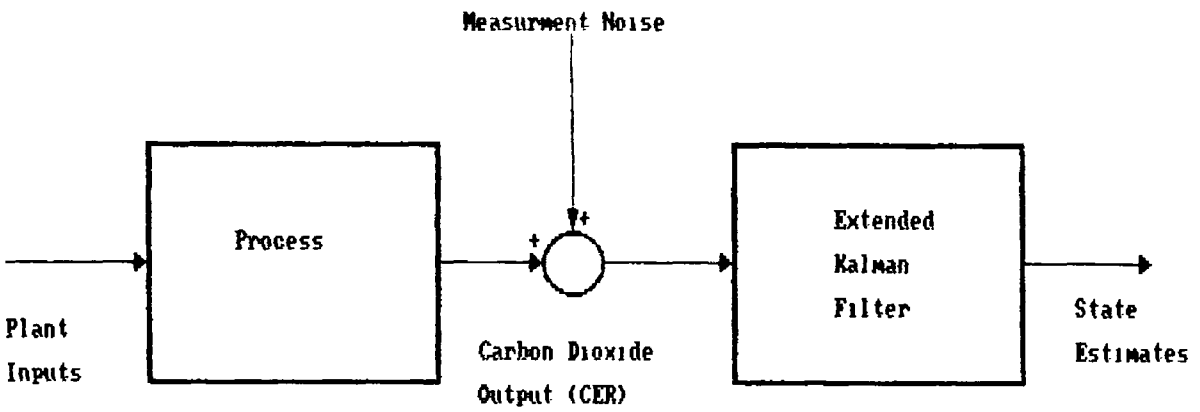

Figure 4.1 State Estimation Scheme.

Fig 4.2a NL Observer,h=0.5

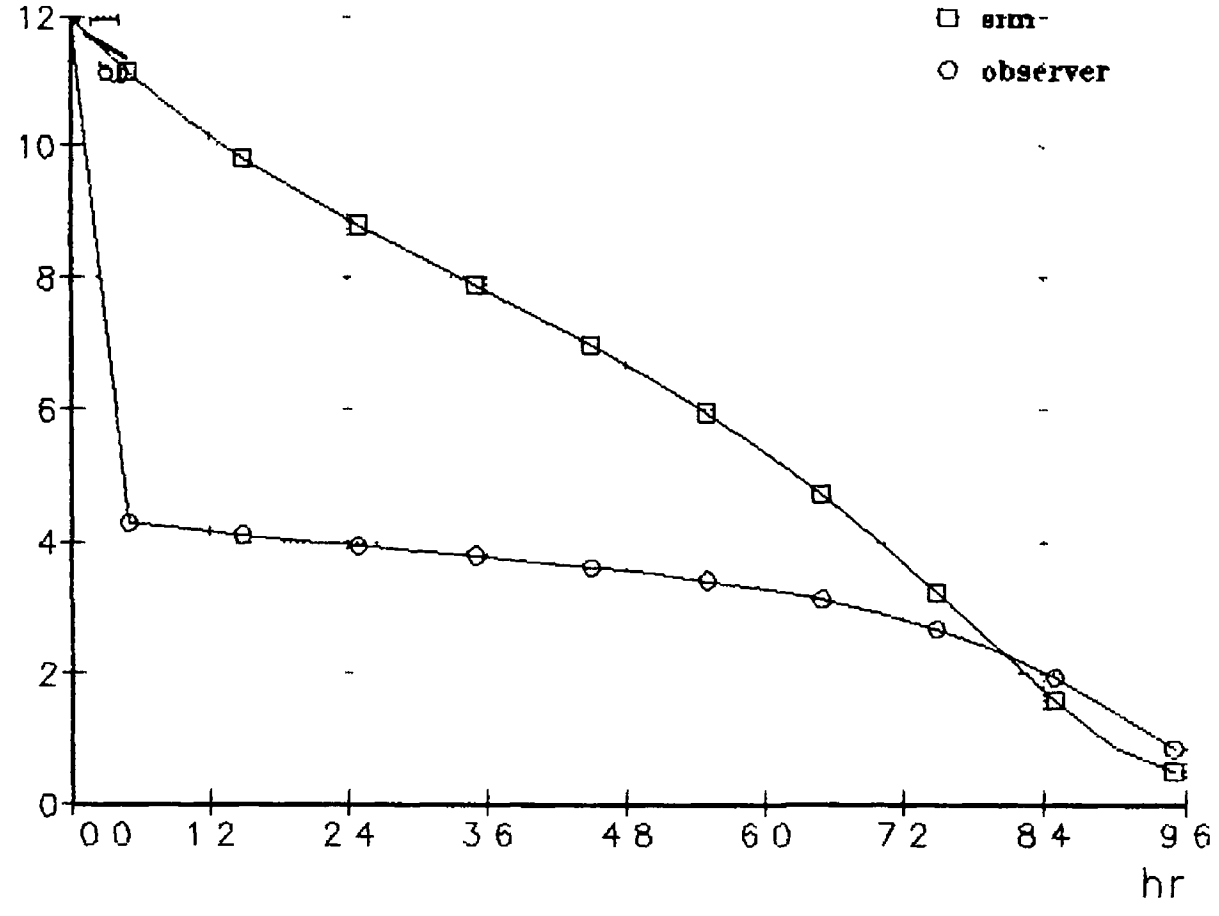

Fig 4.2b NL observer,h=0.05

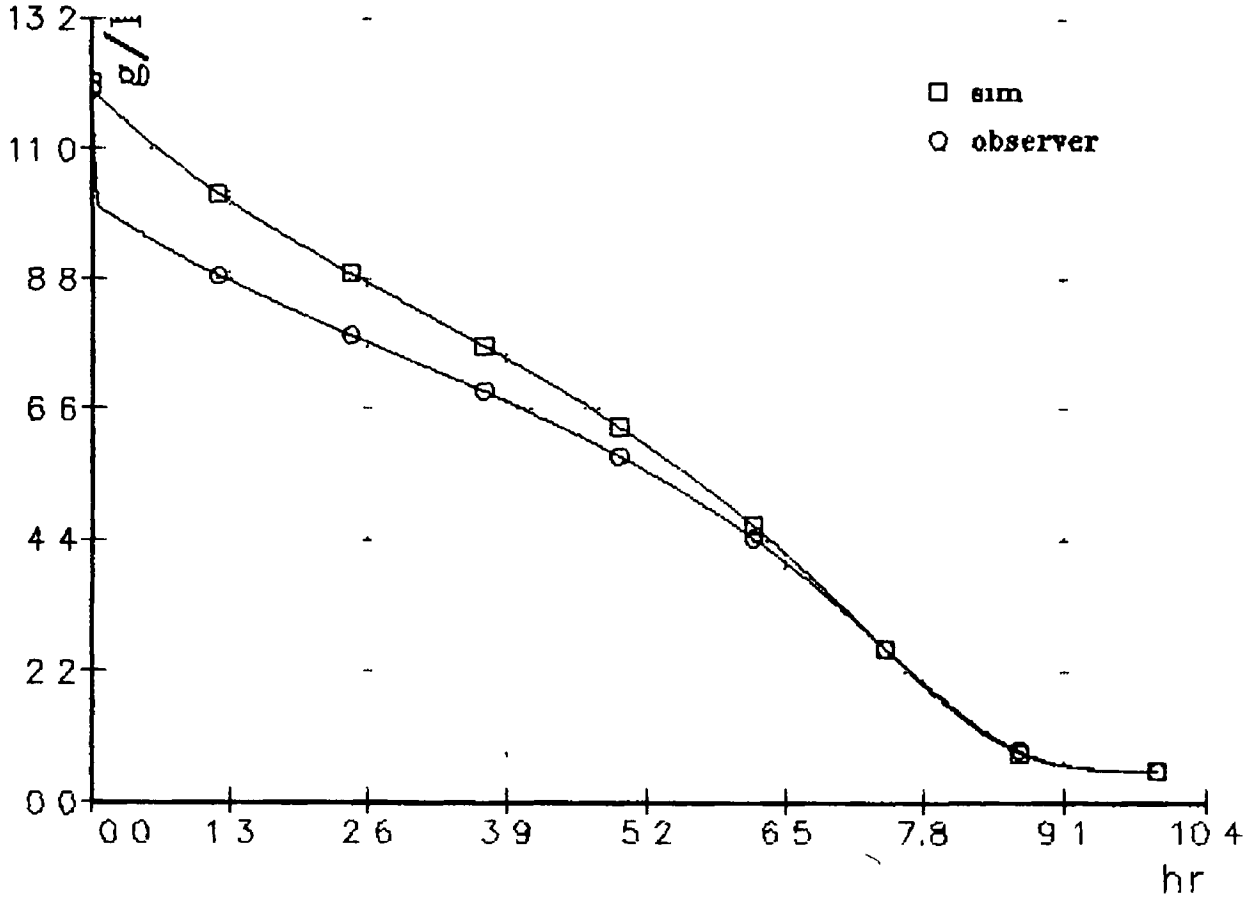

Fig 4.2c NL Observer,h=0.025

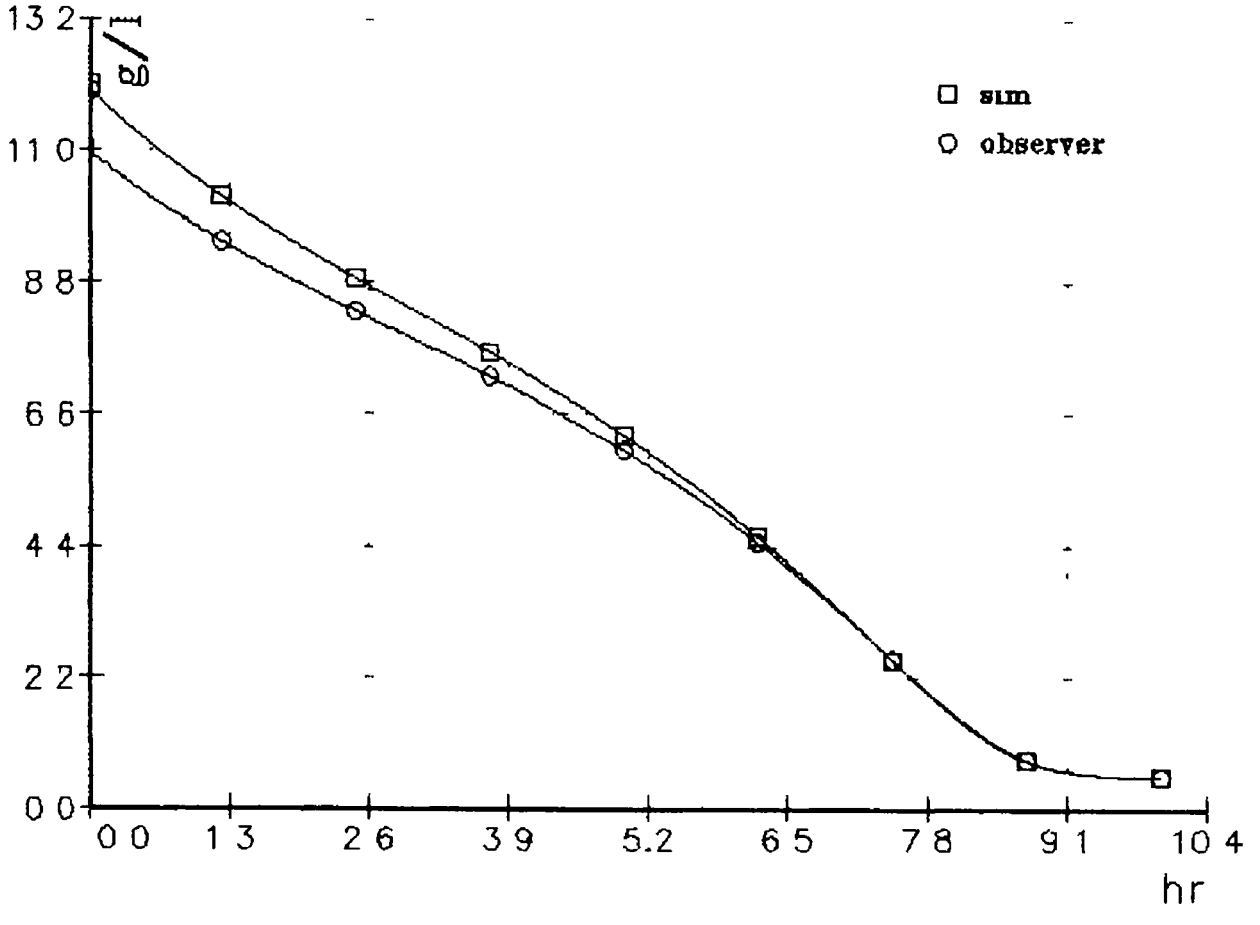

Fig 4.3 NL observer,umax+15%

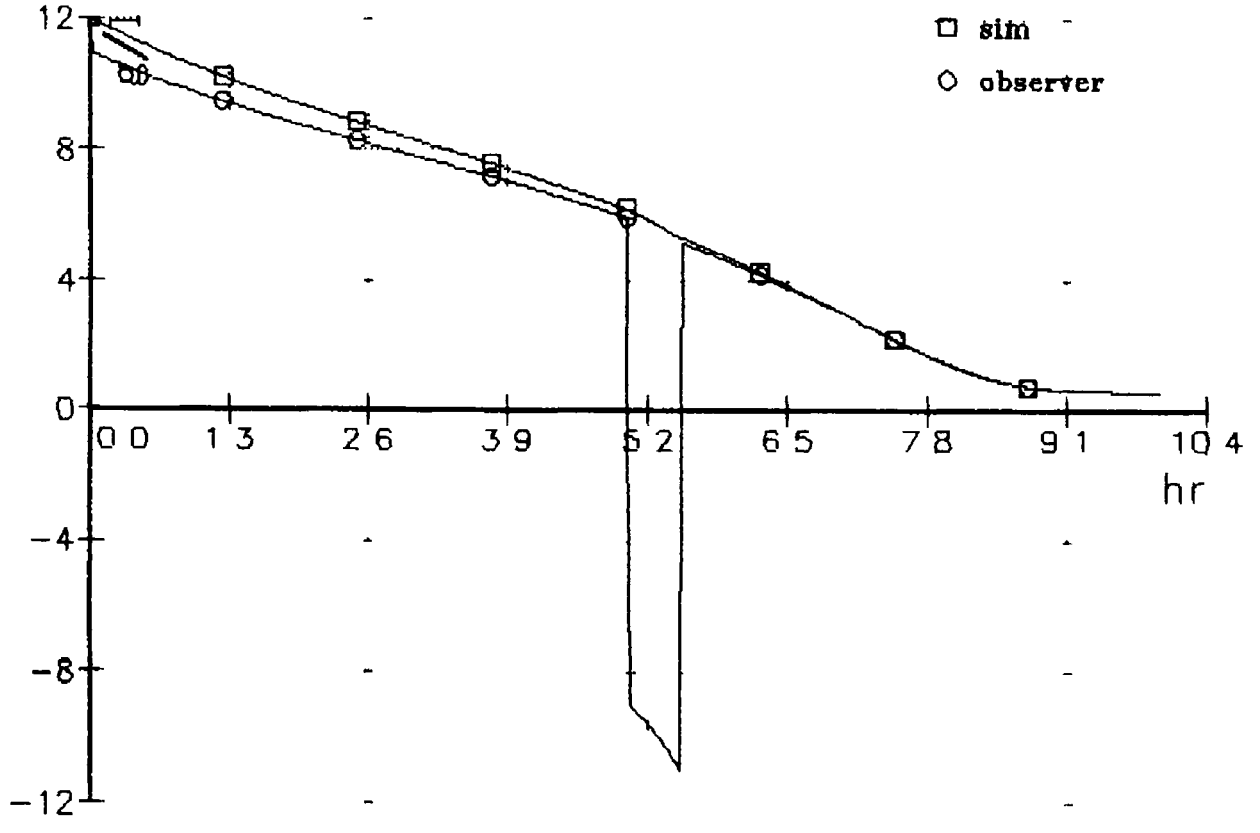

Fig 4.4 NA observer,D=0.42

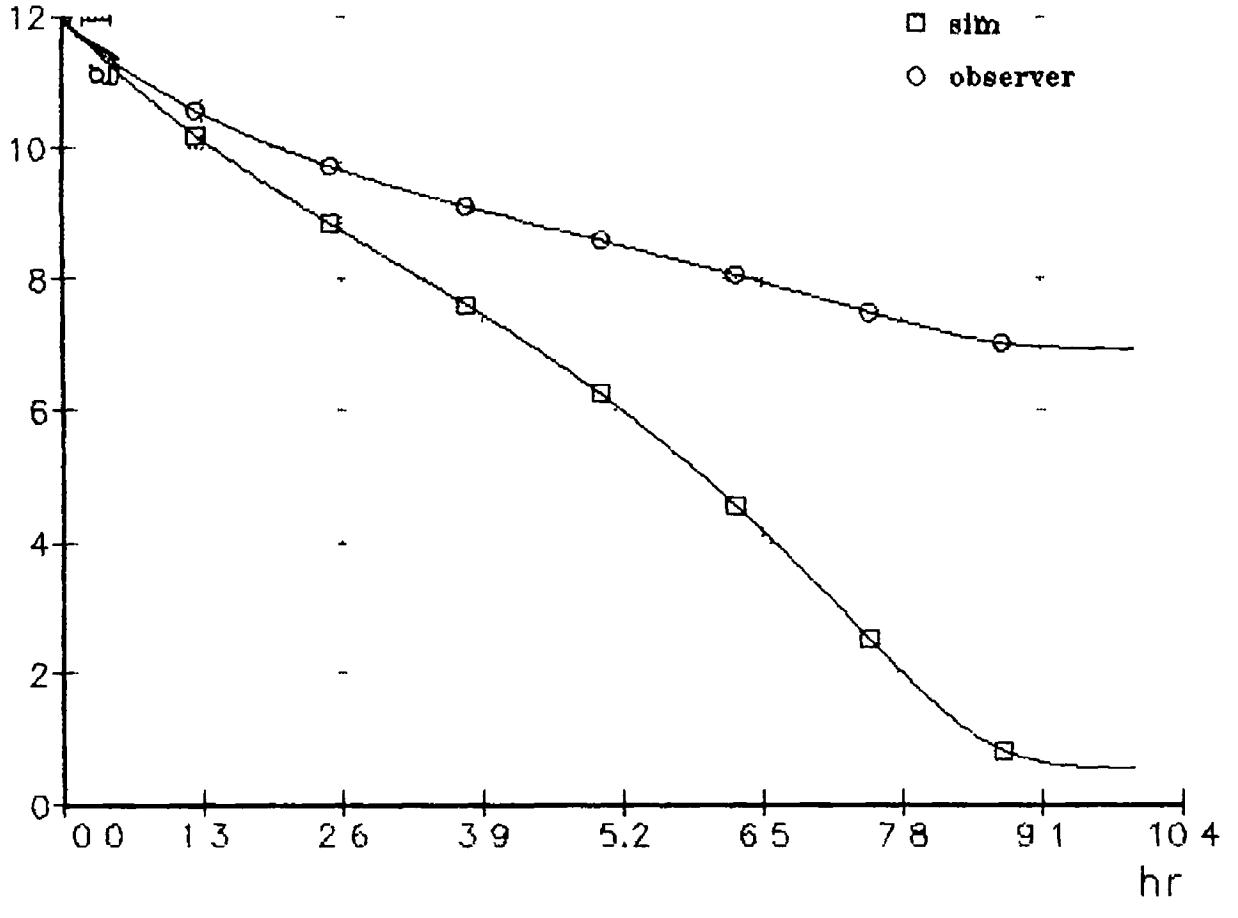

Fig 4.5 NA observer,D=0.75

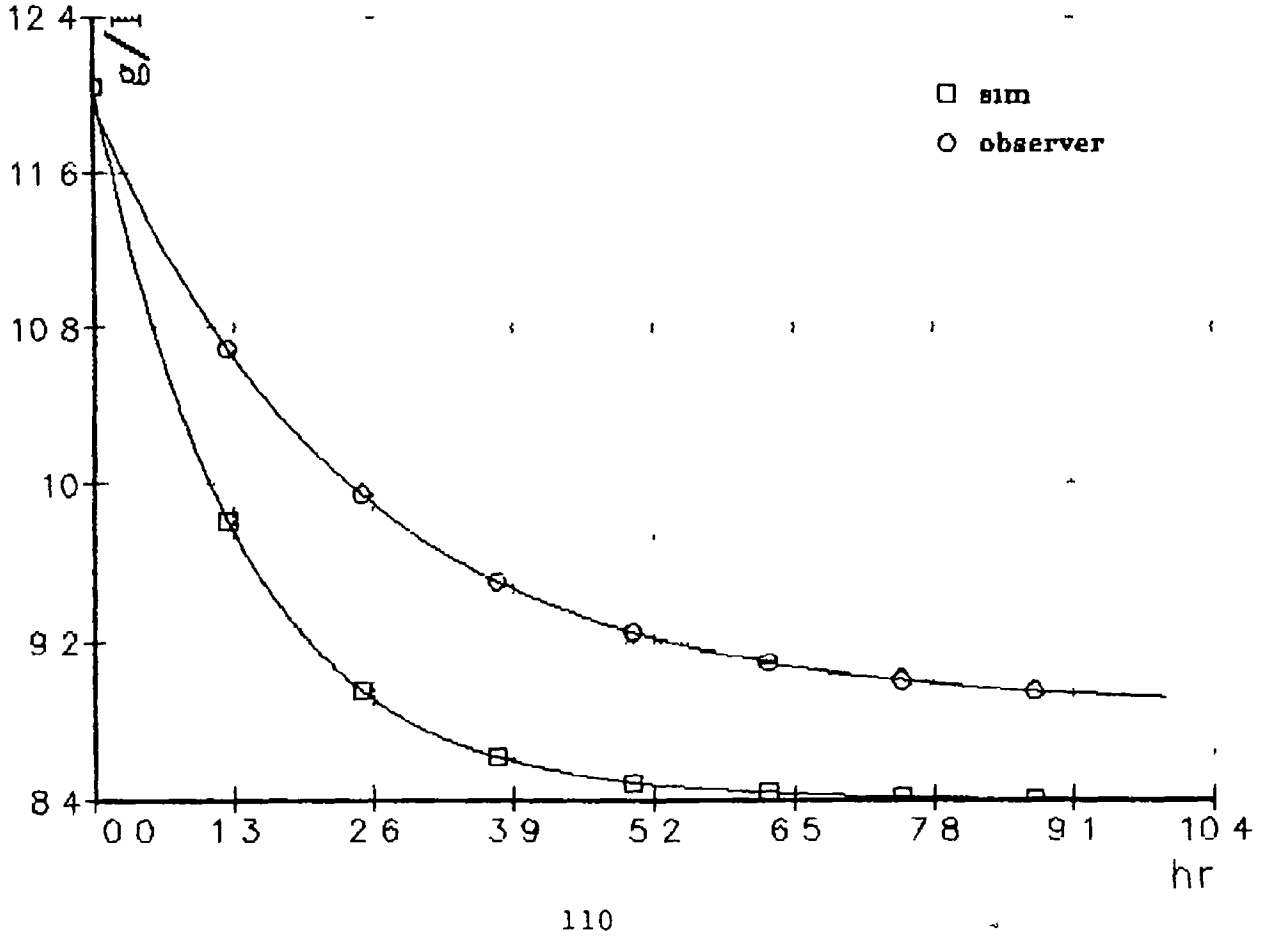

Fig 4.6 NA observer,D=0

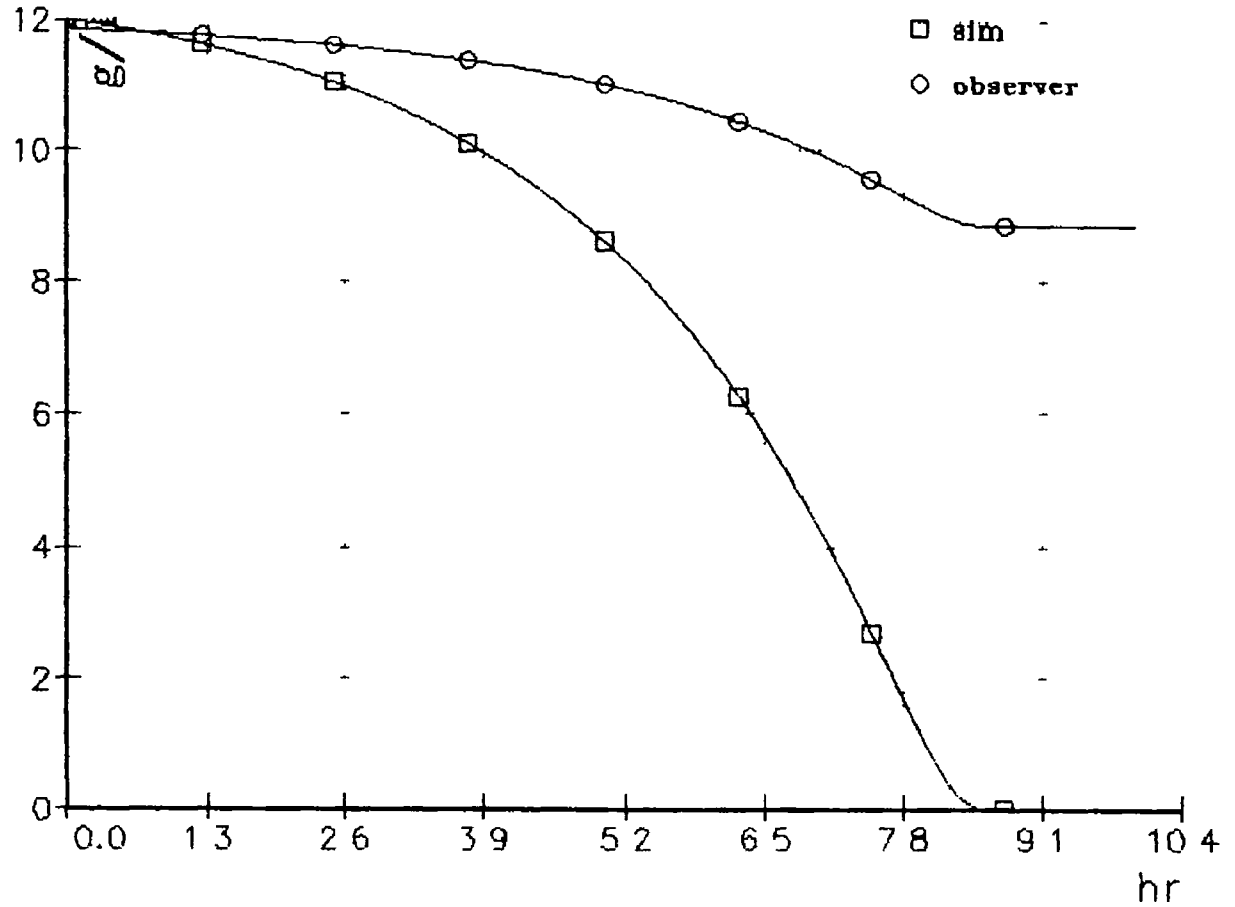

Fig 4.7 CO2 Evolution Rate

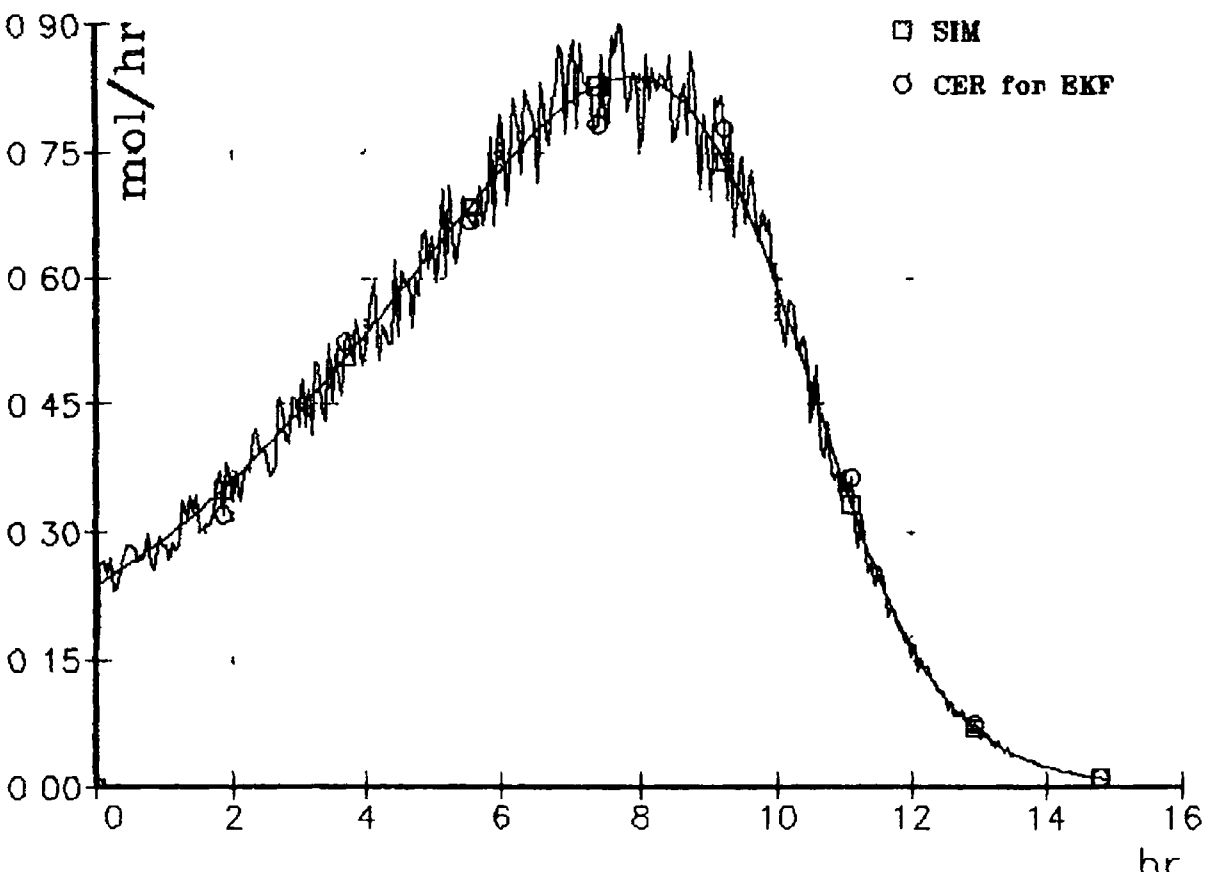

Fig 4.8 EKF – Biomass

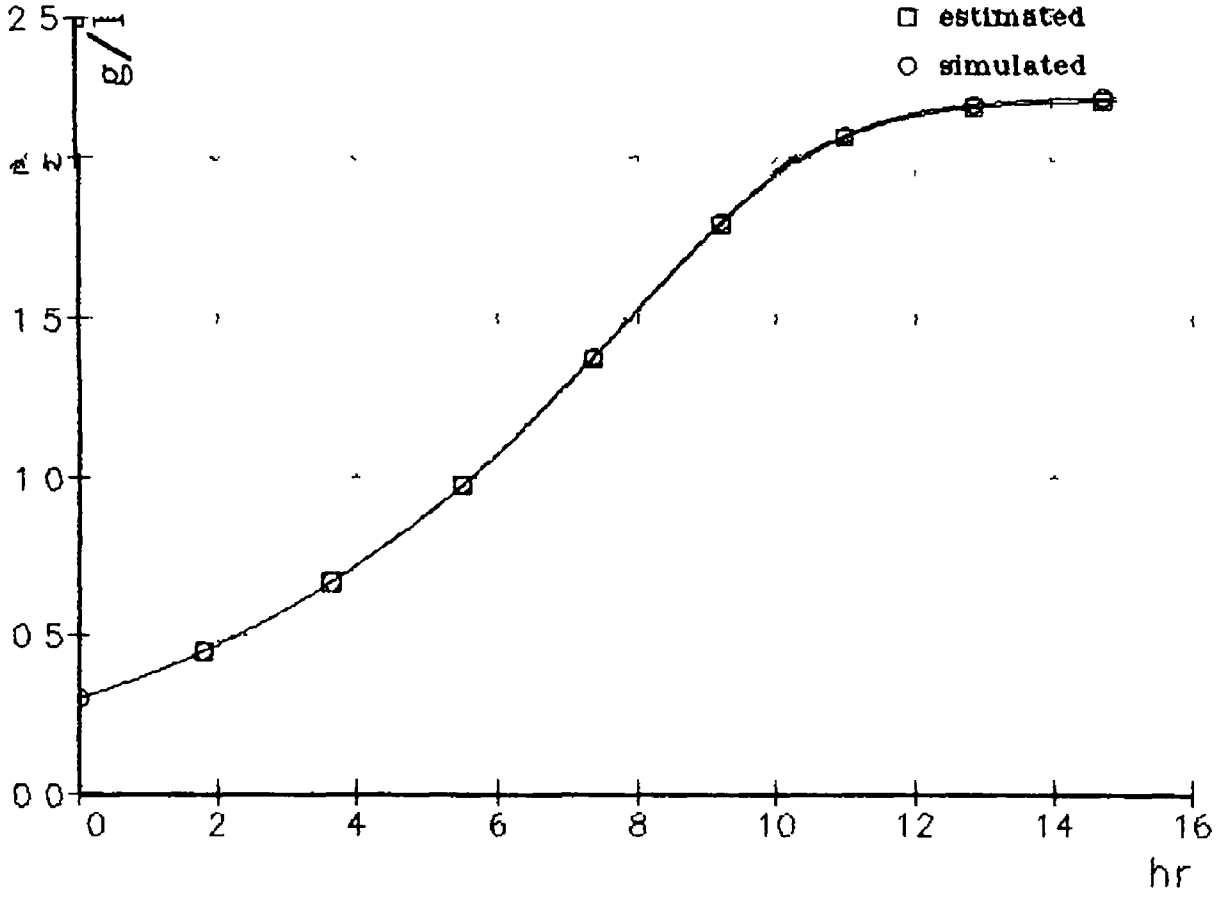

Fig 4.9 EKF – Substrate

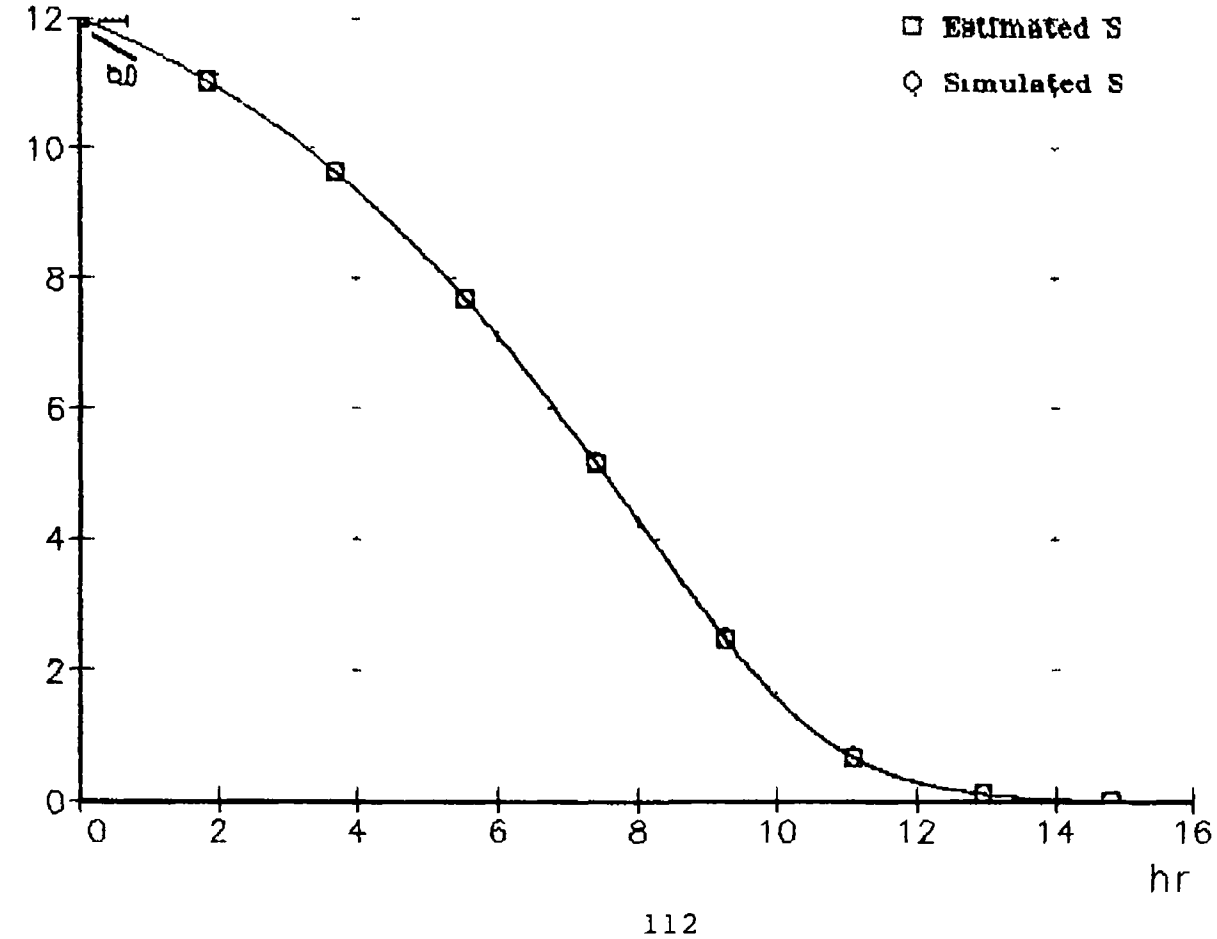

Fig 4.10 EKF – Biomass

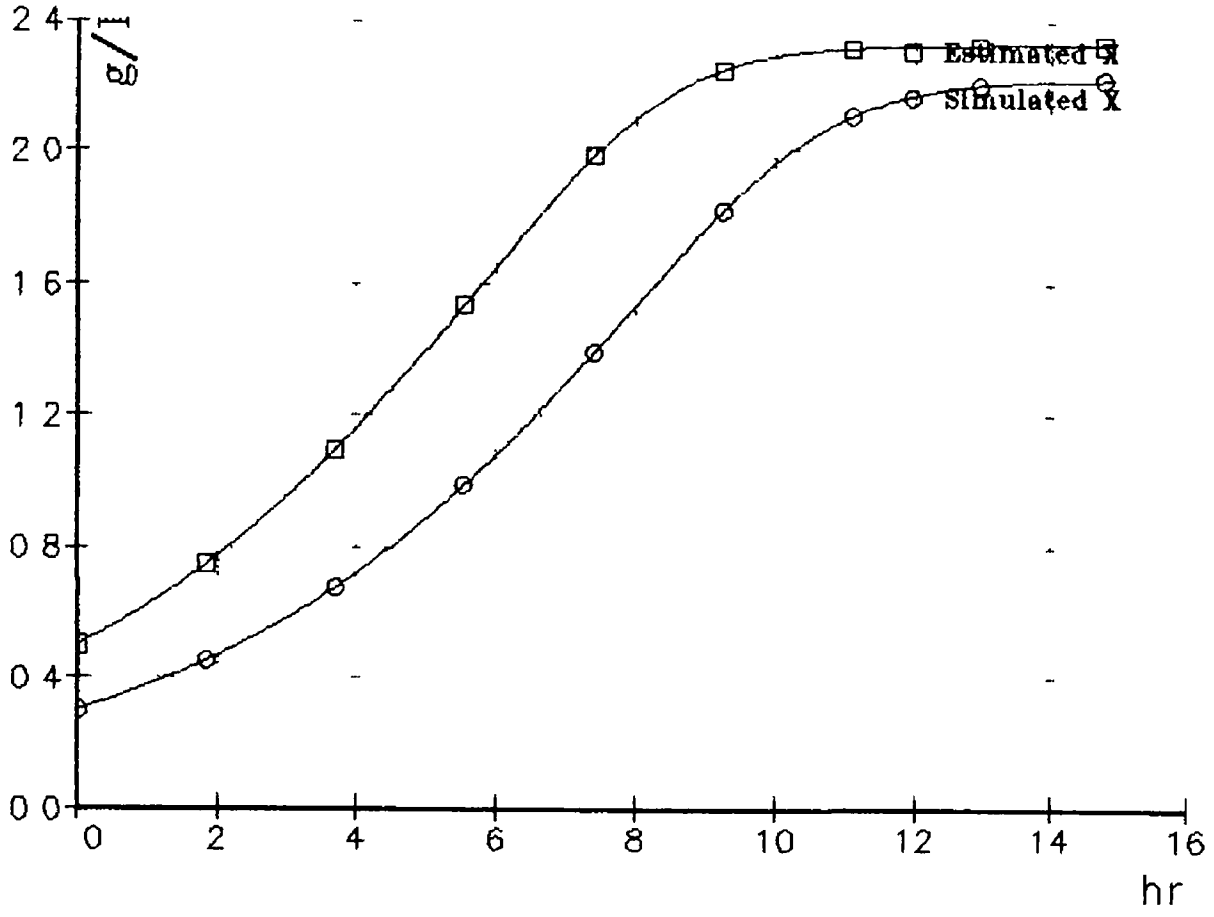

Fig 4.11 EKF – Substrate

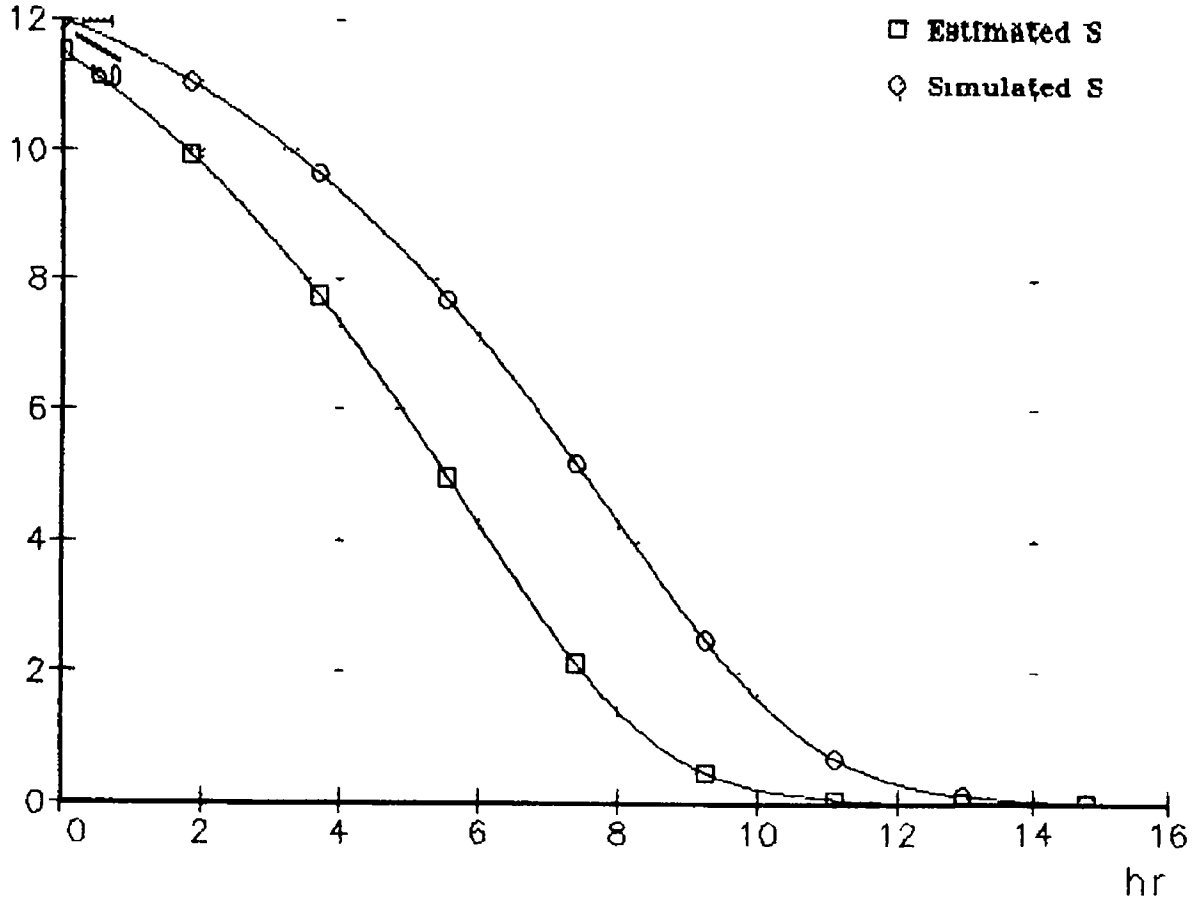

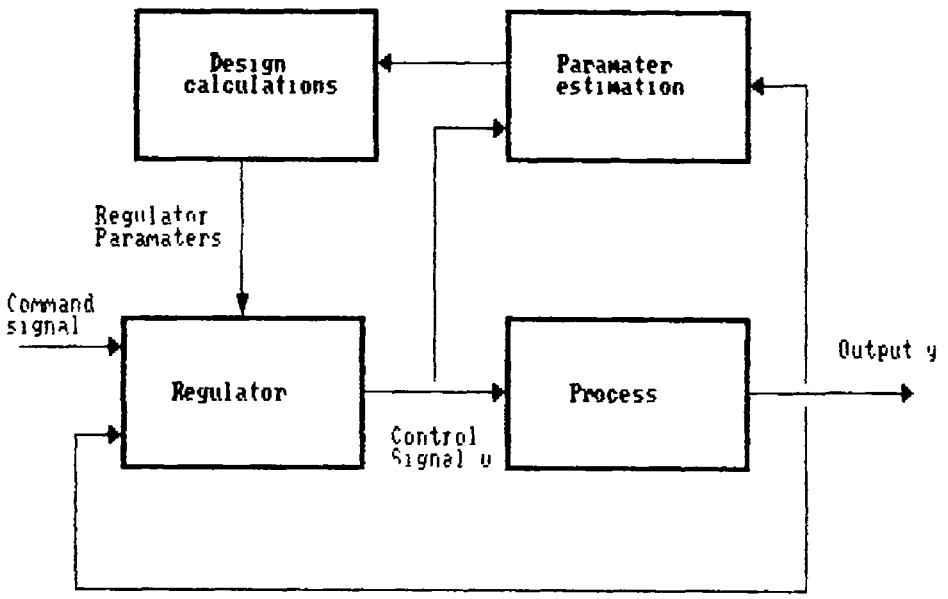

Fig 5.1 Self Tuning Regulator

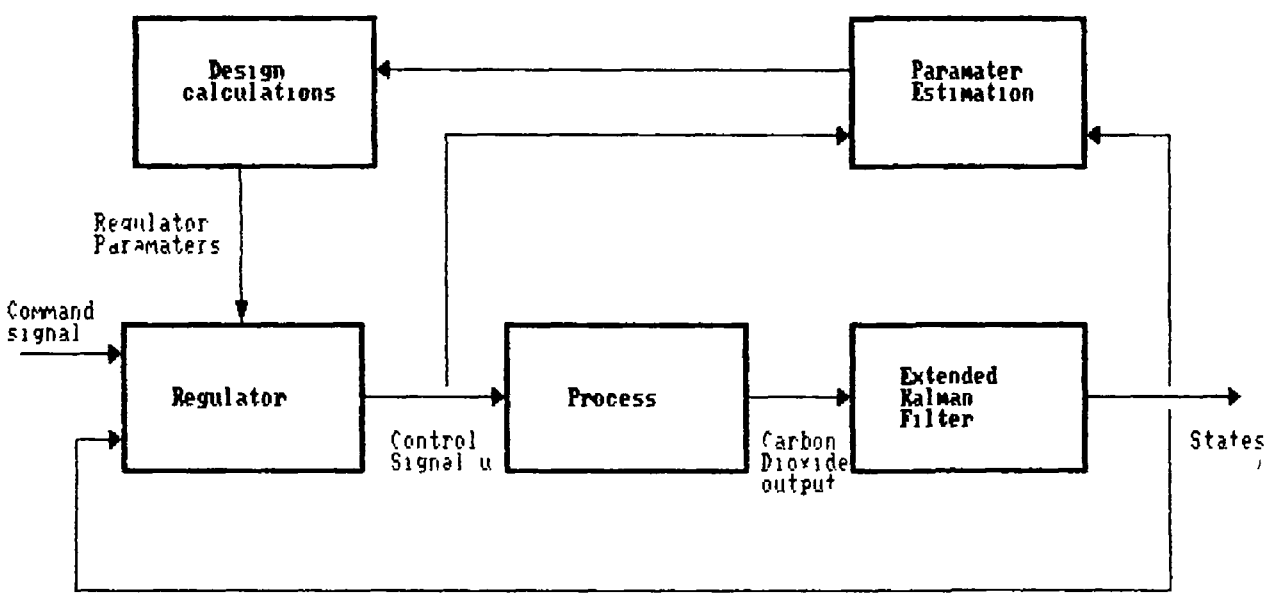

Fig 5.2 Self Tuning Regulator for a Fermentor

Fig 5.3 Model Comparsion

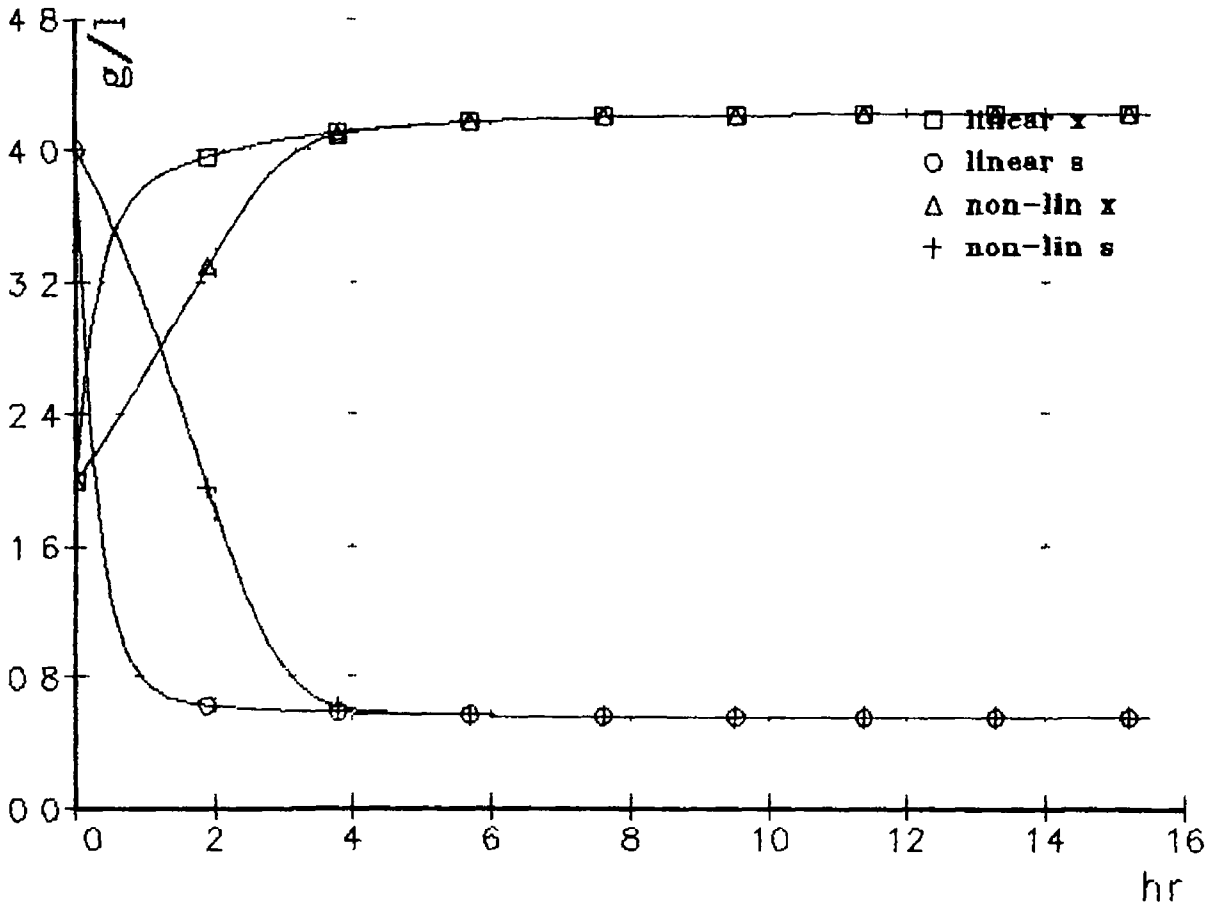

Fig 5.4 Model Comparsion

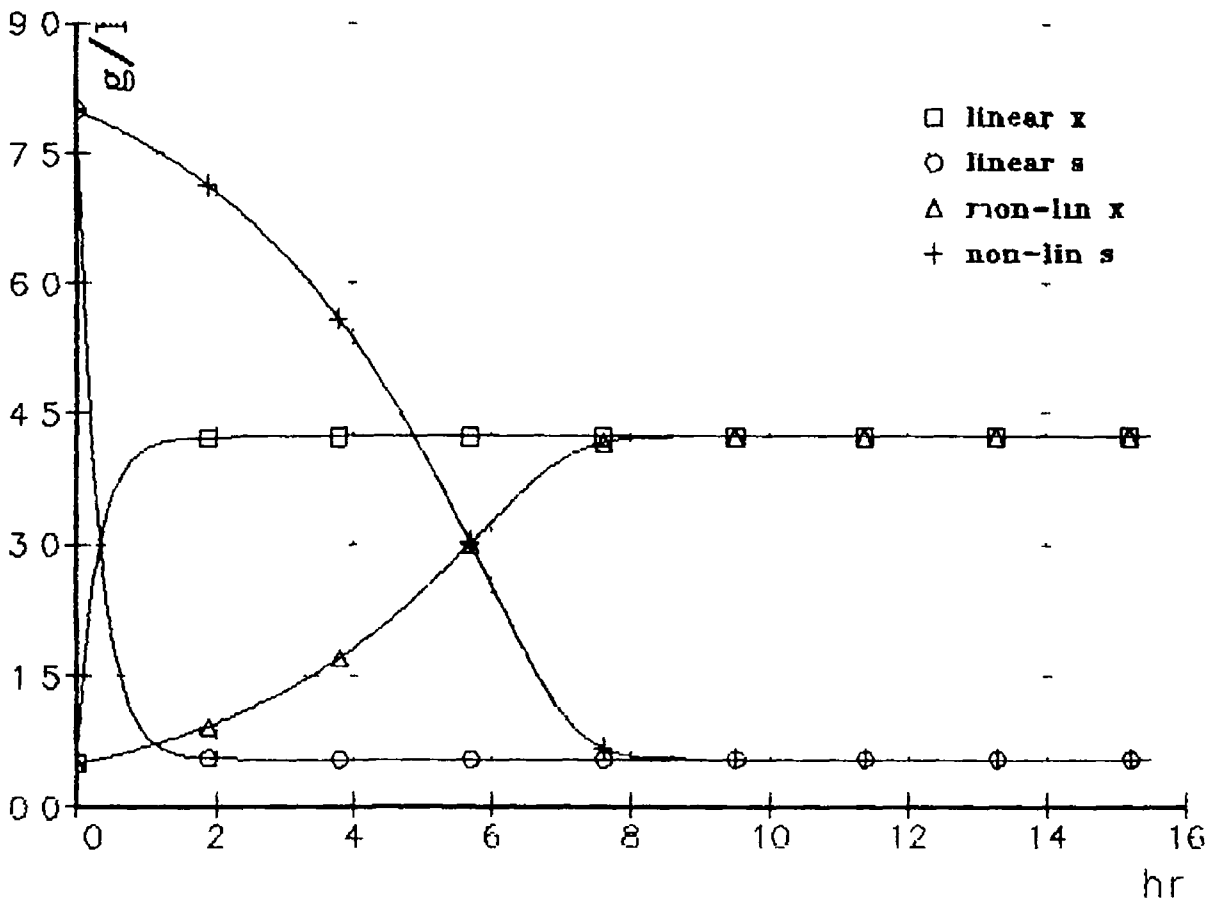

Fig 5.5 Updated equilibrium pt.

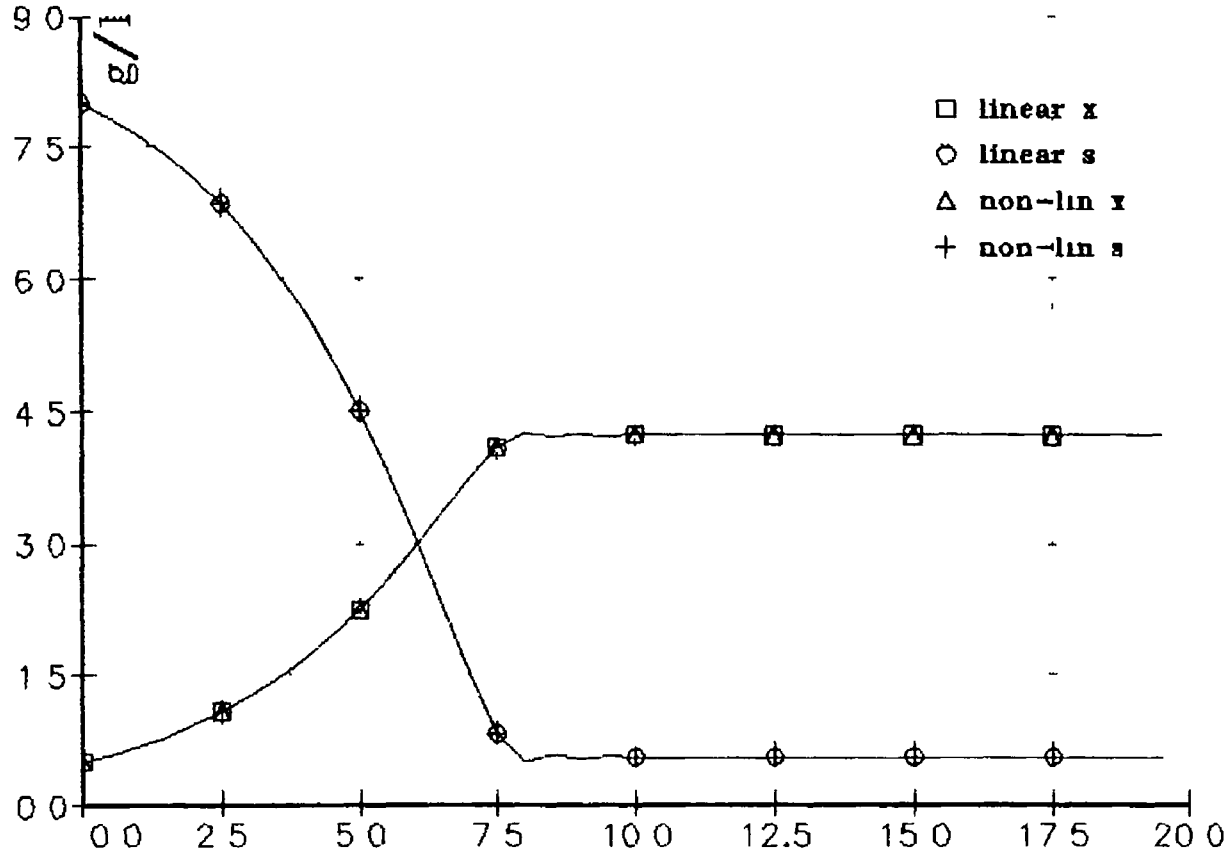

FIG 5.6 SCHEMATIC OF STATE FEEDBACK CONTROLLER FOR FERMENTER.

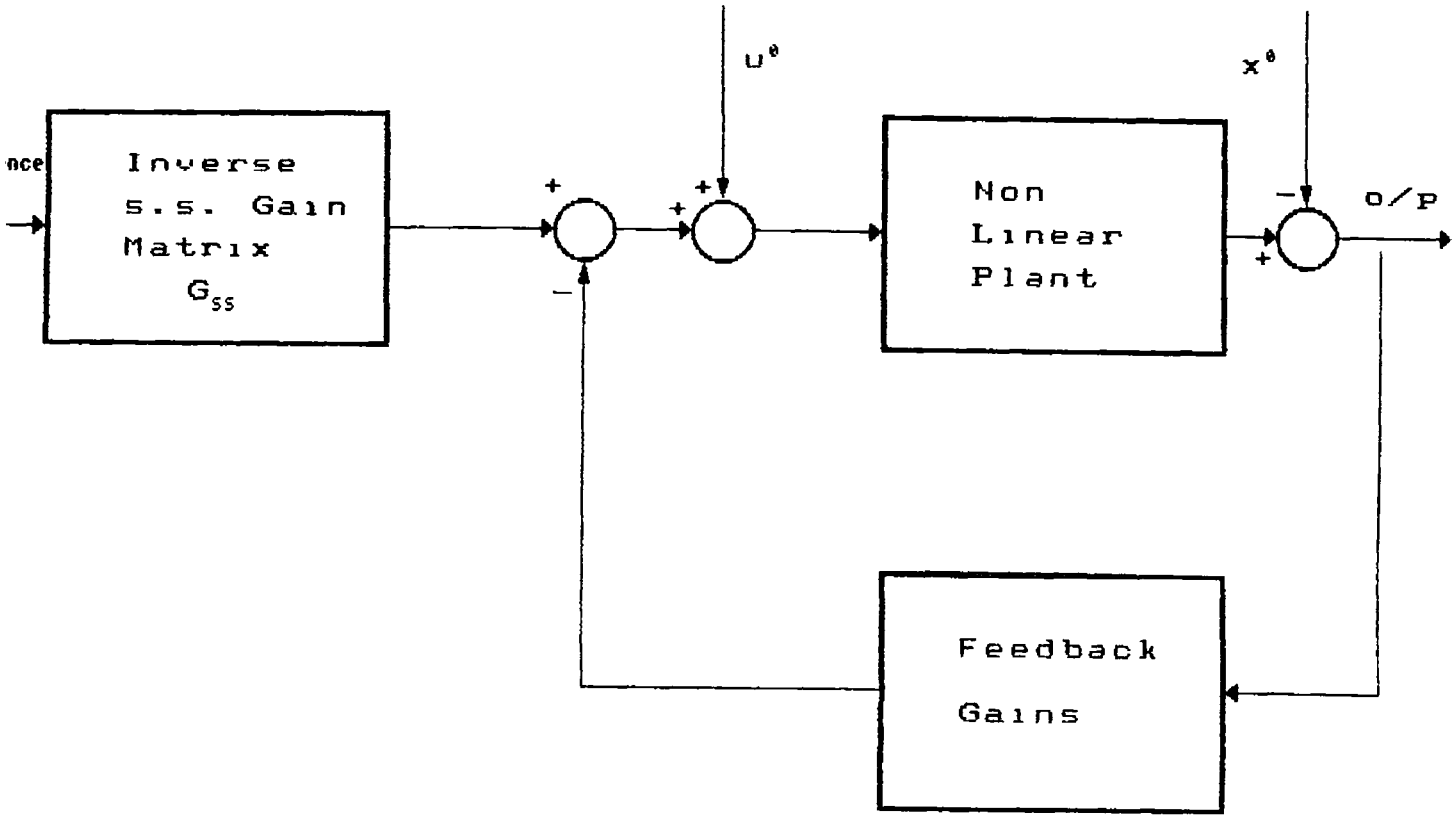

Fig 5.7 Feedback Controller

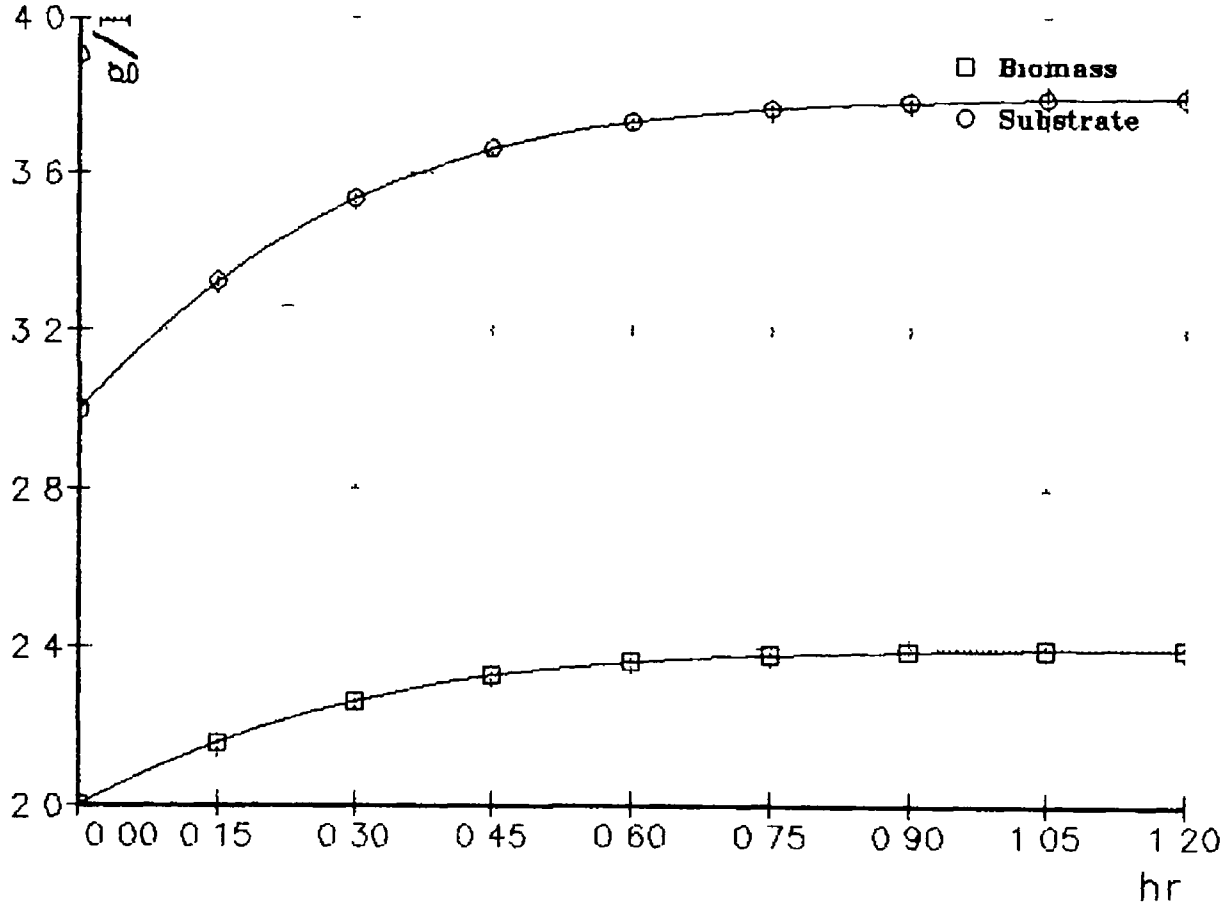

Fig 5.8 Control Inputs

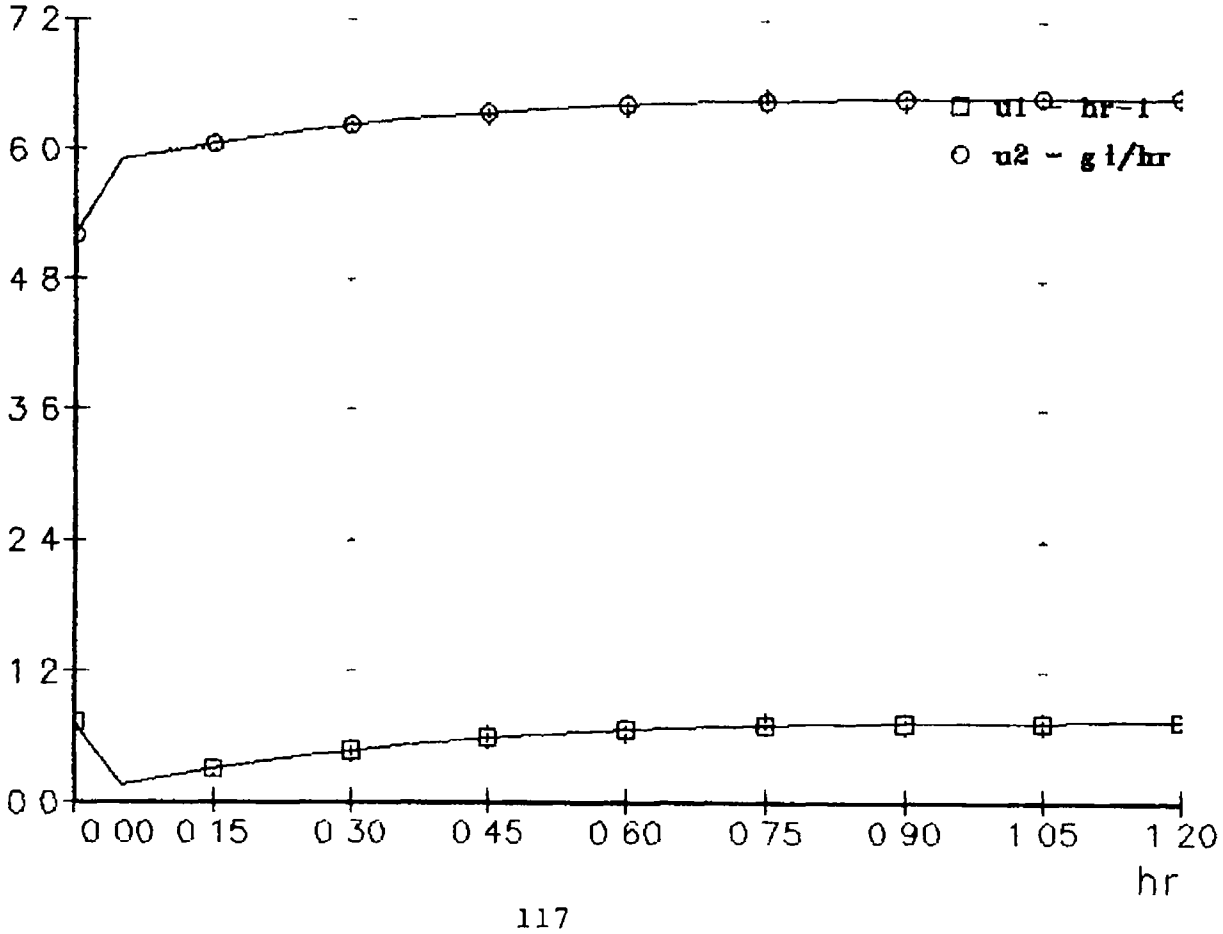

Fig 5.9 Dilution rate

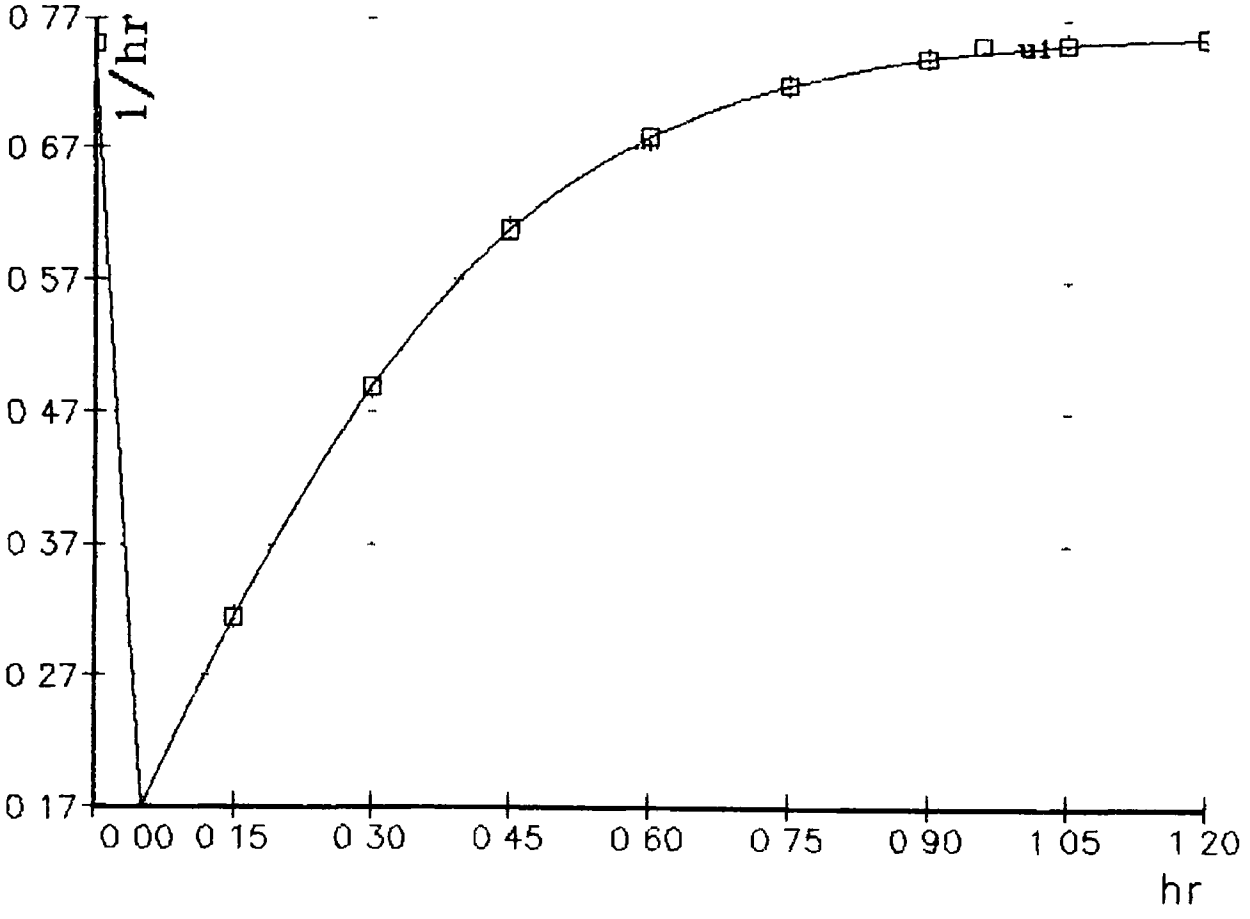

Fig 5.10 Plant o/p-large dev

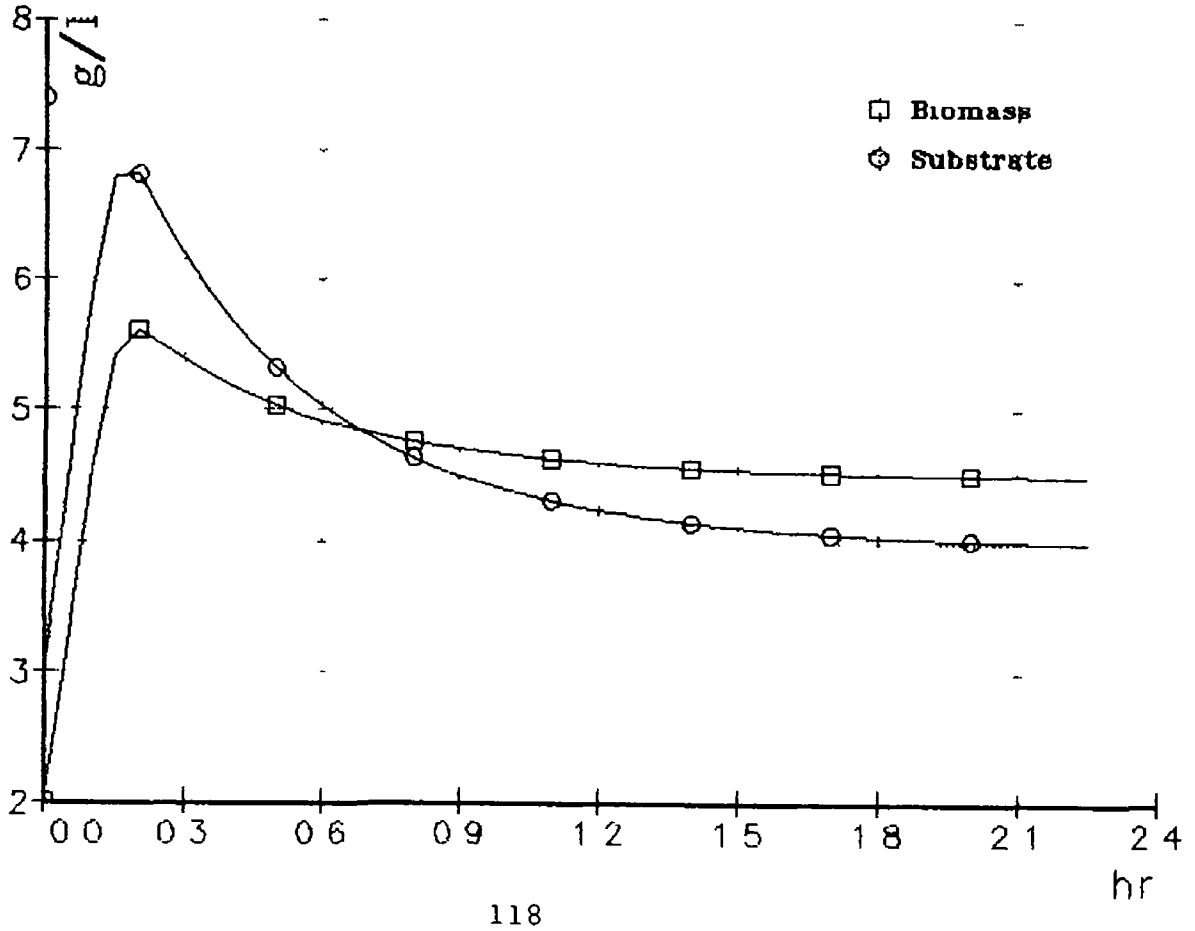

Fig 5.11 Control i/p-large dev

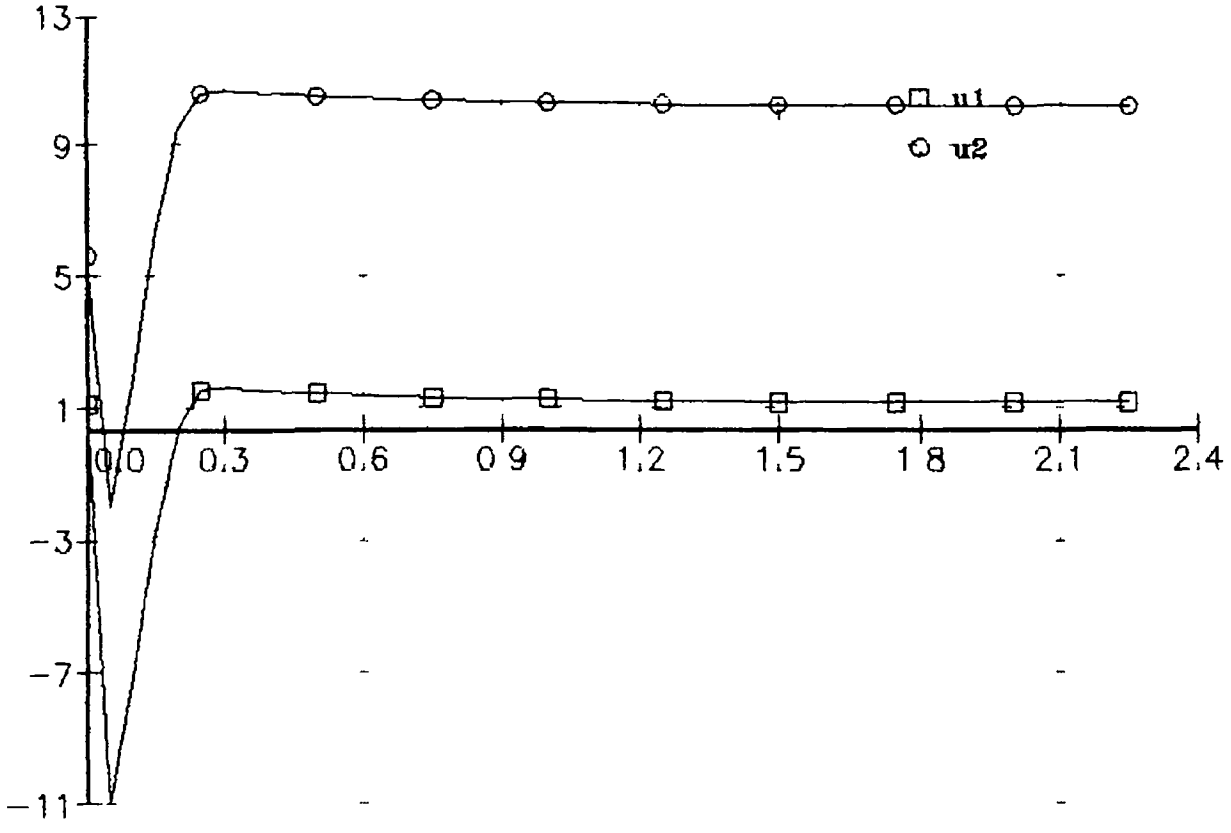

Fig 5.12 Plant o/p set pt. linz.

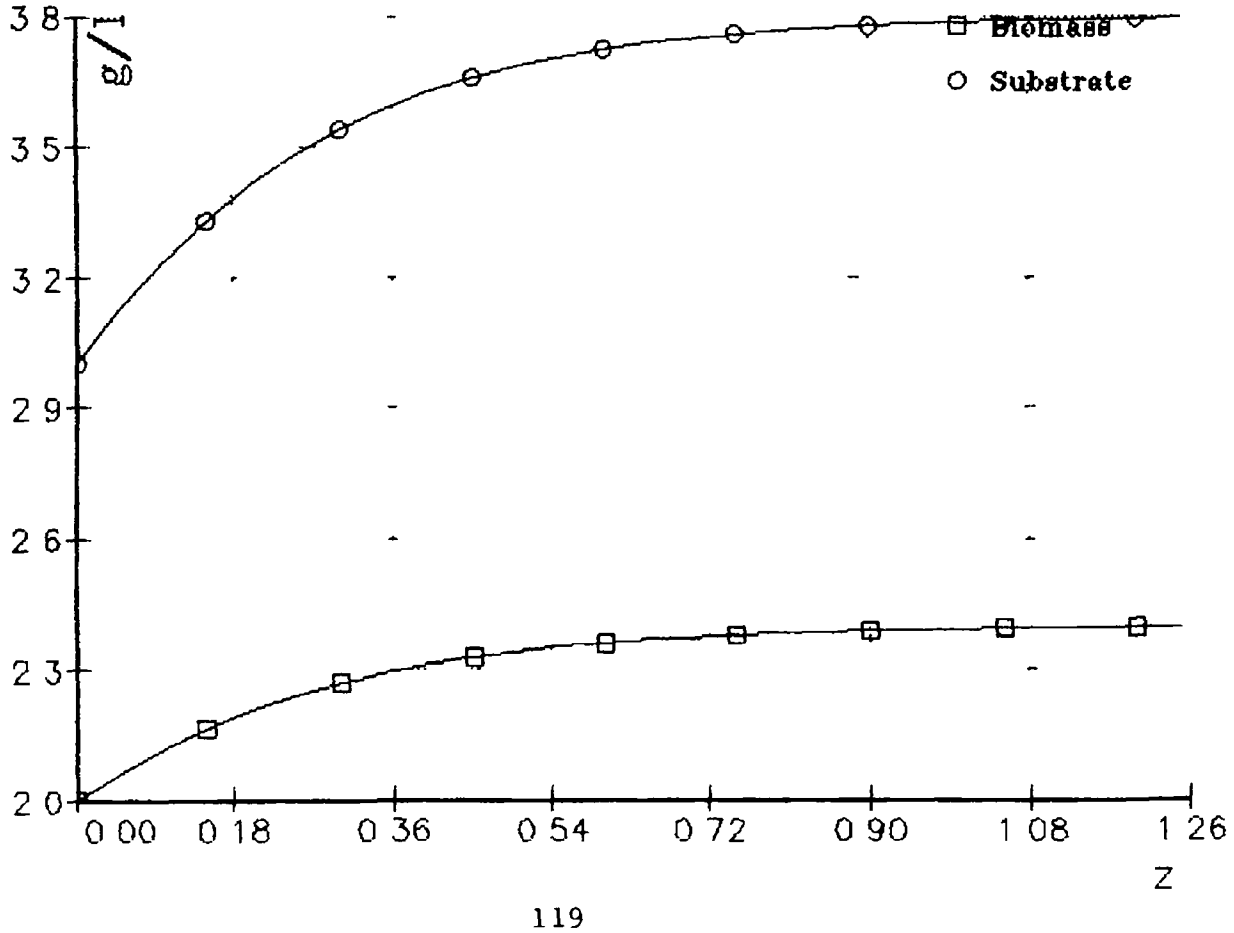

Fig 5.13 u1, set pt linz

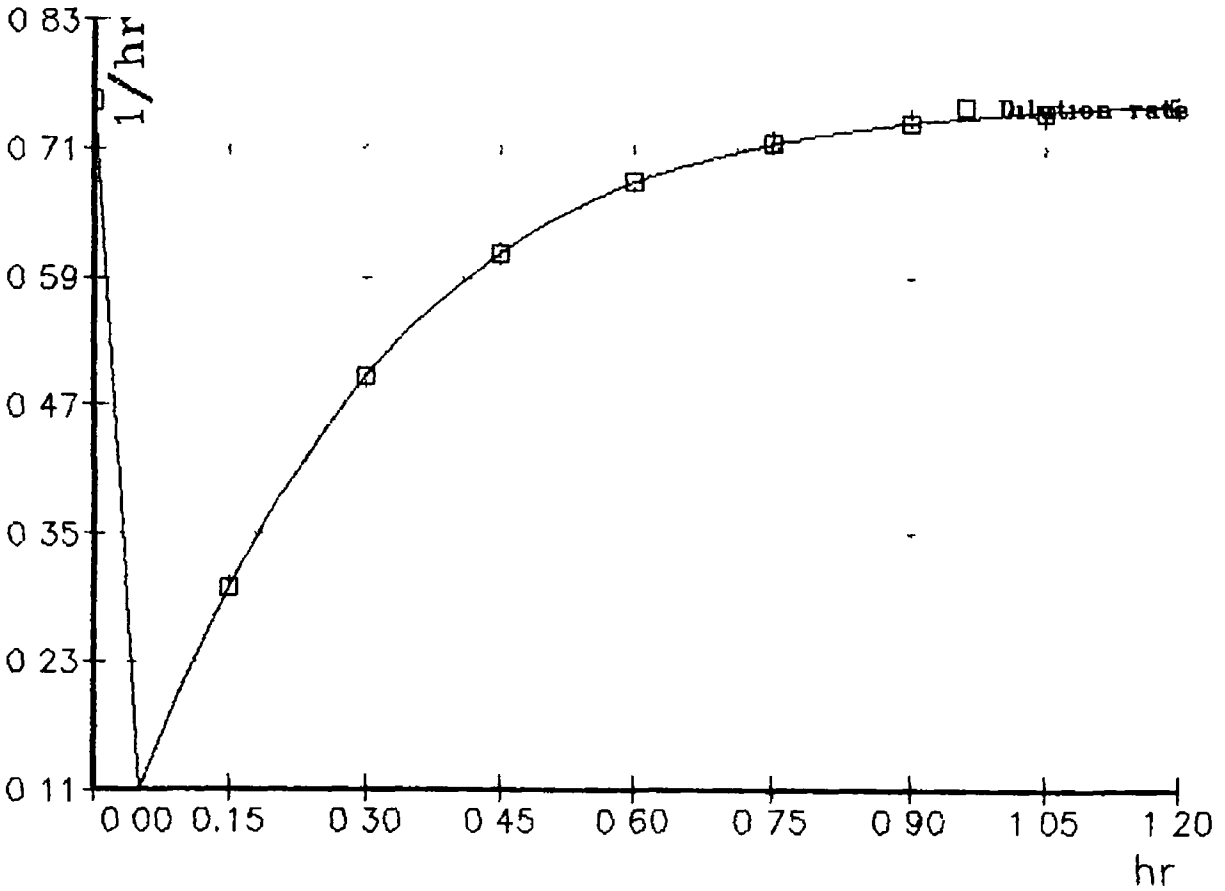

Fig 5.14 set pt. linz-large dev

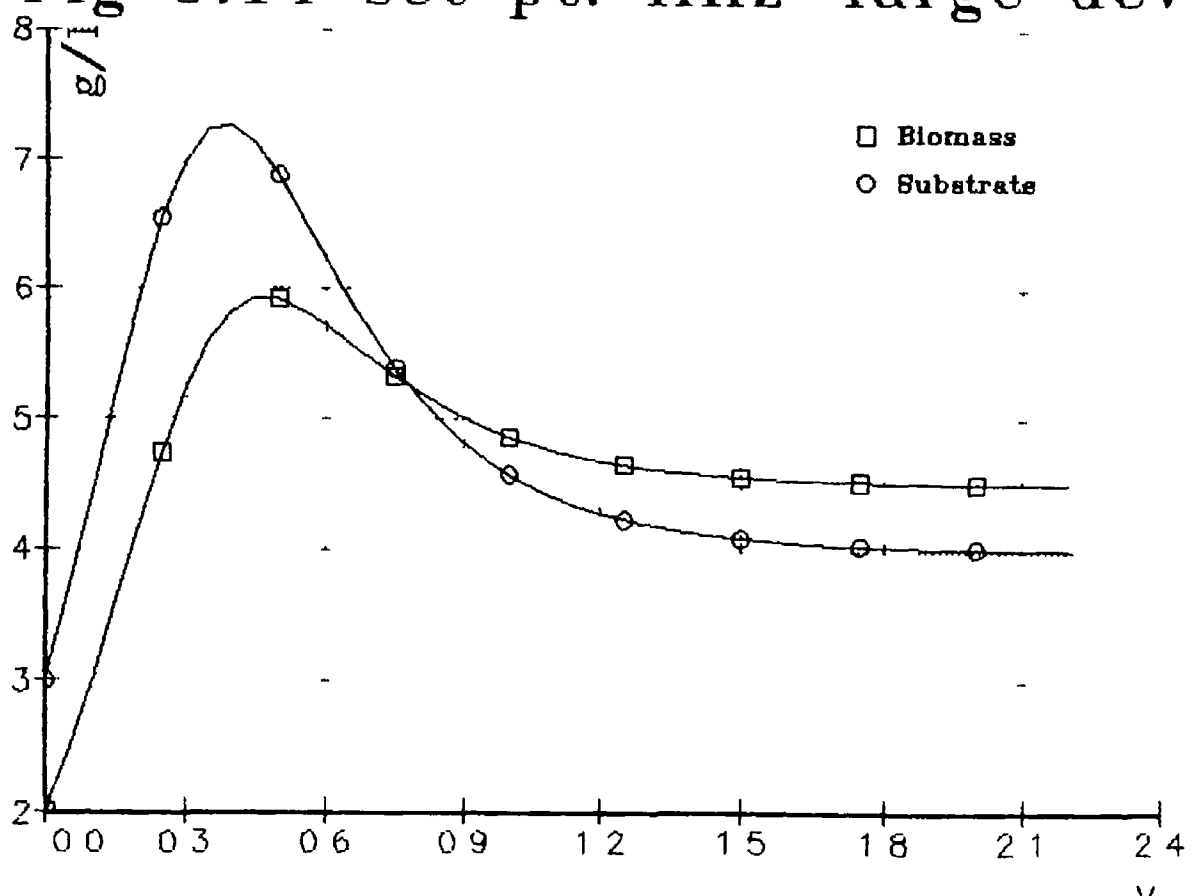

Fig 5.15 Set pt linz-large dev

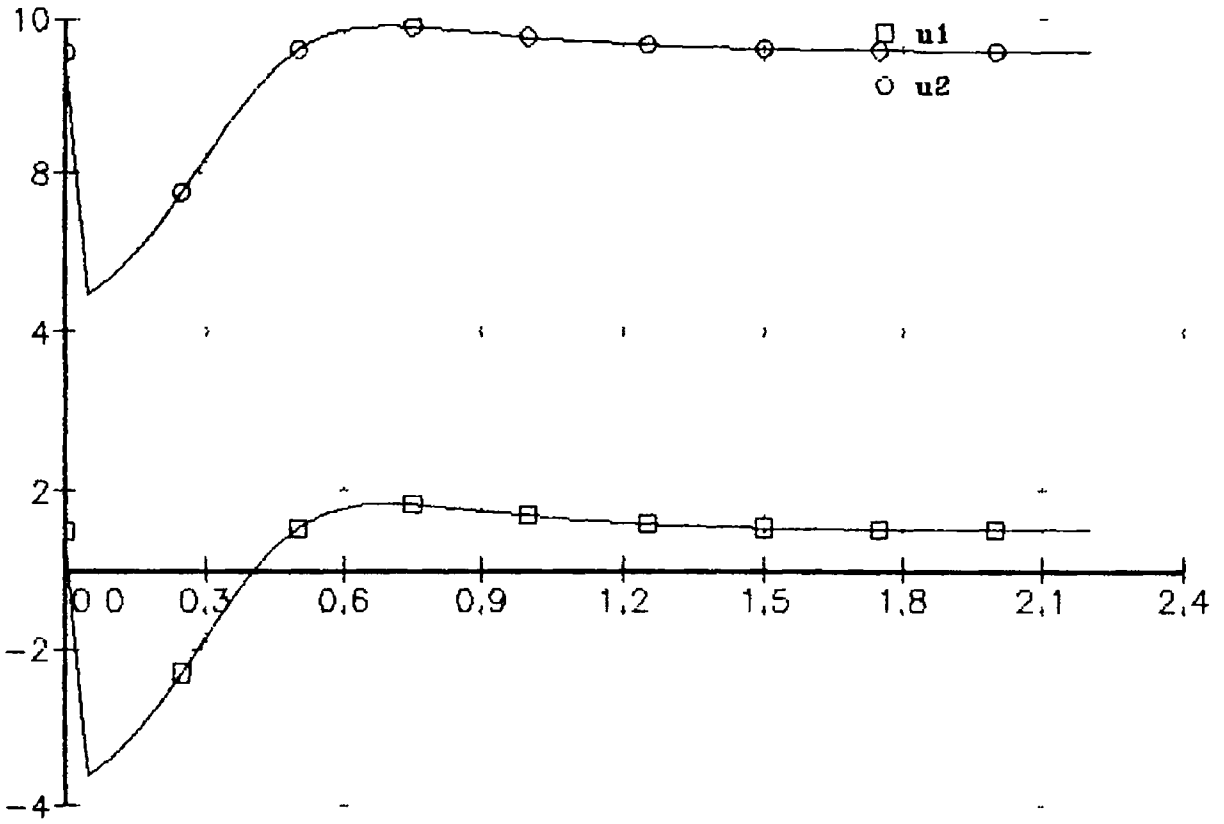

Fig 5.16 Piecewise linz.

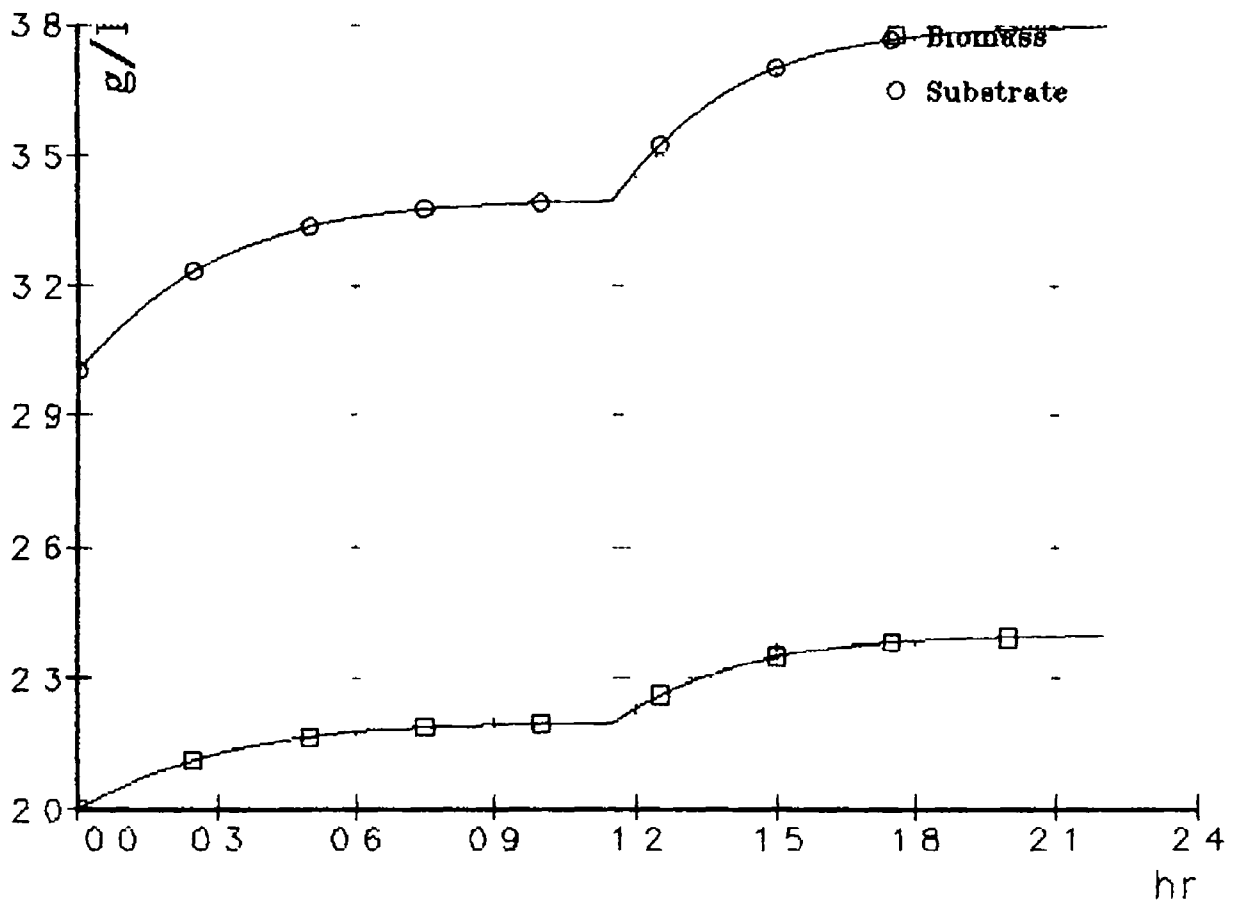

Fig 5.17 Control i/p, p/w linz

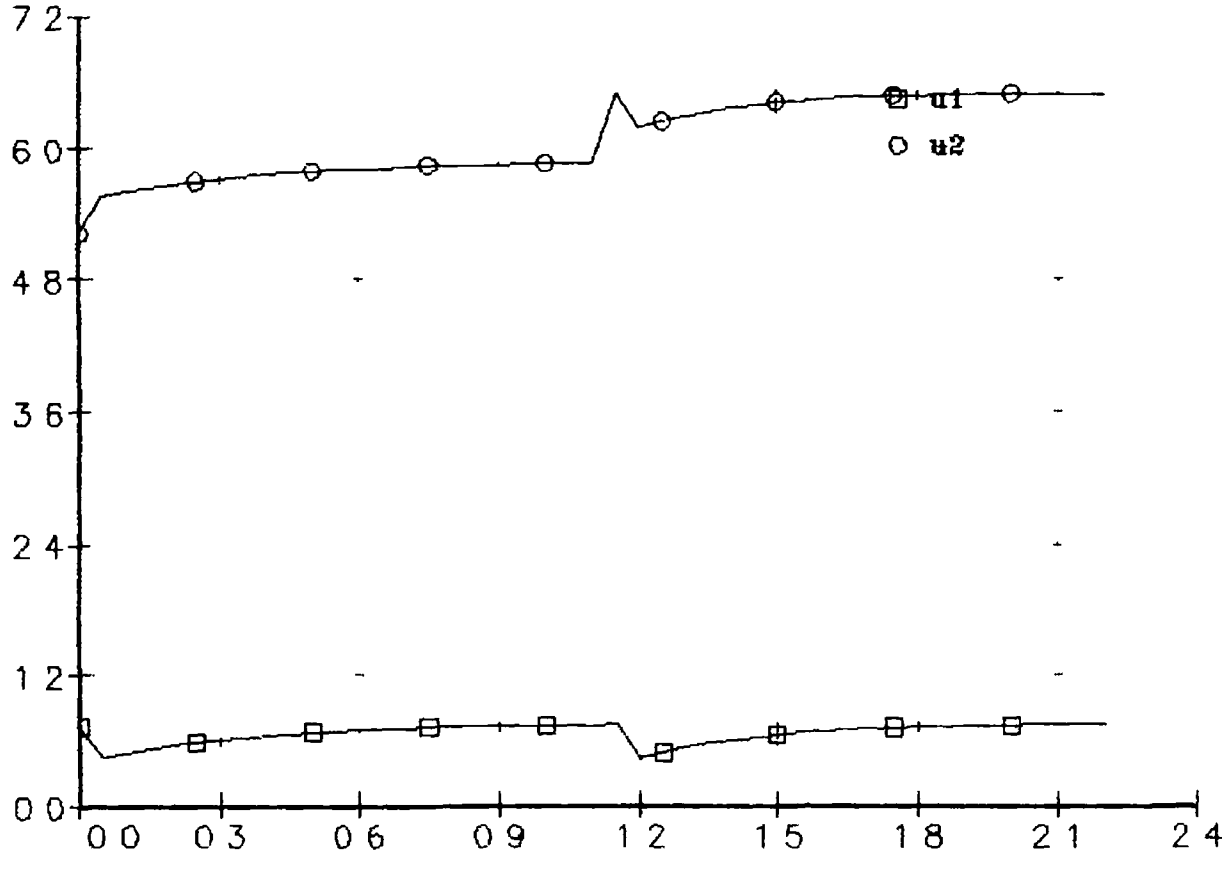

FIG 5.18 SCHEMATIC OF SELF TUNING STATE FEEDBACK CONTROLLER FOR A FERMENTER.

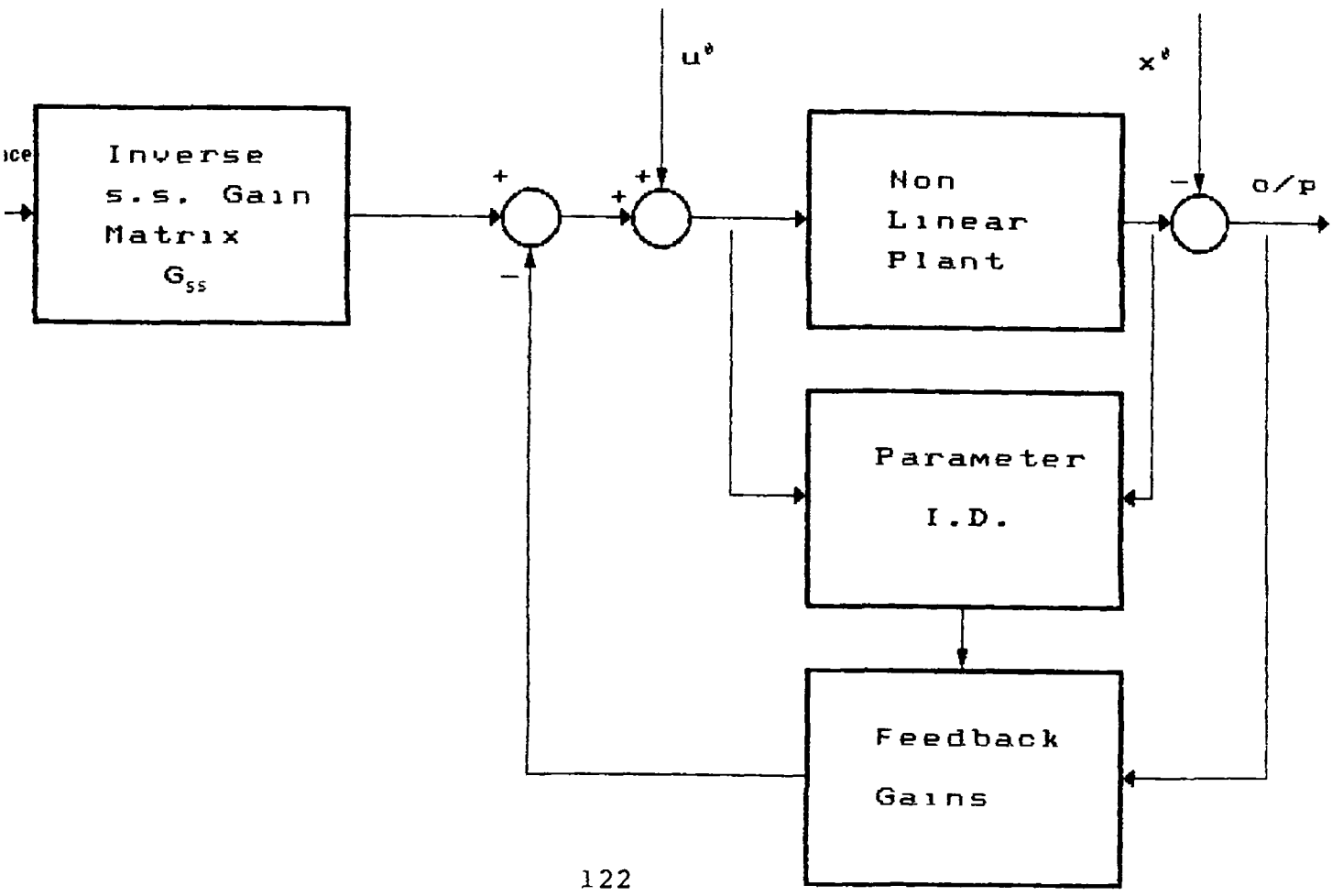

Fig 5.19 Self Tuning Regulator(STR)

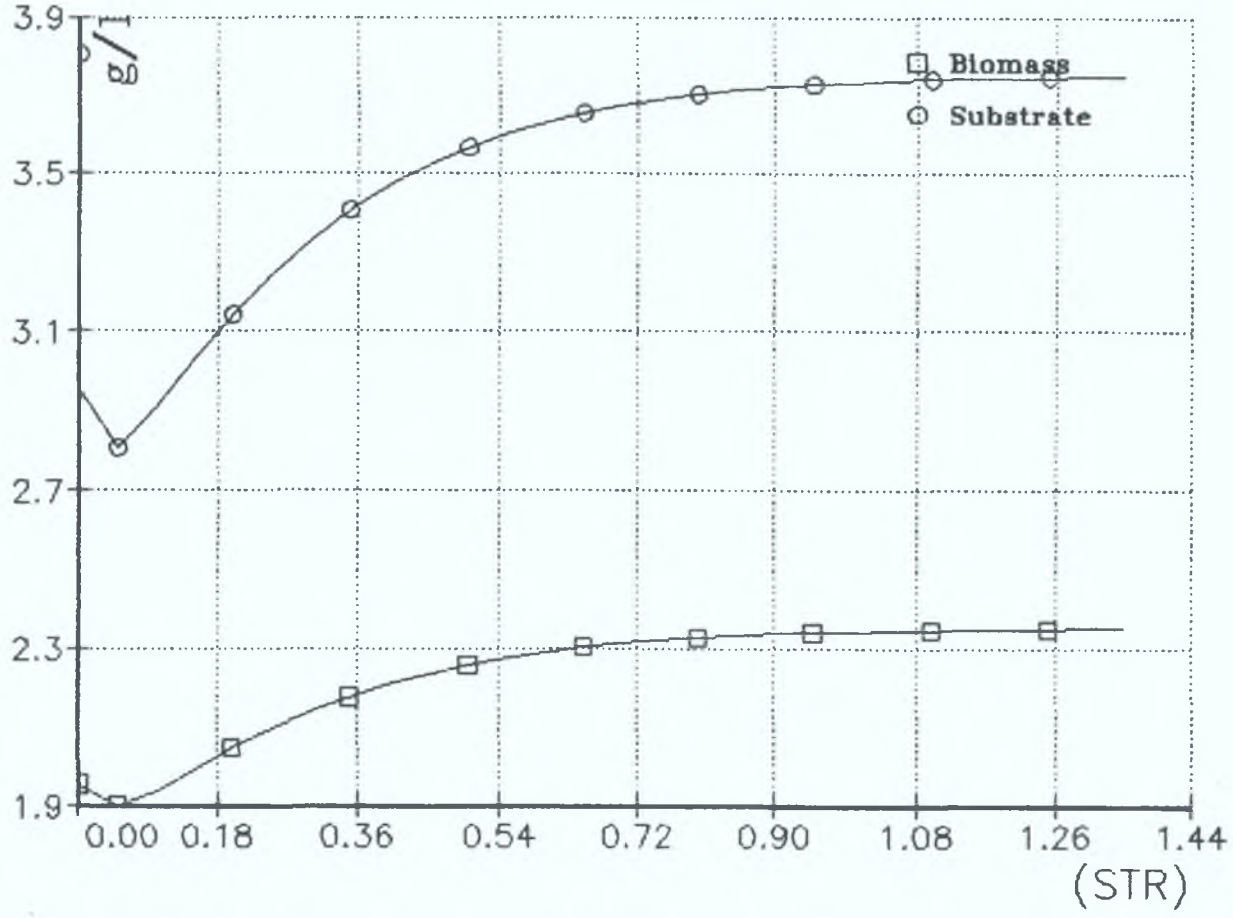

Fig 5.20 STR-Parameter I.D.

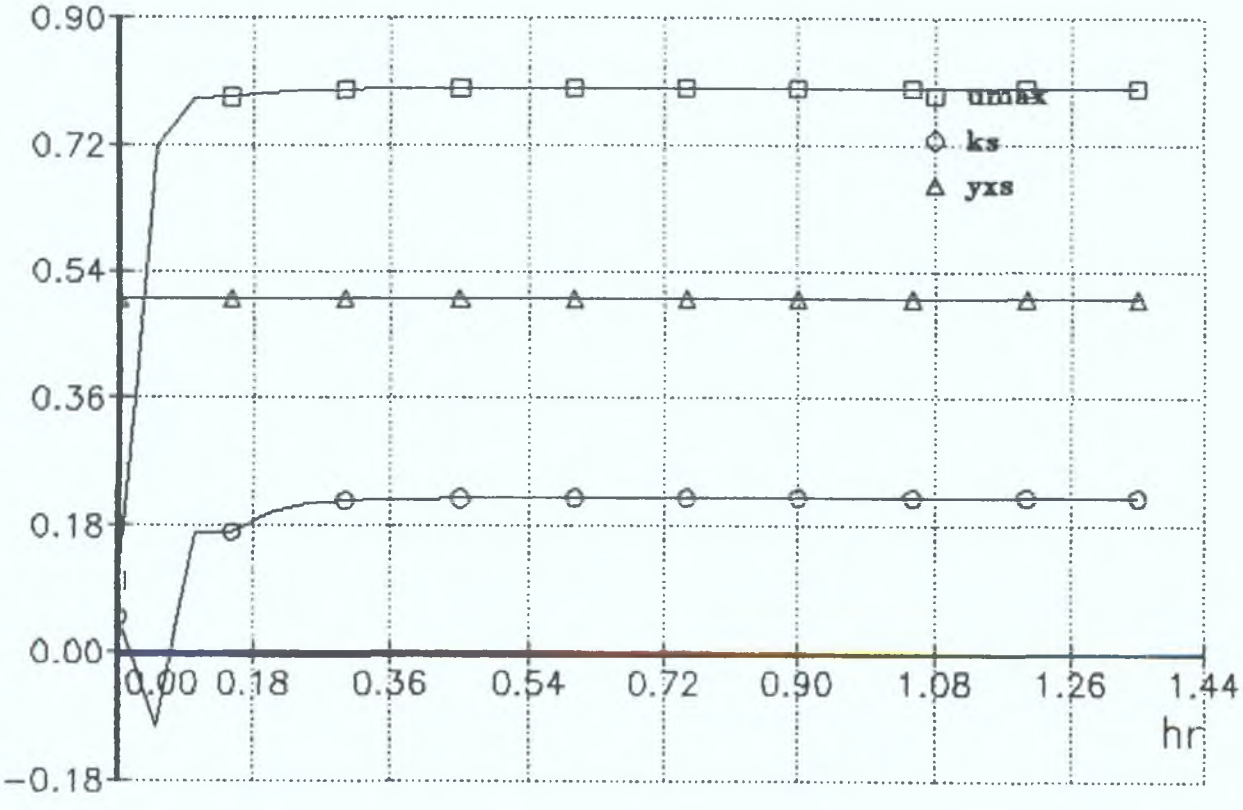

Fig 5.21 STR-Control i/p

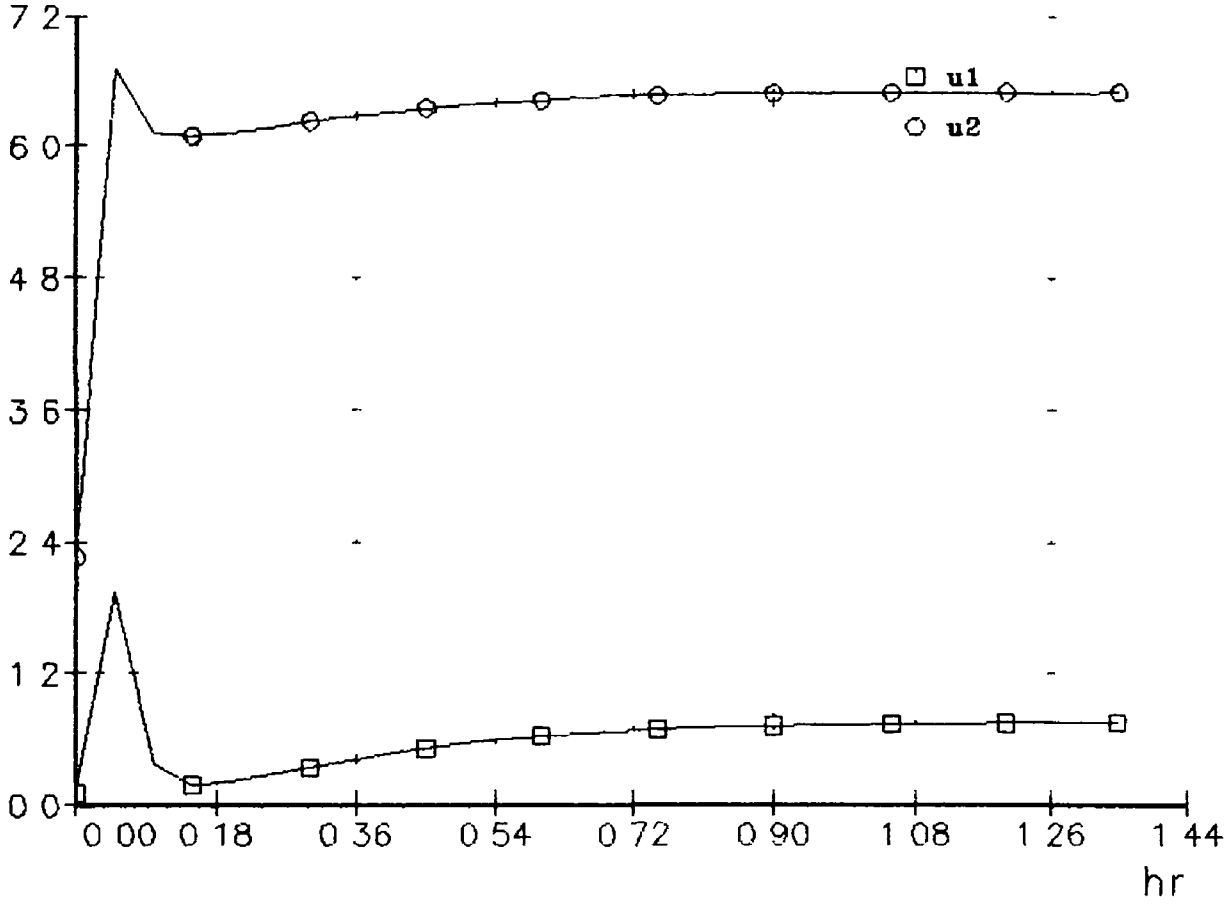

Fig 5.22 STR-States

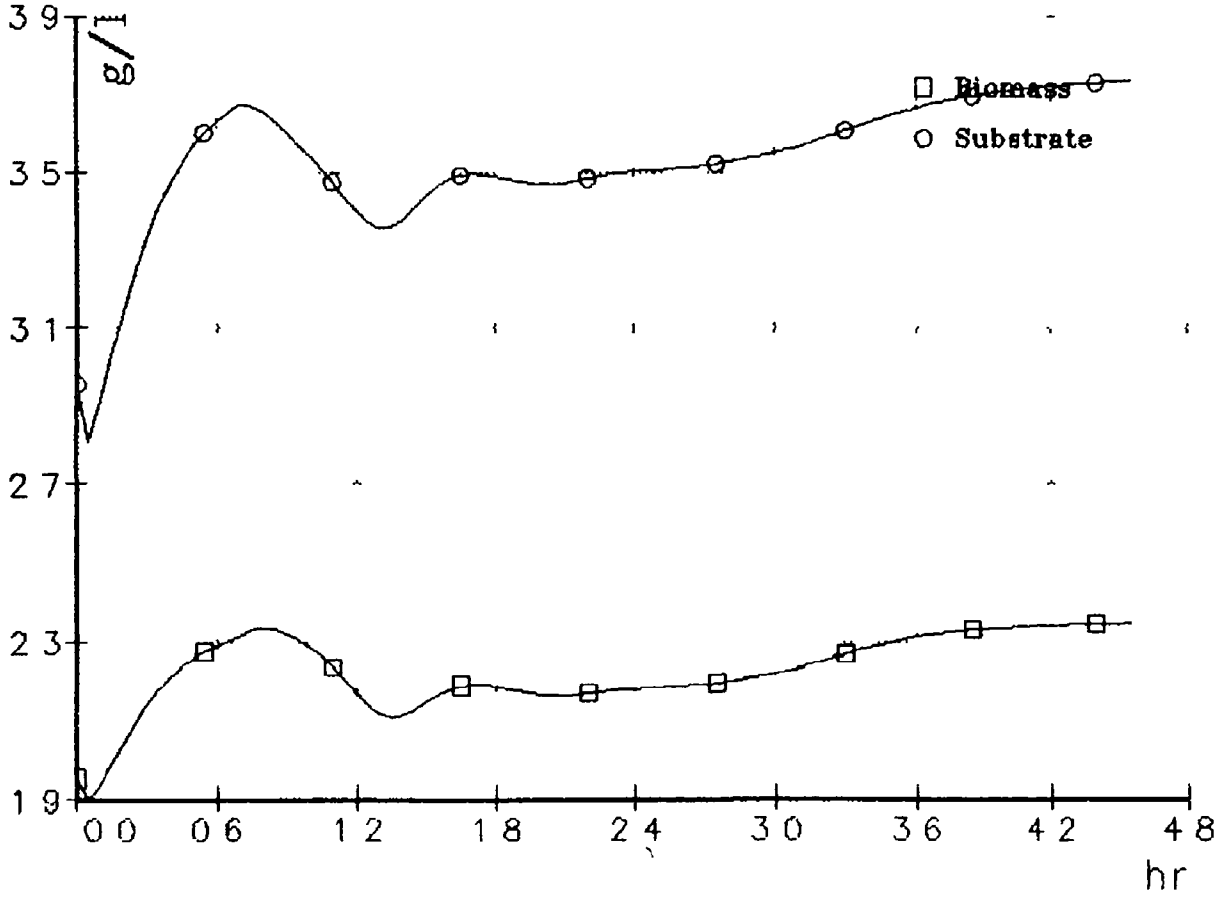

Fig 5.23 STR-Parameter I.D.

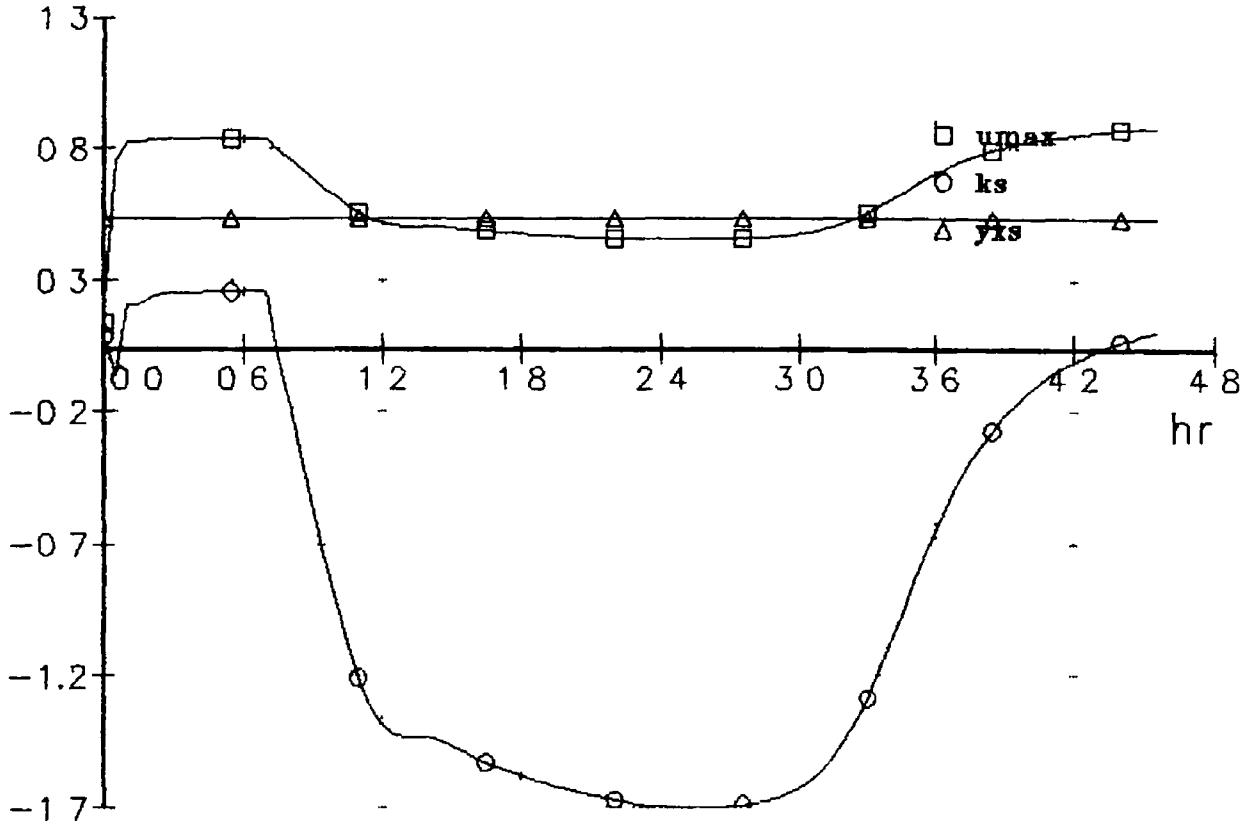

Fig 5.24 STR-Control i/p's

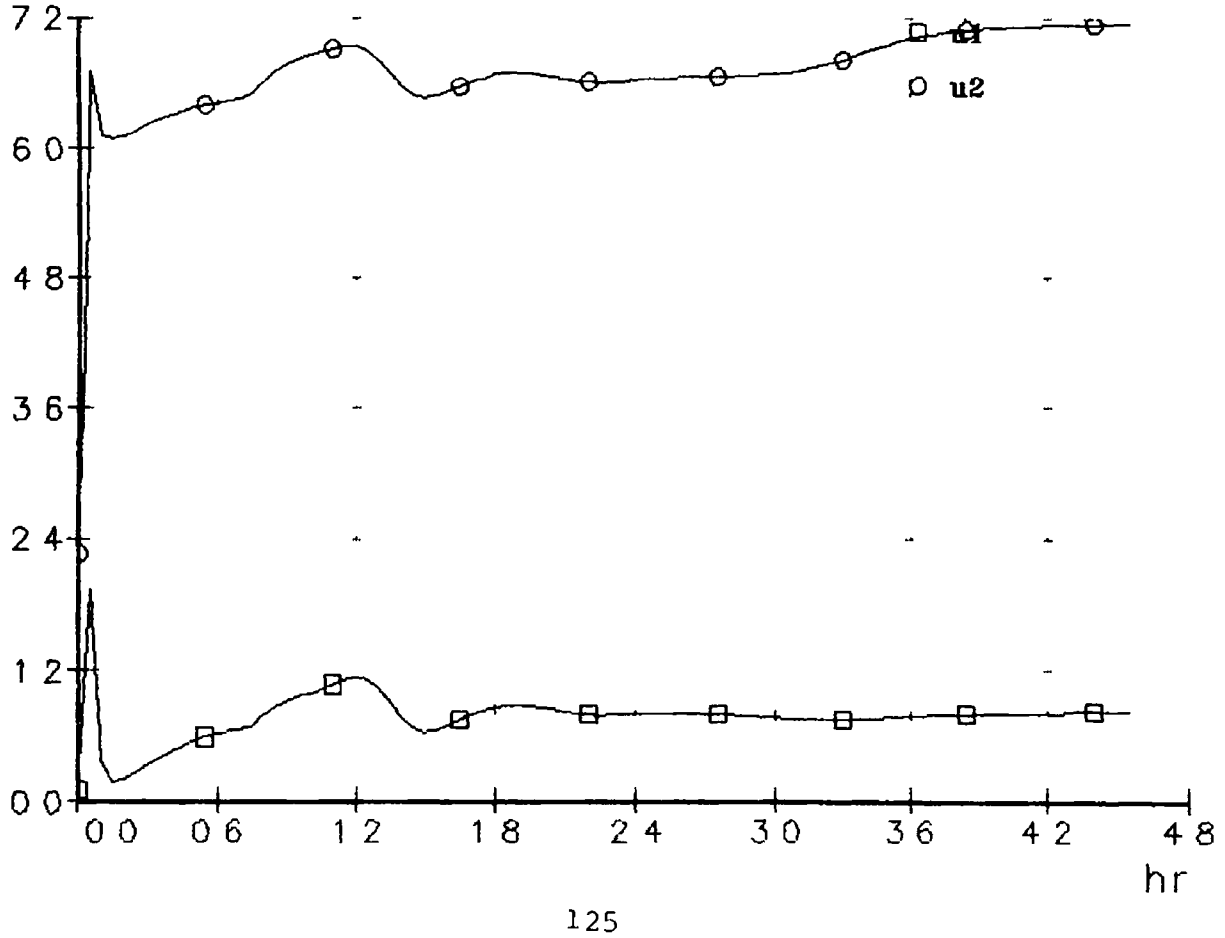

Fig 5.25 STR-States

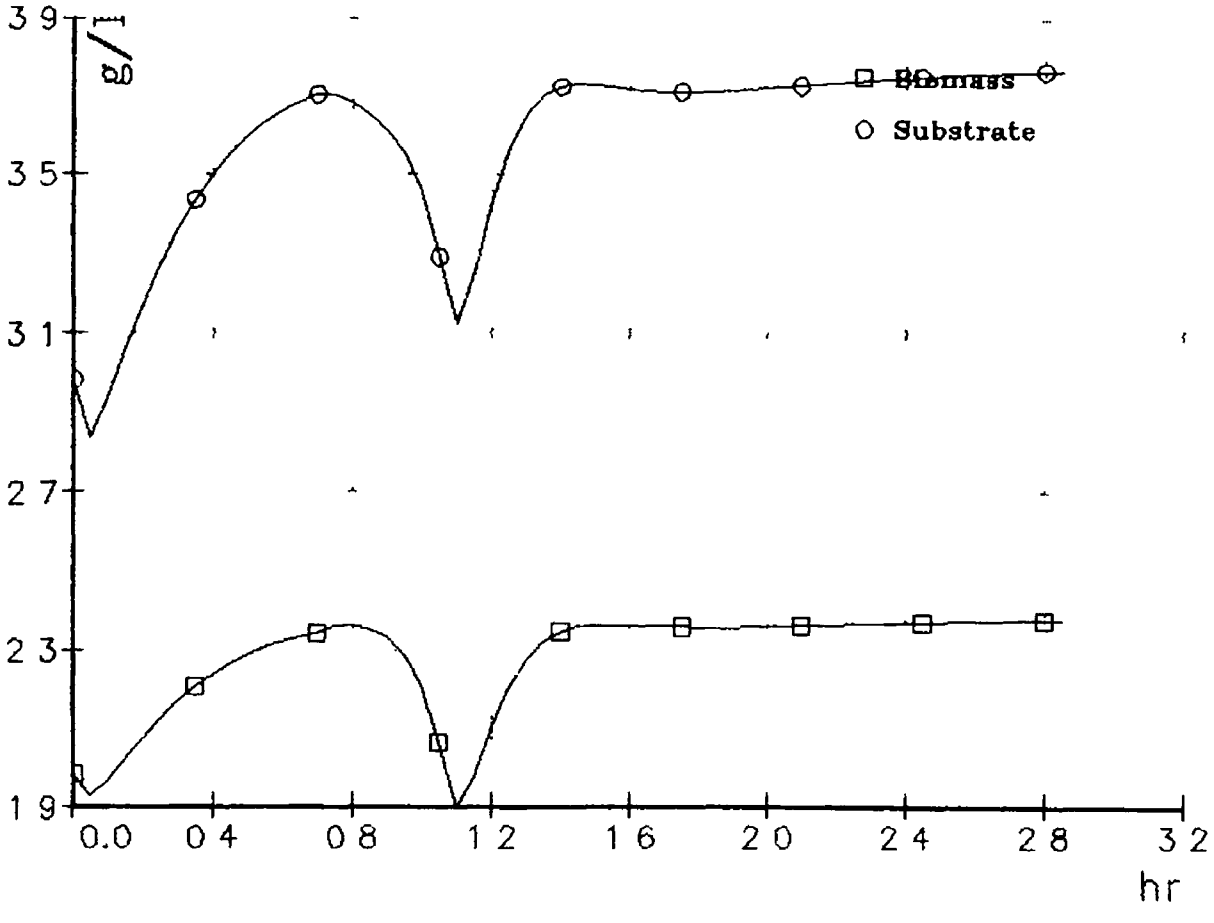

Fig 5.26 STR-Parameter I.D.

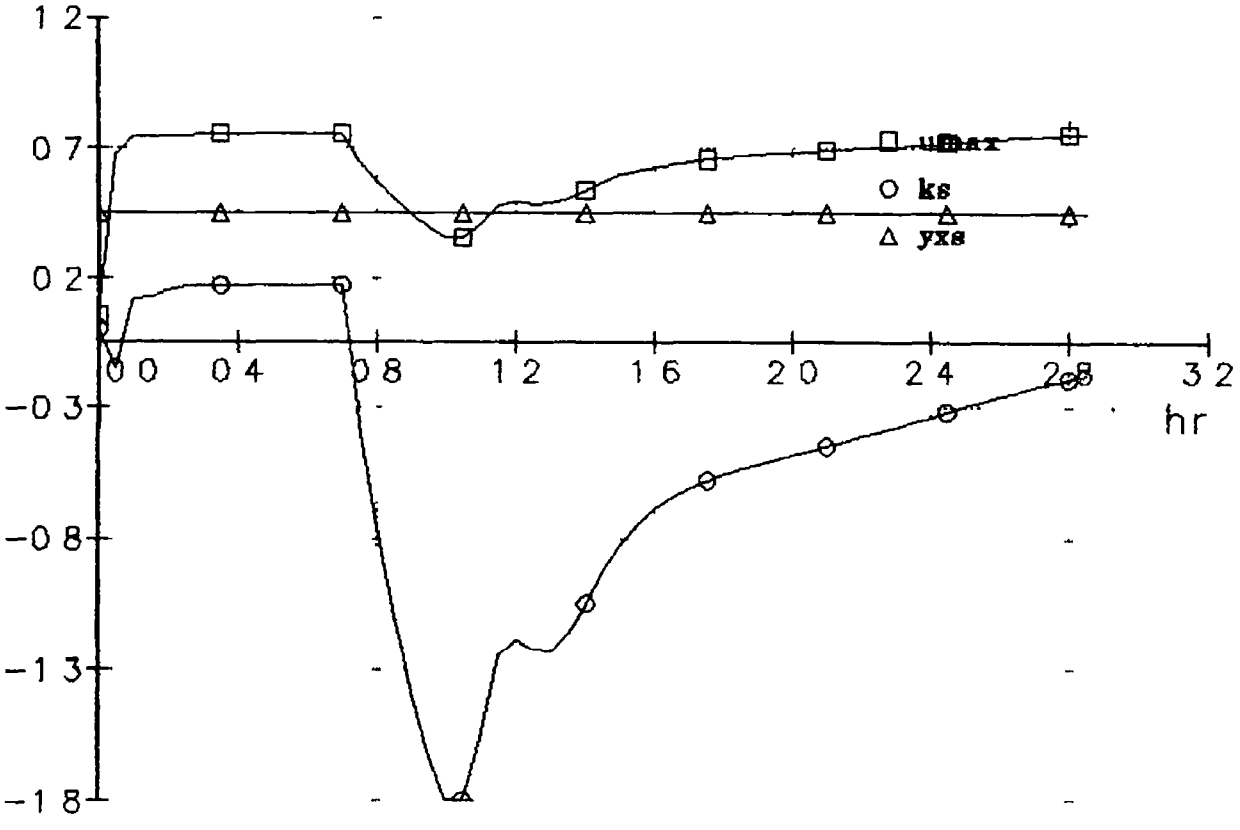

Fig 5.27 STR-Control i/p's

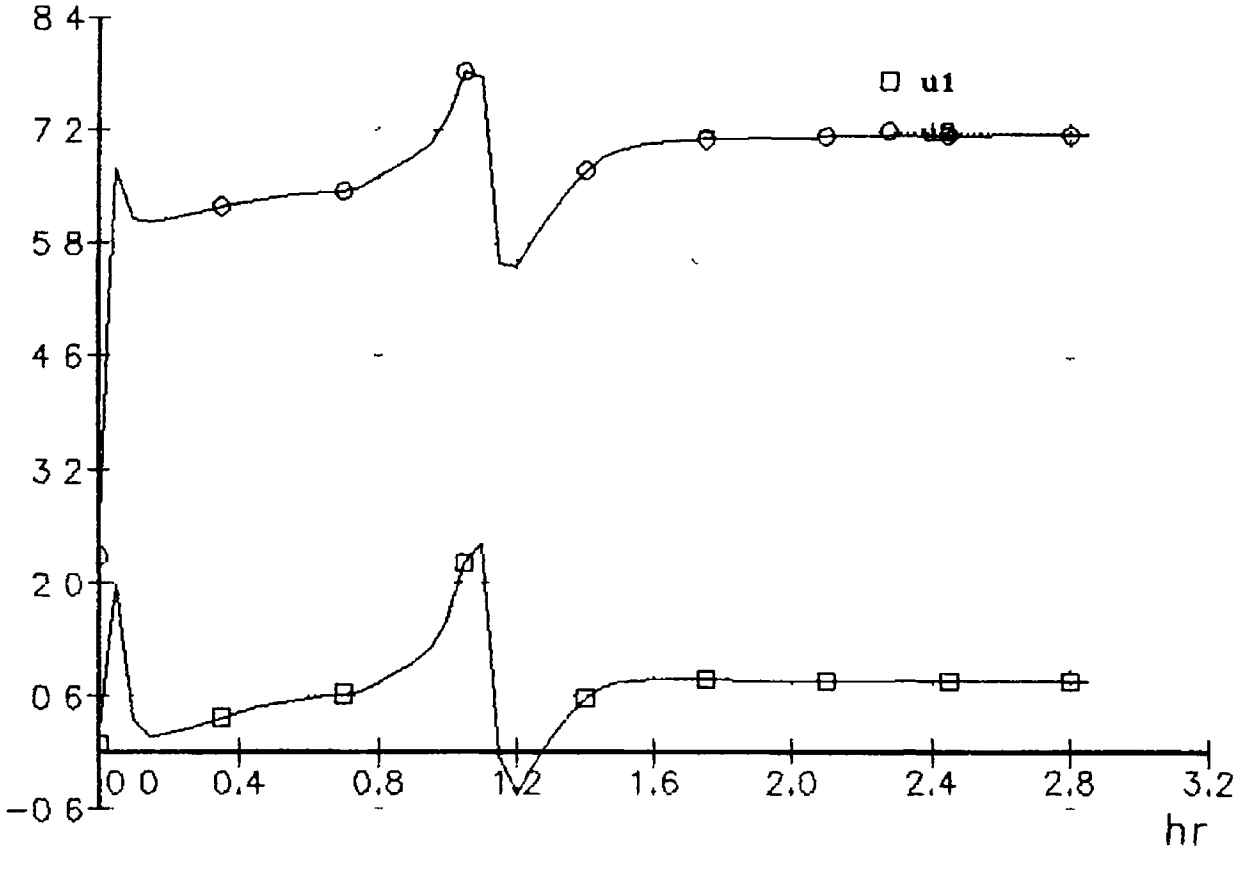

Fig 6.1 Biomass

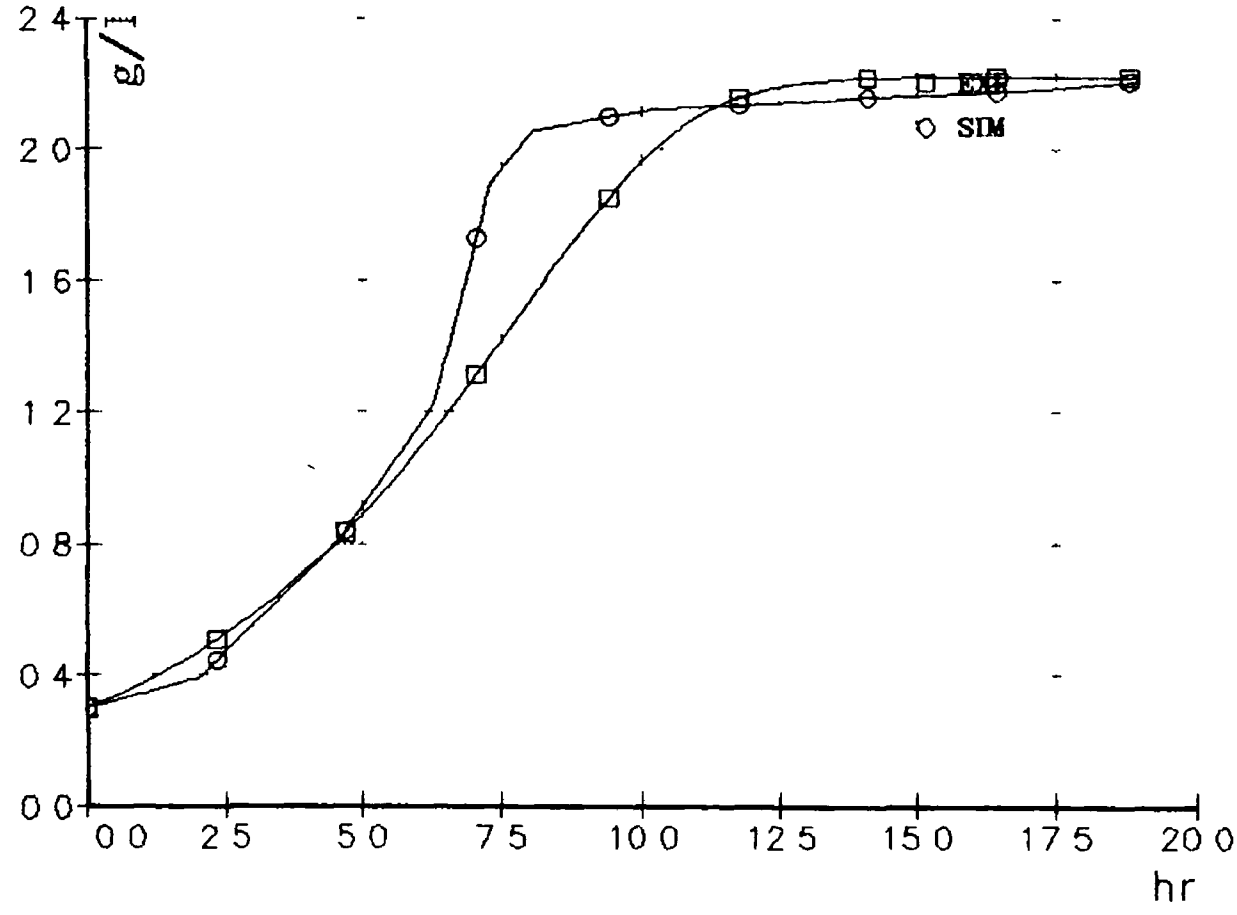

Fig 6.2 Substrate

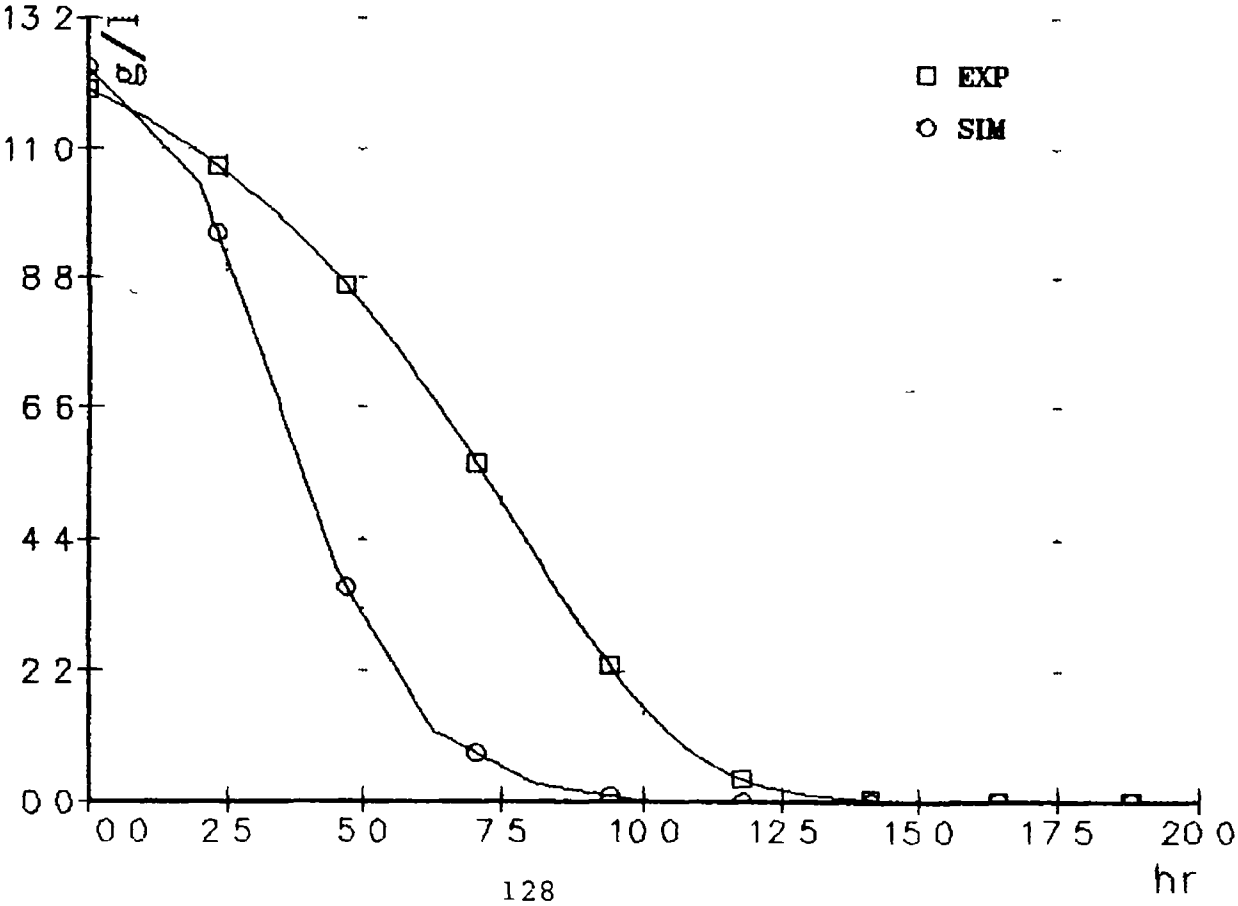

Fig 6.3 Biomass,varying umax

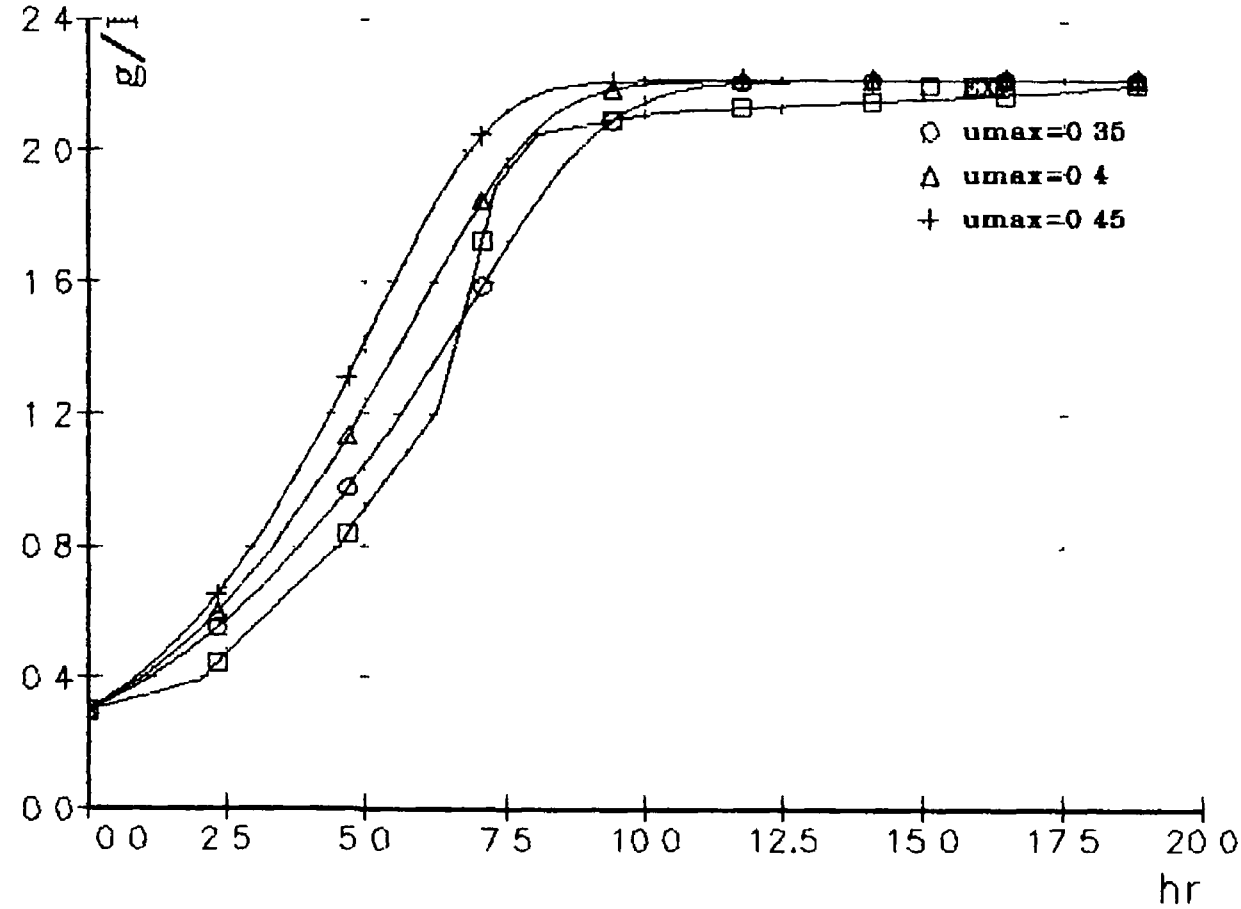

Fig 6.4 Substrate,varying umax

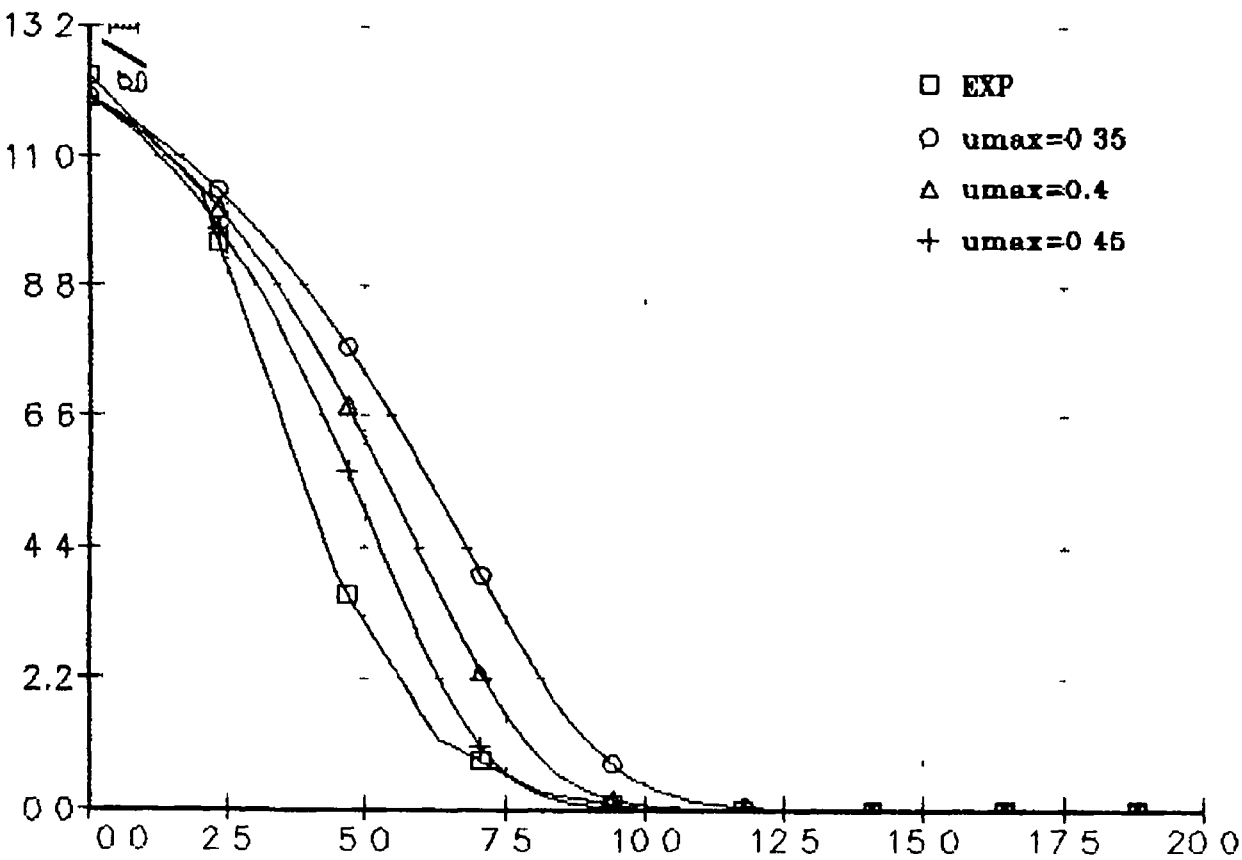

Fig 6.5 Dissolved 02,vary umax

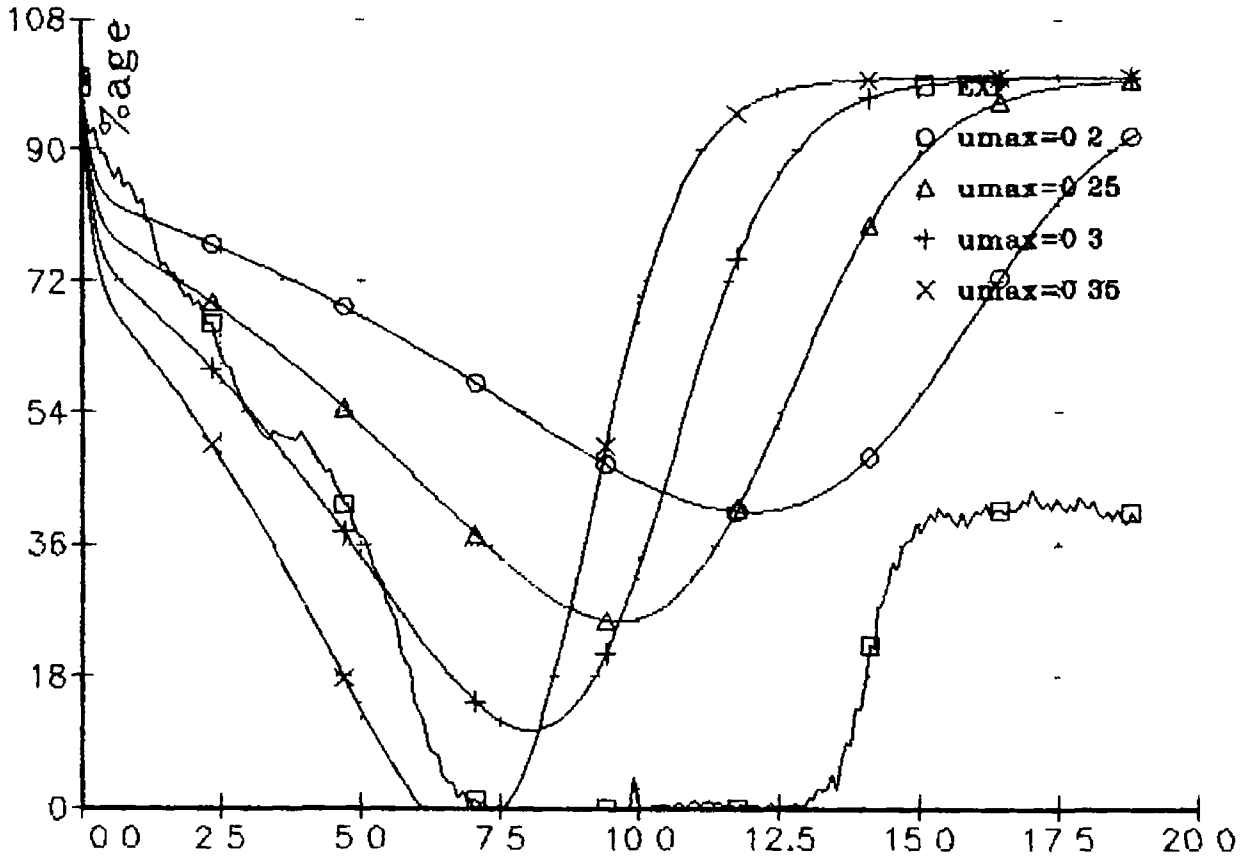

Fig 6.6 Dissolved 02,vary kla

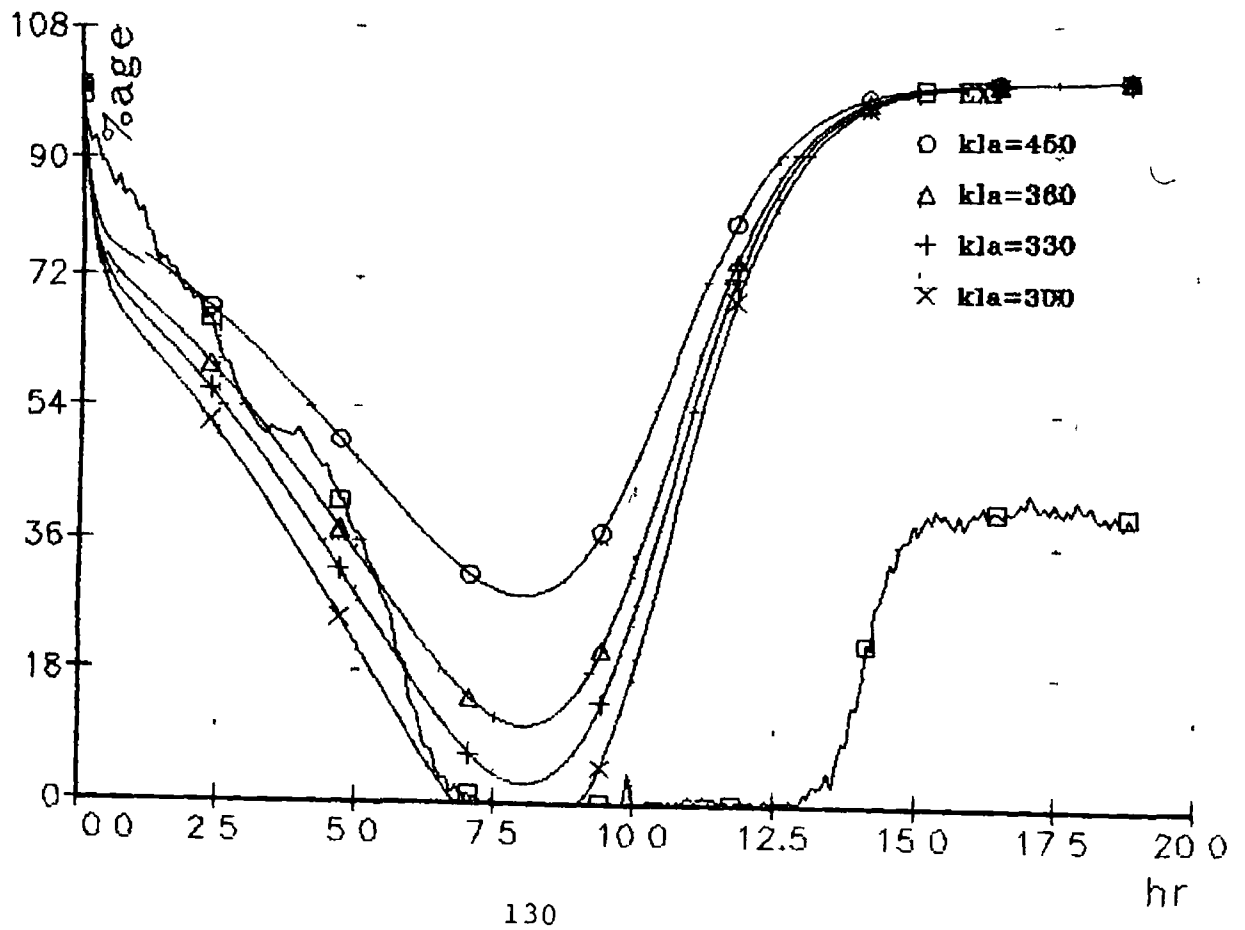

Fig 6.7 Fermentor C02

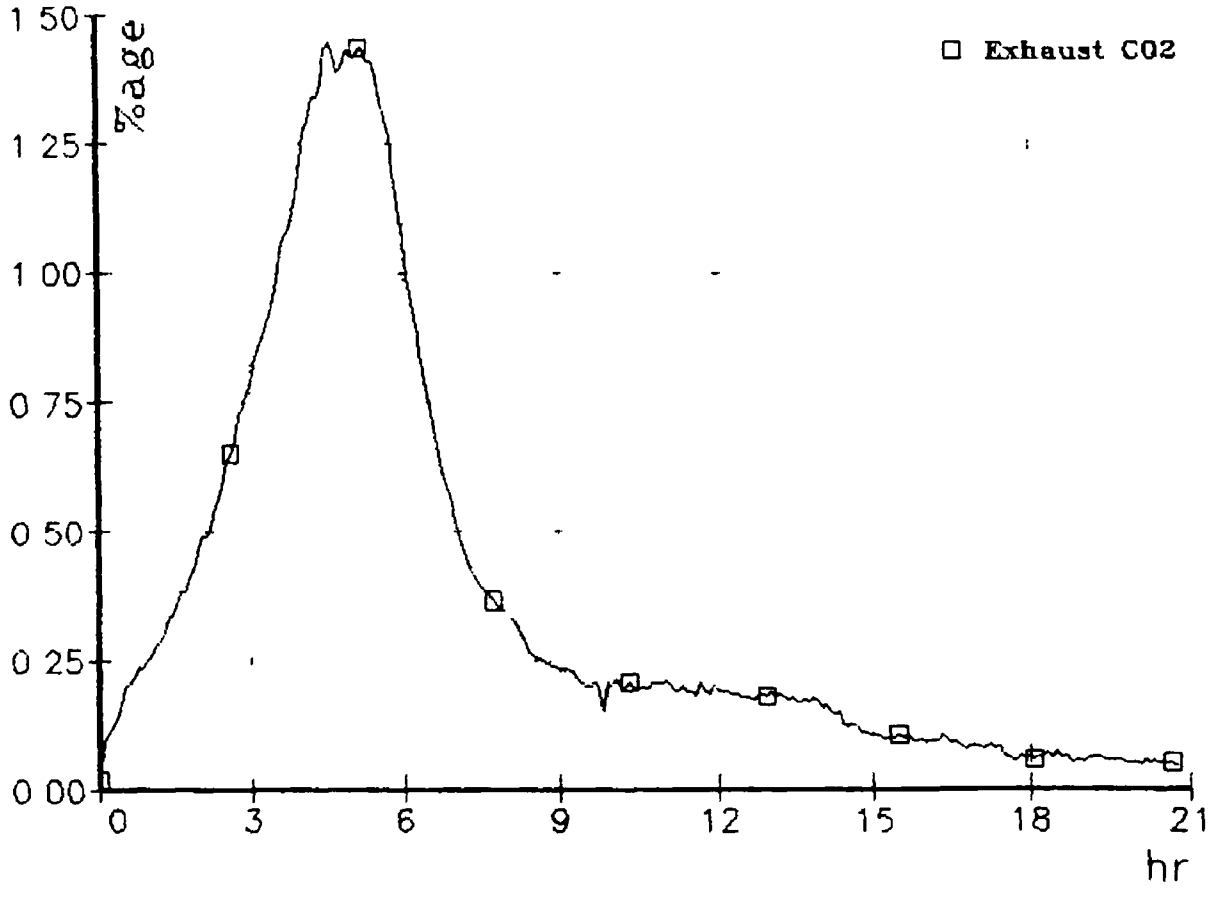

Fig 6.8 Fermentor 02

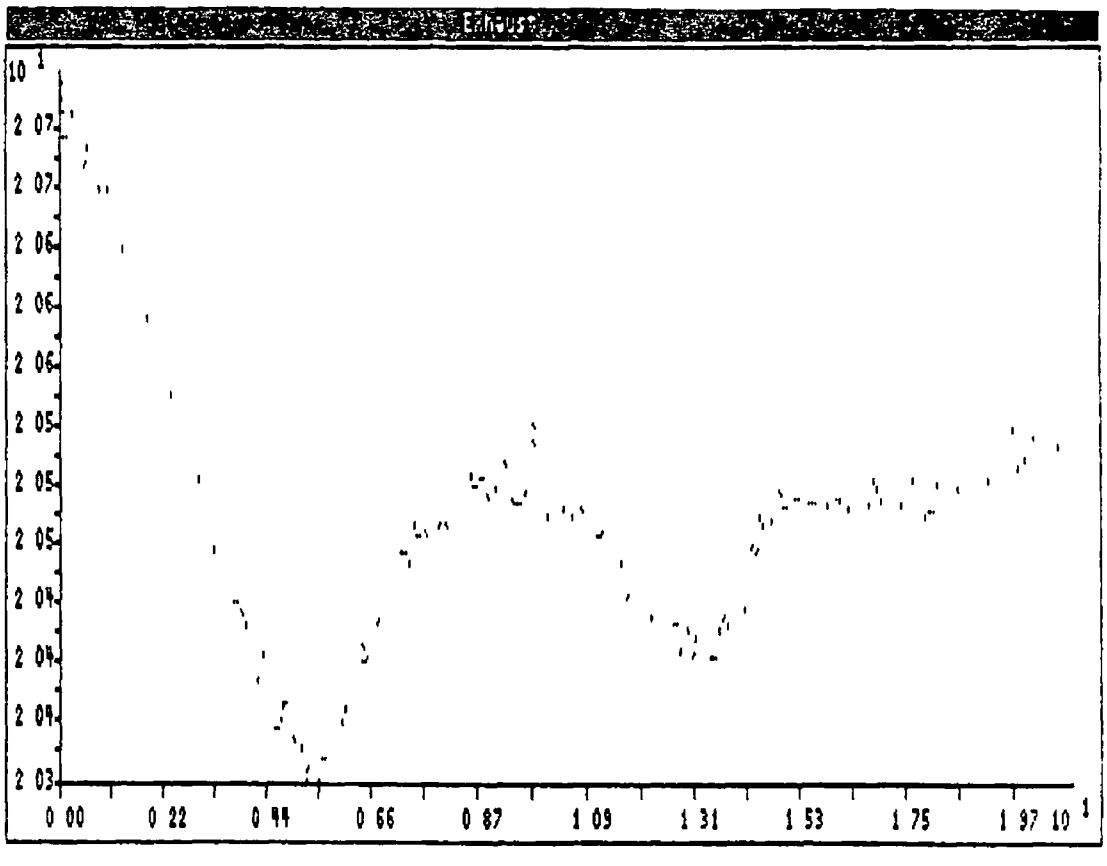

Fig 6.9 Exhaust CO2

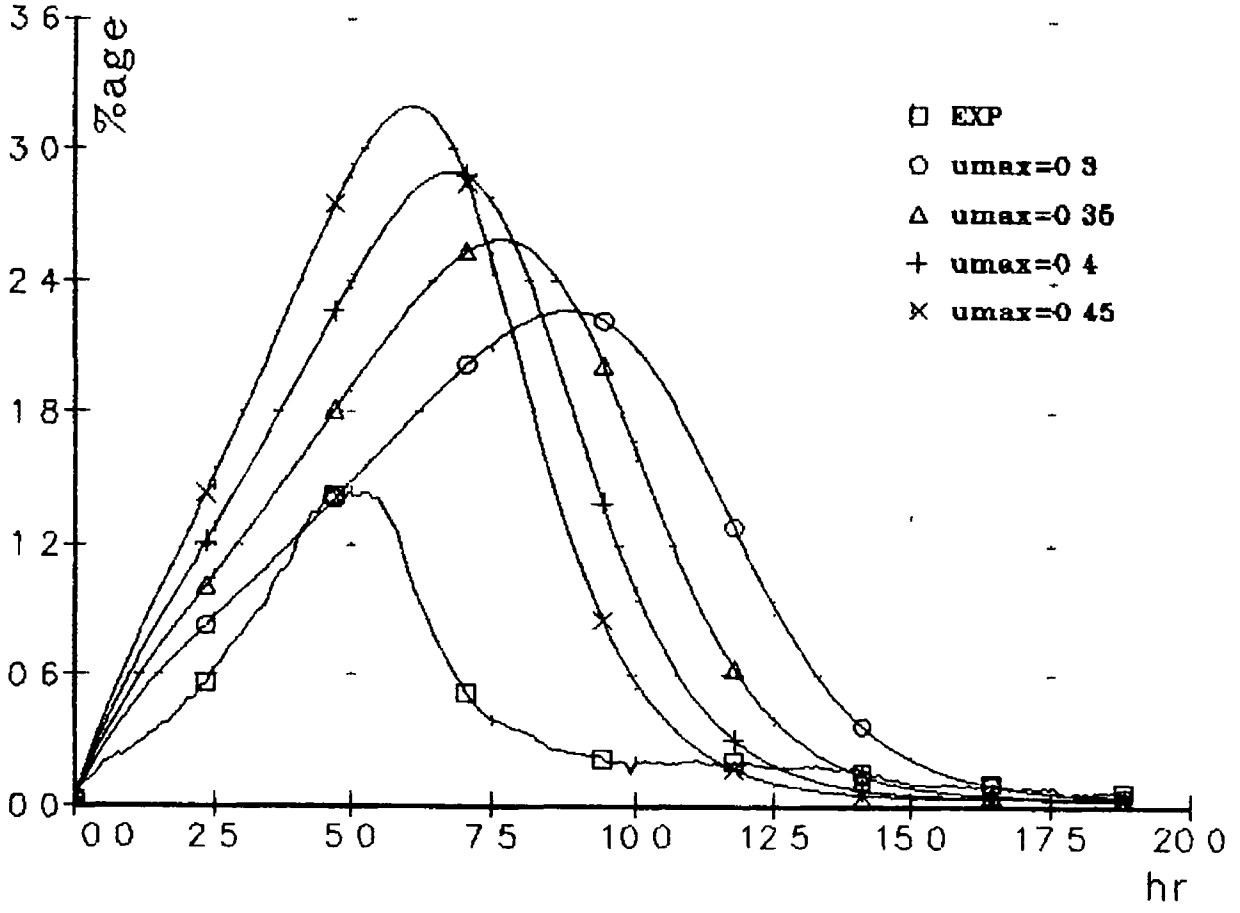

Fig 6.10 Exhaust 02

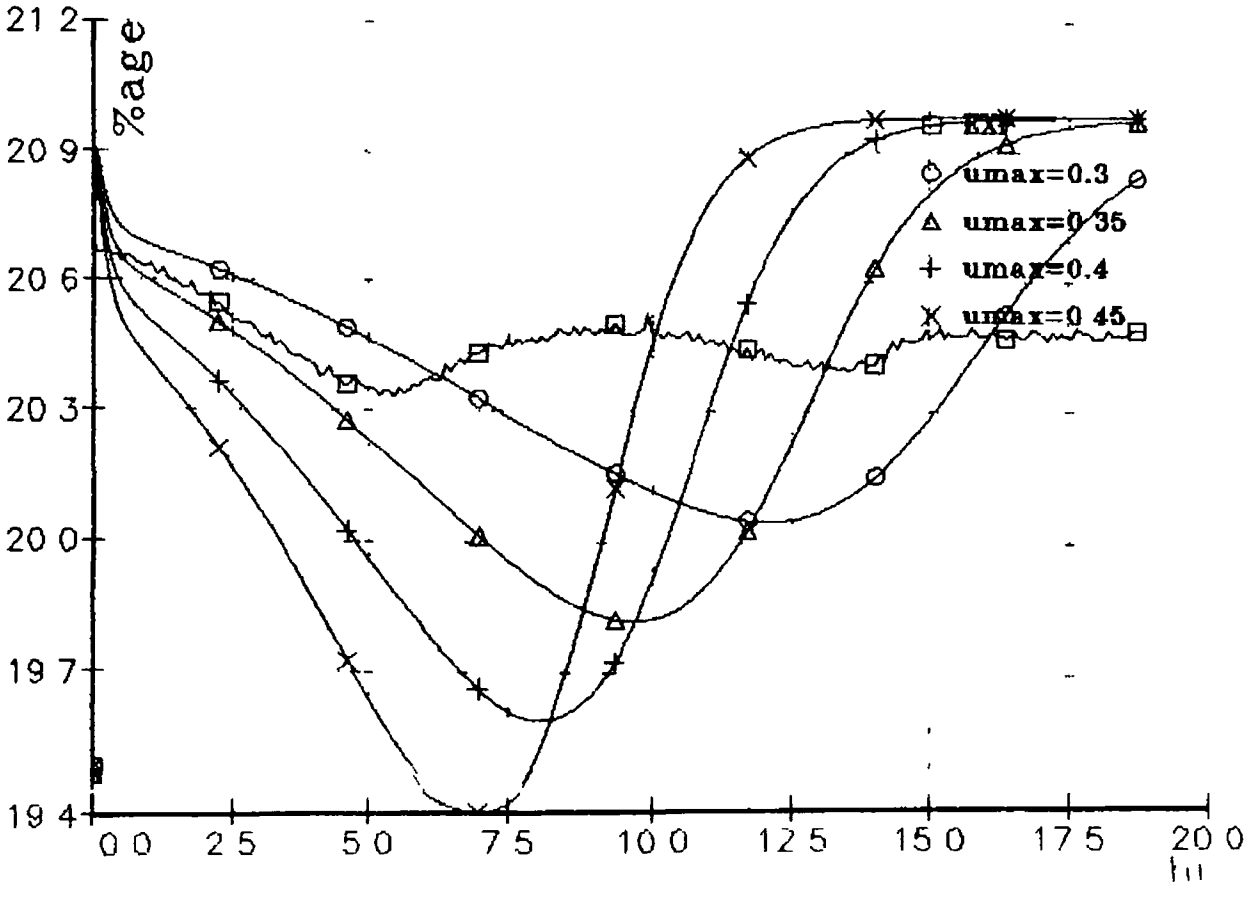

Fig 6.11 Biomass curve fit

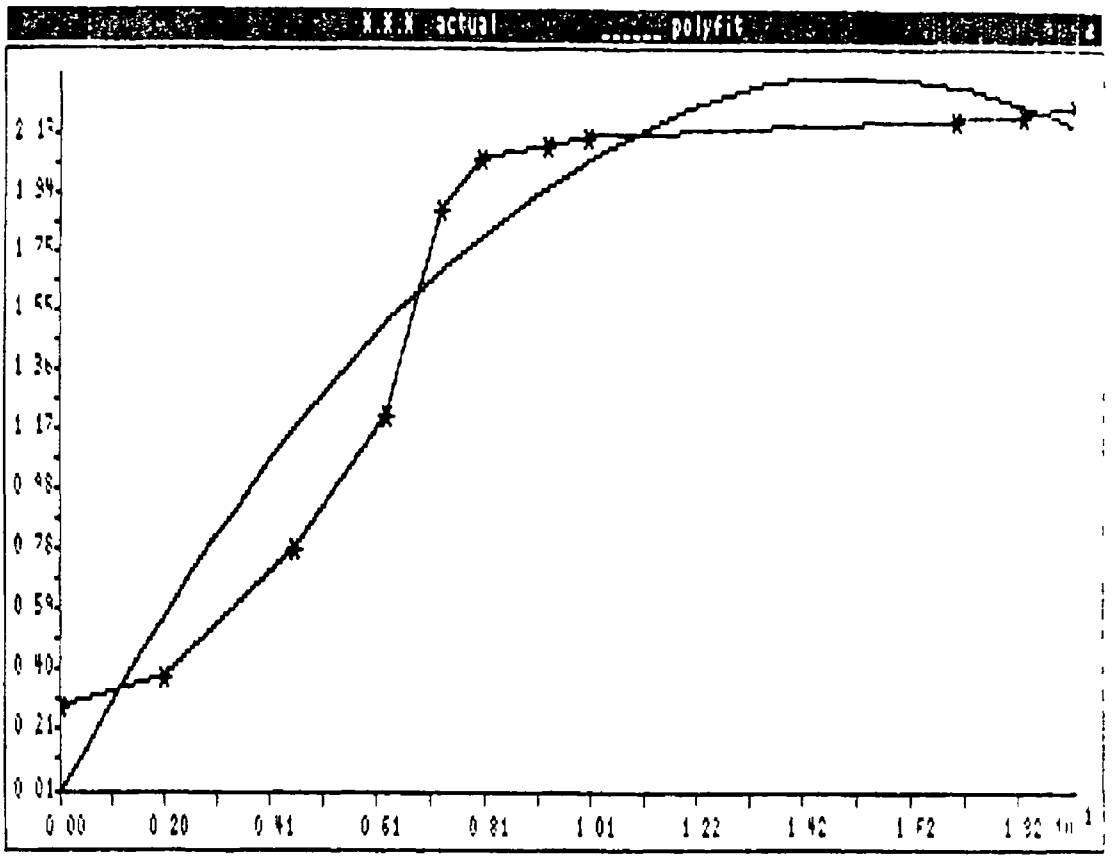

Fig 6.12 Substrate curve fit

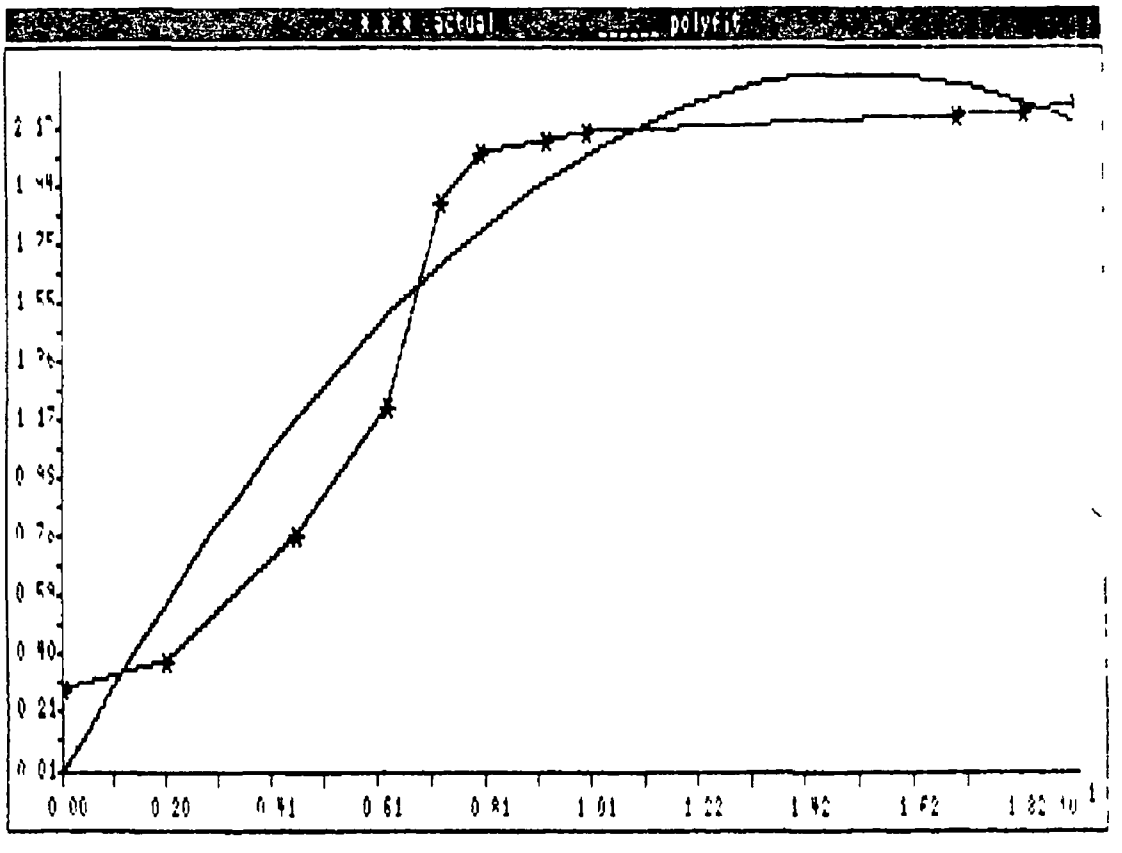

Fig 6.13 Polynominal fit

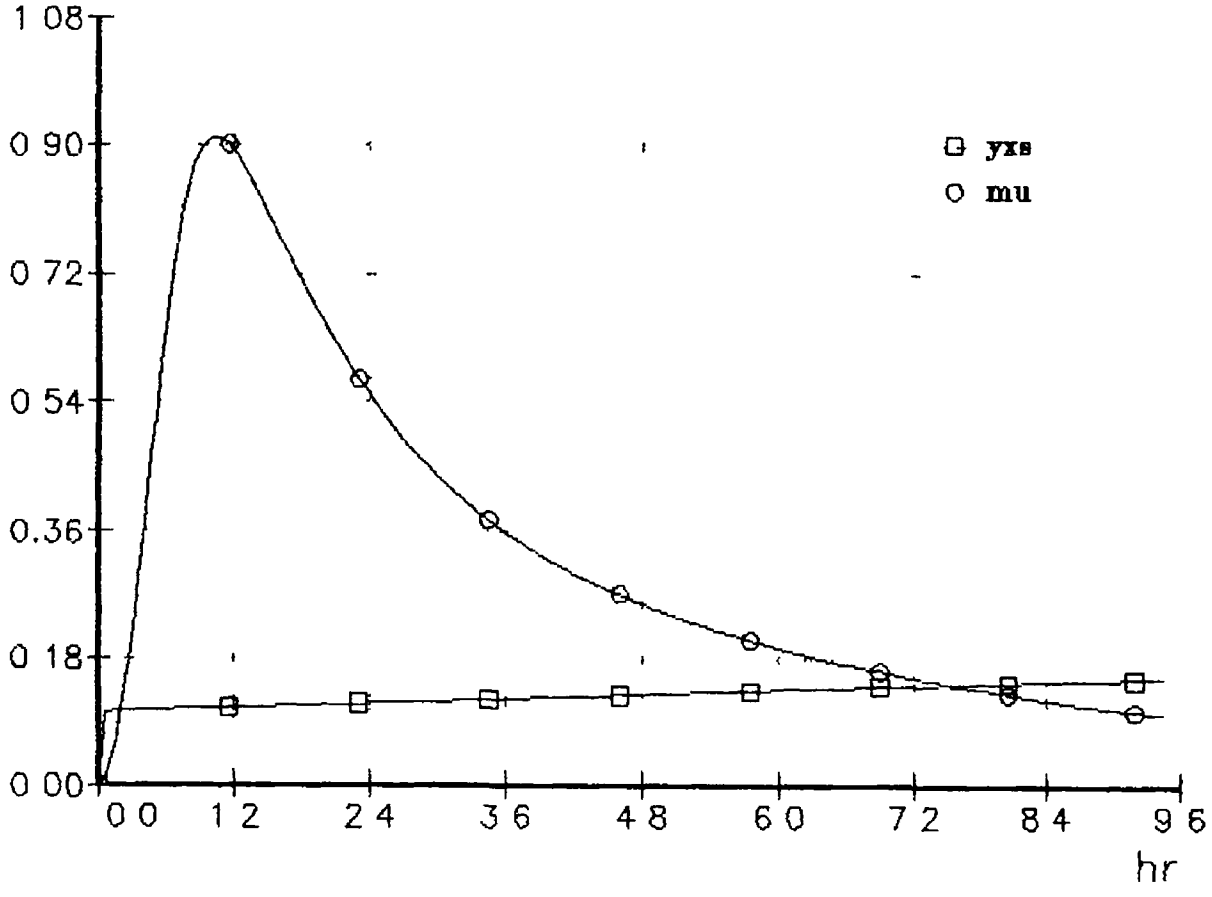

Fig 6.14 Piecewise fit

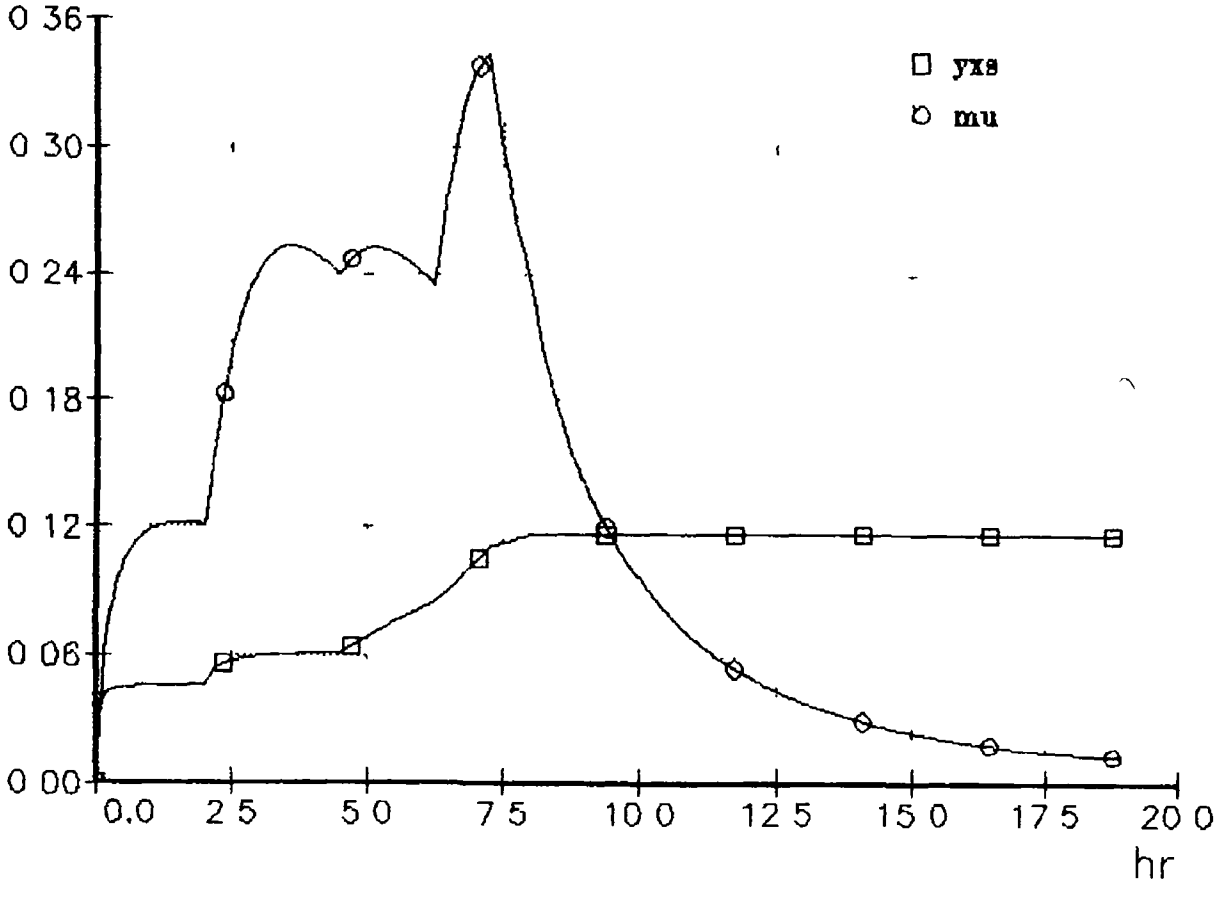

Fig 6.15 French curve fit

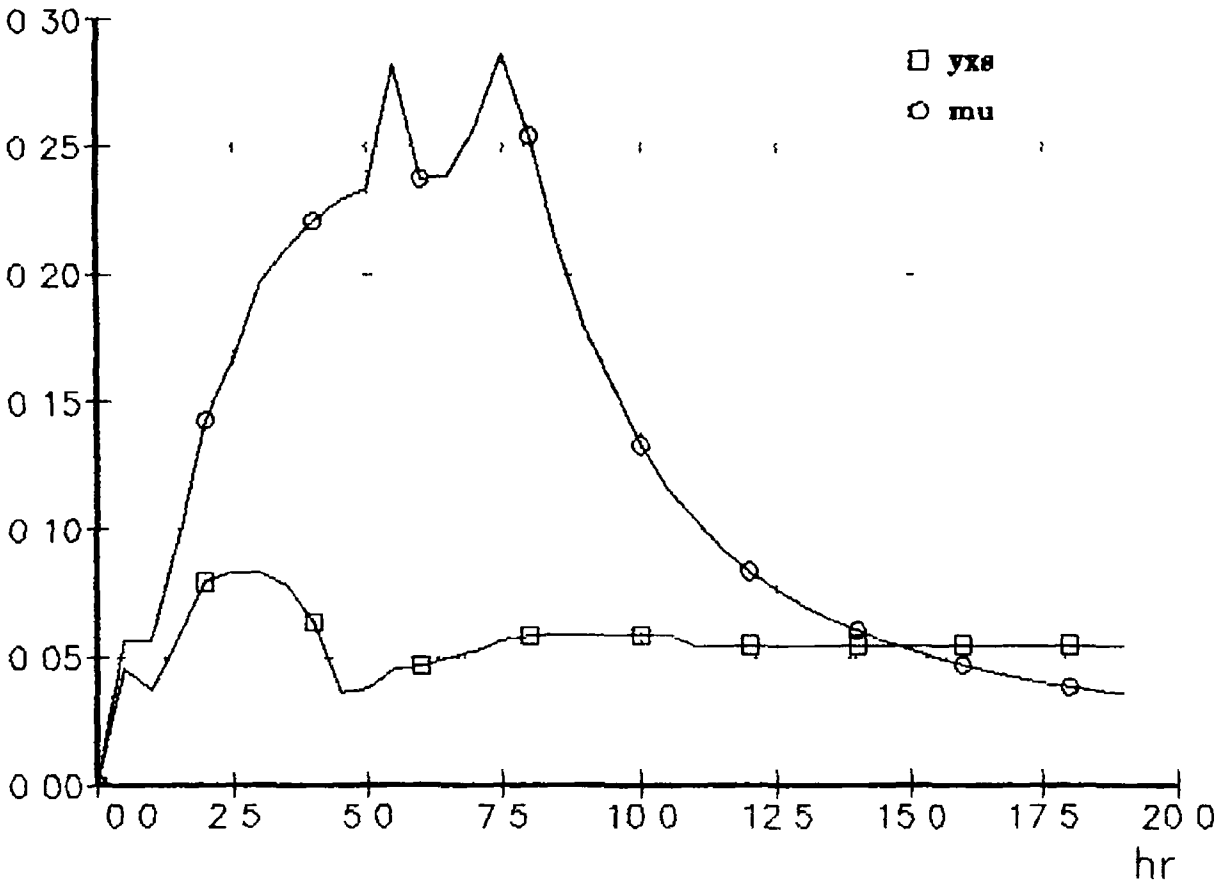

Fig 6.16 Piecewise fit, Monod

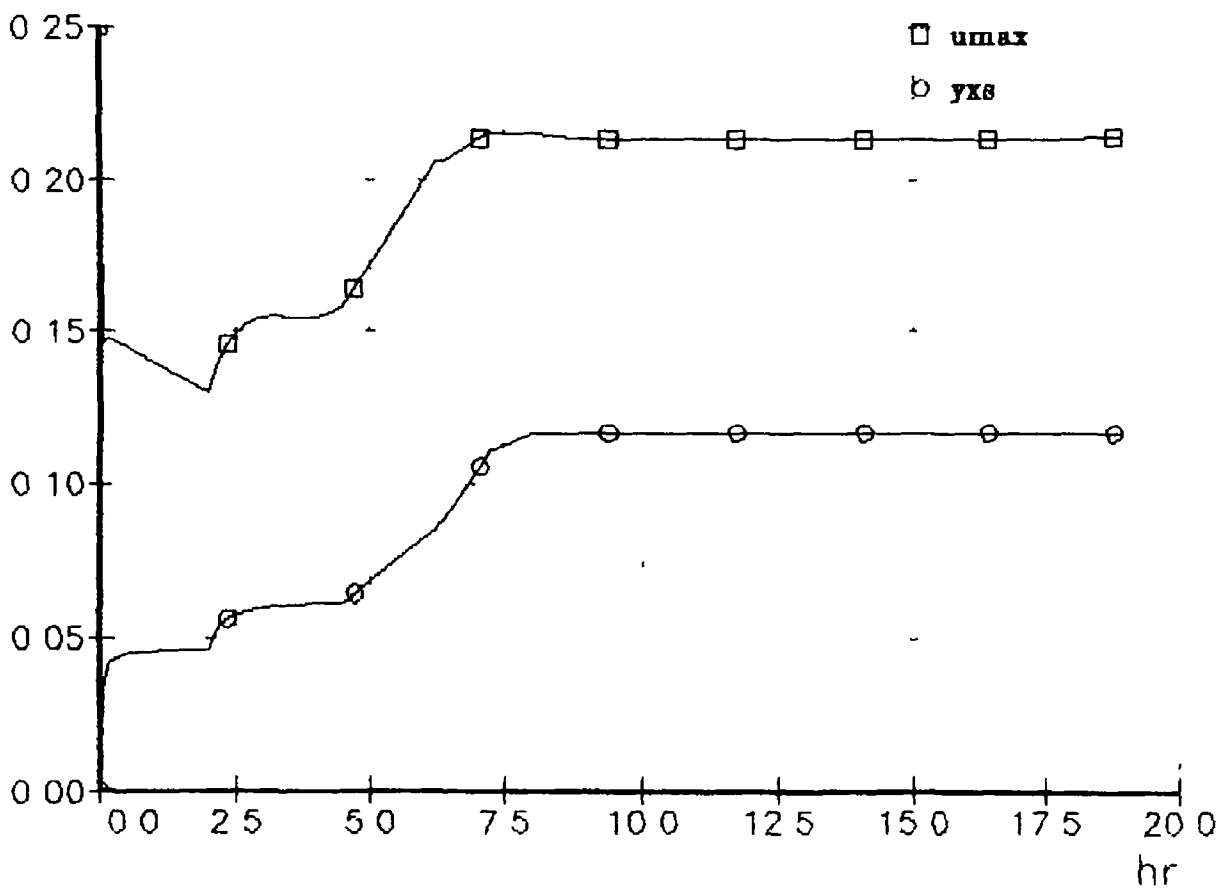

Fig 6.17 Piecewise fit, Monod

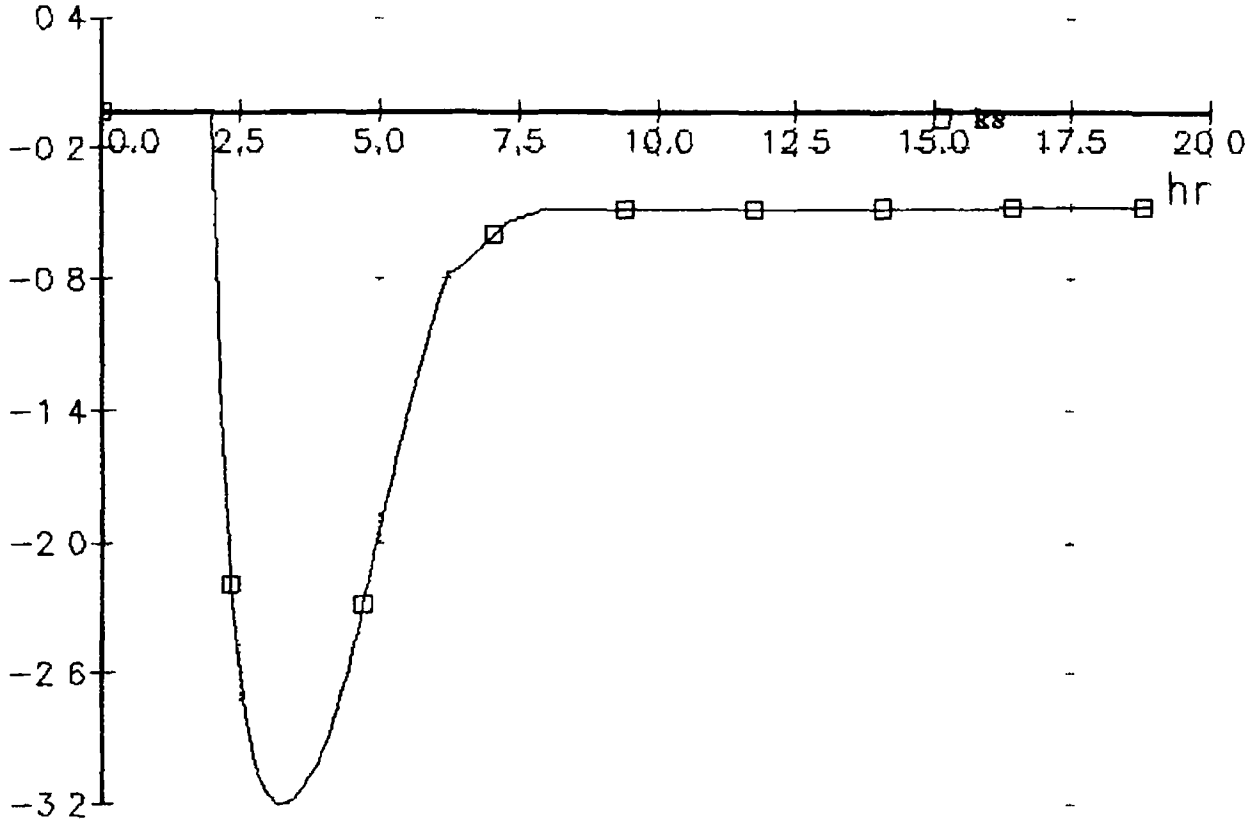

Fig 6.18 Piecewise fit, Ollson

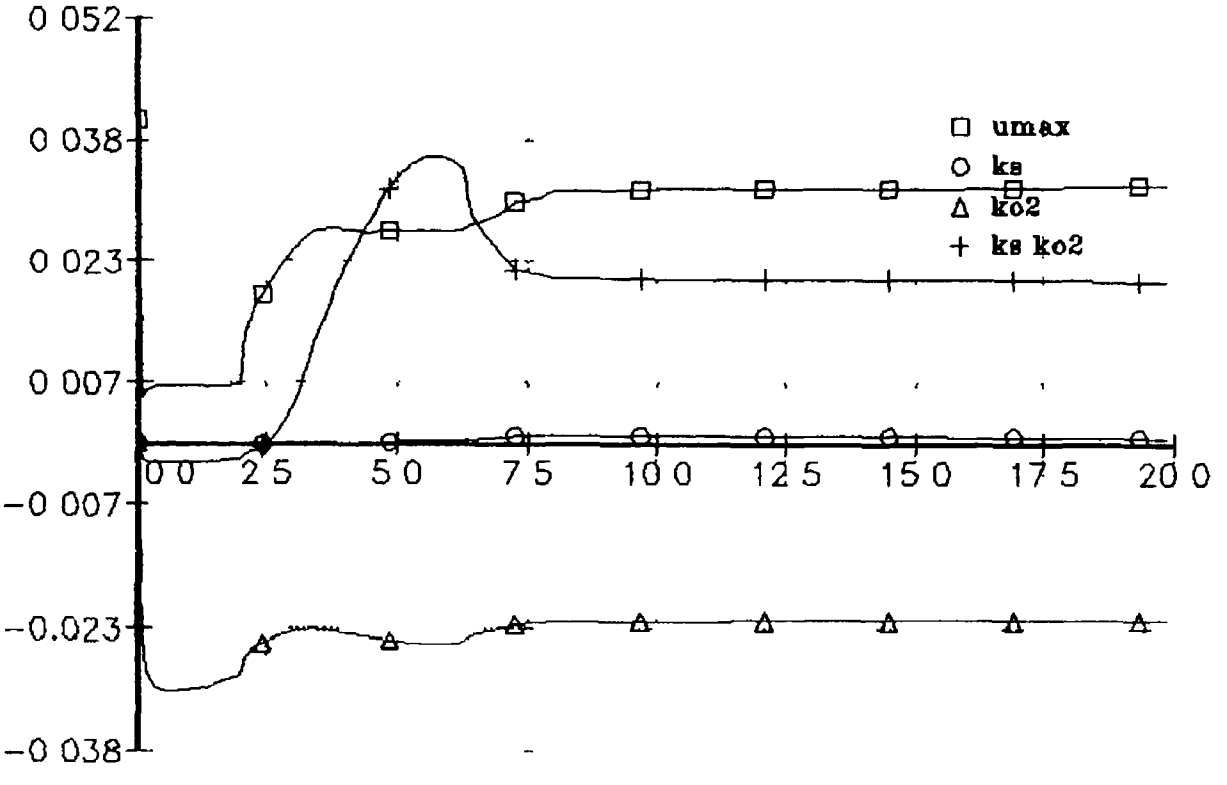

APPENDIX A

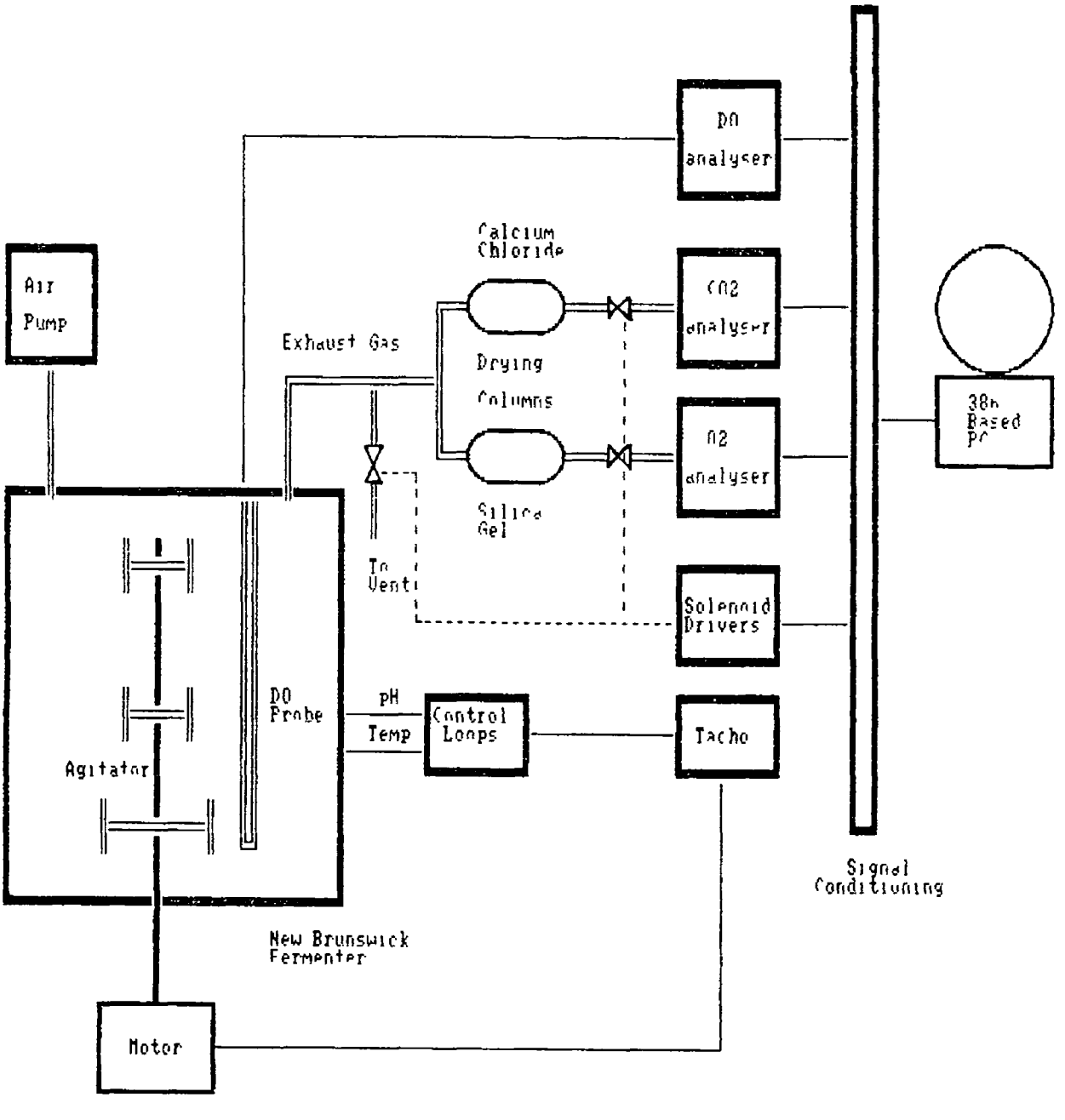

Computer Coupled Fermentation Process